Improvements to the Density-Functional Tight-Binding method: new, efficient parametrization schemes and prospects of a more precise self-consistency

PhD thesis

Zoltán Bodrog

Universität Bremen
2012

Dem Promotionsausschuss an der Universität Bremen, im
Bremen Center for Computational Materials Science
als Dissertation zur Erlangung des akademischen Grades
Doktor der Naturwissenschaften (doctor rerum naturalium)
vorgelegt.
(Tippfehler und ähnliche Fehler wurden korrigiert.)

Tag der Einreichung	10. Januar 2012
Tag der mündlichen Prüfung	23. März 2012

Promotionskommission

Erstgutachter	Prof. Dr. rer. nat. Thomas Frauenheim
Zweitgutachter	Prof. Dr. rer. nat. Gotthard Seifert
Prüfer	Prof. Dr. rer. nat. Thomas Heine
Prüfer	Prof. Dr. rer. nat. Peter Maaß
Vertreter der wissenschaftl. Mitarbeiter	Dr. Bálint Aradi
Vertreter der Studenten	Michael Wehlau

Contents

0.1 Abstract

The Density-Functional Tight-Binding (DFTB) method of quantum-chemical calculations is a pairwise LCAO-based approximation to the Kohn–Sham method of Density Functional Theory (DFT). To put a reader who is not fully familiar with DFT, DFT-like methods and DFTB into context, and to define the chief parts of nomenclature used, a brief introduction to DFT and a more deep one to DFTB is given in this thesis first, with emphasis on the grounds of enhancements in later sections. This initial section is also intended to be a very quick introduction to DFTB, with the minimum necessary insight into Kohn–Sham DFT for a reader who wants to understand the basics of DFTB quickly.

The second part is about improving the treatment of the so-called repulsive part of DFTB energy. It is the quasi-classical energy part specific to DFTB, it is calculated as a sum of pairwise effective potentials, the so-called repulsive potentials, and it is added to the quantum-mechanically calculated Kohn–Sham DFT electronic energy to give the total energy. Parametrization is optimizing these pairwise potentials for every type of atomic pairs, and it has been a lengthy work needing vast amounts of human effort, that has been posing a high barrier of entry into DFTB calculations with atom types not used before. I present a thorough description of a parametrizer automaton to take over this task. The automaton was developed in the course of doctoral research basing this thesis. Intertwined with the description, there are several additional points of possible enhancement revealed, e.g. implementation of new energetical objectives of fitting, and a perspective of possible optimization of electronic parameters. A few examples are also shown to illustrate the capabilities of the parametrizer automaton (of which the halogen-organic set is yet to be published [23]). This section is based on the publication of this part of work, see [5].

As a completely different answer to the parametrization problem, fully derived formulae of calculating the DFTB pairwise repulsive energy, instead of fitting, are presented at the end of the second part. Directly calculated repulsive potentials may be at least a good starting guess in cases when quick calculations of bigger error tolerance are needed. These results will be published soon in a separate article [6].

In the third part of this thesis, several pieces of enhancement are proposed to the electronic part of DFTB method itself. They affect the so-called Self-Consistent-Charges part of second-order DFTB, which implements iterative self-consistent Kohn–Sham calculations in DFTB, or more accurately an approximation of it based on the point-like representation of atomic charge fluctuations. Improvements of SCC are centered around making the effective interaction between point-like atomic excess charges more precise. First, a multipole expansion is suggested instead of the point-like charges. Second, the effective interaction profiles between atomic charge centres can be improved by semiempirical calculations, instead of the present heuristic interpolation formulas between chemical hardness and long-range Coulombic interaction. Most of the proposals described here were published in [4].

0.2 Kurzfassung

Die density-functional tight-binding (DFTB) Methode der quantenchemischen Kalkulationen ist eine paarorientierte Approximation der Kohn–Sham-Methode der Dichtefunktionaltheorie (DFT). Für die, die DFT, bzw. DFTB nicht ganz detailweise kennen, und auch um die weitere Entwicklungen vorzubereiten, beginnt eine kurze Einleitung zu DFT und eine mehr tiefgreifende Einleitung zu DFTB diese Dissertation. Dieses erste Teil ist vorgehabt auch eine sehr kurze Einleitung für die zu sein, die DFTB mit dem kleinsten Eingriff zu DFT oder mit DFT-Hintergrund schnell verstehen möchten.

In dem zweiten Teil werden Verbesserungen der Handlung von dem sogenannten repulsiven Anteil der DFTB-Energie beschrieben. Es ist das quasiklassische Energieanteil, das spezifisch zu DFTB ist, und es wird als eine Summe von Paarpotentialen – die sogenannten Repulsivpotentialen – neben dem elektronischen Energieanteil gerechnet. Die Fittung von dieser Paarpotentialen für jedem Typ von Atompaaren, die Parametrisierung heisst, ist ohne Automatisierung ein sehr langer Prozess, der intensive Menschliche Arbeit nimmt, und deshalb eine hoche Barrierie gegen neue DFTB-Kalkulationen anzufangen gibt. Hier wird, aber, ein Automat, das die Parametrisierung machen kann, vorgeschlagen und detailreich beschrieben. Die Parametrisierungsautomat wurde im Ramen der Doktorandforschung, die auch das Material dieser Dissertation gegeben hat, entwickelt. In der Beschreibung des Automaten werden auch mögliche Richtungen der Weiterentwicklung geschrieben, z. B. Implementation neuerer energetischen Zwecke der Parametrisierung, oder Optimierung elektronischer Parameter. Auch in diesem Teil werden einige Beispile der Nützlichkeit des Automaten dargestellt (von denen das Beispiel mit halogen-organischen Parametern wird in Kürze publiziert [23]). Dieses Teil ist auf [5] gegründet.

Am Ende des Kapitels wird ein komplett unterschiedliche Lösung zum Parametrisierungsproblem vorgeschlagen. Völlig herabgeleitete Formeln der direkten Kalkulation der Repulsivenergie anstatt der gefitteten Repulsivprofilen stehen hier. Die direkt kalkulierte Repulsivenergie kann ein guter Tipp am Anfang einer DFTB-Kalkulation sein, wann man schnelle Resultaten, aber keine höhere Präzisität braucht. Diese Methode und Resultaten sind auch in Kürze zu publizieren [6].

In dem dritten Teil dieser Dissertation werden mehrere methodologische Verbesserungen des elektronischen Anteils der DFTB Methode geschrieben. Sie gehen um dem sogenannten Self-Consistent-Charges (selbstkonsistente Ladungen) Teil der DFTB von zweiter Ordnung, das approximative Selbstkonsistenz in DFTB als eine Kohn–Sham Methode implementiert (durch ein Bild von Punktladungen, die atomare Ladungsfluktuation representieren). SCC-Entwicklung enthält zwei größere Hauptgebiete. Das erste geht über das Punktladungsbild bei Ladungsfluktuationen, und schlägt eine Entwicklung der Ladung-Ladung Wechselwirkung durch Multipolenreihen vor. Das zweite schlägt verbesserungen von dem Wechselwirkungsprofil zwischen Ladungen vor, von denen eine ist die, die diese Profile semiempirisch anstatt der heutigen heuristischen Interpolation zwischen der atomaren Härte und der coulombischen Grenzwert kalkuliert. Fast alle Vorschläge geschrieben in diesem Teil wurden in [4] publiziert.

0.3 Summarium operis

Methodus nomine 'Density-Functional Tight-Binding' (DFTB) in chemia quantica est approximatio calculationum in theoria functionalis densitatis (DFT) algorithmo Kohn–Sham factarum, quae fundamenta in integralibus pro geminis atomorum calculandis et basi minimali utendo habet. Contextum construendi causa eis, qui non maxime periti in DFT, methodis similibus atque in DFTB sint, nec non ad nomenclaturam sectionibus sequentibus scriptam introducendam habetur introductio in prima thesi, quae altitudines DFT minime, DFTB autem maxime tractat. Introductio haec est scripta etiam eis, qui in DFT iam periti aut DFT tangere non volentes methodum DFTB ipsam celerrime intellegere volunt.

In media thesi tractatur pars energiae in DFTB nomine energia repulsiva appellata atque investigantur producenda parametra. Producenda parametra est optimanda pars energiae quasi-classica, ad DFTB specifica, quae summa potentialium effectivorum pro geminis atomorum, vulgo potentialium repulsivorum, calculatur et ad energiam methodo Kohn–Sham calculatam additur. Haec potentialia repulsiva omnibus geminis typorum atomorum adiustenda fuerunt tamen labor immensis vires humanas maxime dissipans. Situatio haec obstitit novis calculationibus methodo DFTB cum typis atomorum prior non praesentibus. Automaton problema hoc solvens propono et describo, quod in cursu quaestionis doctoralis materiam huius dissertationis quoque producentis creatum est. Complexae in descriptione habentur etiam partes automati meliorem faciendi, e.g. implementatio obiectivorum ad adiustanda parametra novorum energeticalium et perspectiva optimandorum parametrorum electronicorum. In hoc capite sunt etiam exempla nonnulla parametrisatorem automaticum multum bene functum illustrantia scripta (quorum parametra inter halogenia et elementa organica optimata brevi tempore publicanda sunt [23]). Hoc caput contenta maxime ab articulo has res describenti [5] ducit.

Altera solutio problematis parametrorum est calculatio potentialium repulsivorum arte 'ab initio' facta, cuius formulae perfecte derivatae in ultimo capite sunt scripta. Expectantur repulsiva sic calculata utilia esse in situationibus, quibus calculationes celeriter currere oportet, errores autem magis tolerandi sunt. Repulsiva hoc modo calculata sunt etiam publicanda [6].

In parte dissertationis tertia mutationes ad methodum DFTB ipsam et partem electronicam meliorem fiendam propono. Has mutationes partem Self-Consistent-Charges (onera electrica sibi consistentia) methodi DFTB, implementantem calculationes sibi consistentes iterativas ad modum Kohn–Sham faciendas, sive praecisius approximationem earum oneribus electricis punctis formatis utendam, afficiunt. SCC-DFTB possit melior fieri a melioribus interactionibus inter illas fluctuationes onerum electricorum. Ad primum continet hoc thema expansionem multipolis constructam loco onerum punctis similium. Ad secundum habentur hic interactionum functiones semiempirice calculatae, loco interpolationis multum heuristicae. Plurimae harum theseon sunt etiam in [4] publicatae.

0.4 Összefoglalás

A DFTB (Density-Functional Tight-Binding) módszer egy olyan kvantumkémiai számítógépes eljárás, mely a sűrűségfunkcionálelmélet (Density-Functional Theory, DFT) Kohn–Sham-féle megfogalmazásának atomi párokon alapuló minimális bázisú közelítése. A DFT-ben, DFT-szerű eljárásokban, illetve a DFTB-ben mélyen nem jártas olvasók számára, valamint a későbbi fejlesztések megalapozásául e disszertáció elején egy igen rövid bevezetés olvasható a DFT-be, majd a DFTB-nek egy nagyon részletes leírása következik. Ezt a bevezető részt – szándékom szerint – tankönyveszerűen is olvashatják azok, akik a DFT alapjainak minimális érintésével, vagy kész DFT-s háttérrel szeretnék gyorsan megérteni a DFTB működését.

A második rész a DFTB-energiának az úgynevezett repulzív részét, e repulzív rész kezelésének javítását, illetve a DFTB parametrizálását járja körül. Maga a parametrizálás azoknak a párpotenciáloknak (az úgynevezett repulzív potenciáloknak) az optimalizálását jelenti, amelyeknek az összegeként a DFTB-re jellemző kváziklasszikus energiarészt, a repulzív energiát számoljuk – az elektronok Kohn–Sham-energiájával együtt ez adja a DFTB-ben számolt teljes energiát. Ezeknek a párpotenciáloknak az optimalizálása minden atompártípusra egy rendkívül hosszadalmas és sok emberi erőfeszítést igénylő feladat, mely igen nehézzé teszi azt, hogy a DFTB-vel eddig nem számolt atomtípusok kémiáját számoljuk. Javaslatot teszünk azonban egy automatikus parametrizálóeljárásra, mely ezt a munkát könnyebbé teszi, illetve nagyrészt elvégzi. A parametrizálóeljárást az e disszertáció alapját képező doktori kutatások keretében fejlesztettem ki. A parametrizálóautomata leírásába szőve annak lehetséges továbbfejlesztési irányait is felvázolom, példa ilyenre a jelenleg meglevőkön felüli energetikai célfüggvények definiálása, vagy az elektronikus paraméterek optimalizációja. E fejezetben néhány példával illusztrálom is az automata képességeit (a példák közül a halogén-szerves paraméterek önálló publikációként is meg fognak jelenni [23]). A fejezet eredményei publikációként meg is jelentek [5].

A parametrizálás problémájának eddigiektől teljesen eltérő megoldását adja a repulzív energia közvetlen, nem félempirikusan illesztett számítása. Ennek képleteit minden részletre kiterjedően szintén közlöm. A számított repulzív energia jó kiindulópont lehet olyan számítások esetén, ahol gyorsan kell eredményeket produkálni, azonban az eredmények nagy pontossága nem feltétlenül szükséges. E megoldás rövidesen publikációként is megjelenik [6].

A disszertáció harmadik részében javaslatot teszek magának a DFTB eljárásnak, azaz az elektronikus résznek a fejlesztésére is. Ezek a fejlesztési javaslatok a DFTB-n belül az SCC (Self-Consistent-Charges, azaz önkonzisztens töltések) nevű részt érintik, mely a DFTB-n belül másodrendben teszi lehetővé az önkonzisztens Kohn–Sham-féle számítást, pontosabban annak egy közelítését, mely az atomi töltésfluktuációk ponttöltésszerű modelljén alapul. Az SCC fejlesztése ezen töltésfluktuációk kölcsönhatásait teszi pontosabbá. Ehhez az első módszer a ponttöltések helyett multipólussorok használata. A második módszer az SCC pontosítására a töltések közti effektív kölcsönhatási profilok pontosabb meghatározását tűzi ki célul, ezen belül is félempirikus módszerrel, nem pedig az eddig jellemző heurisztikus interpolációval, mely a kémiai keménységet a távoli Coulomb-kölcsönhatással kötötte össze. Az ebben a szakaszban szereplő javaslatokat szintén publikáltuk [4].

Chapter 1

An introduction to the DFTB method

1.1 What we shall know about DFT now

1.1.1 What is density functional theory?[1]

Although quantum mechanics brought a deeper-than-ever-before understanding of microscopic world, and a revolution in physics connected therewith, practical computations with the quantum mechanical machinery are impossibly complicated even with a perturbative treatment of fairly small systems, e.g. small molecules. Solution of the

$$\varepsilon|\Psi\rangle = \hat{H}|\Psi\rangle \tag{1.1}$$

stationary Schrödinger equation for the ground state of the system is far from trivial when Ψ is a multi-particle wavefunction with N particles. The spatial representation of Ψ in this case uses $3N$ spatial coordinates, while that of $\hat{H}$ uses $6N$, and because of electron-electron interactions, all of these are inseparably connected in the integro-differential Schrödinger equation.

However, quantum chemistry, as a prevalent, 'killer' application of quantum mechanics, quickly came out with the most successful simplification scheme of the above problem, the density-based calculation of electronic configurations. This means changing the Schrödinger equation or the equivalent

$$E(\Psi) = \langle\Psi|\hat{H}|\Psi\rangle = \text{min.}, \quad \langle\Psi|\Psi\rangle = 1 \tag{1.2}$$

variational problem to another variational problem, but the new problem searches for the ground-state electronic density, not the ground-state wavefunction.

$$E(\varrho) = \text{min.}, \quad \int_{\mathbf{x}} \varrho(\mathbf{x}) d\mathbf{x} = N \tag{1.3}$$

In the presence of a $\hat{V}_{\text{ext}}$ external electric potential, the above energy func-

[1] For a thorough foundation and description of this topics, see [29].

tionals of wavefunction or density split to two parts,

$$E(\Psi) = \int \dots \int \Psi(\mathbf{x}_1, \dots, \mathbf{x}_N) \left[-\sum_i \frac{\Delta_i}{2} + \sum_{i \neq j} \frac{1}{|\mathbf{x}_i - \mathbf{x}_j|} + \sum_i V_{\text{ext}}(x_i) \right] \times$$
$$\Psi(\mathbf{x}_1, \dots, \mathbf{x}_N) d\mathbf{x}_1 \dots d\mathbf{x}_N = F(\Psi) + \int V_{\text{ext}}(\mathbf{x}) \varrho(\mathbf{x}) d\mathbf{x}$$
$$= E(\varrho) = F(\varrho) + \int V_{\text{ext}}(\mathbf{x}) \varrho(\mathbf{x}) d\mathbf{x}. \tag{1.4}$$

Note that the last term in $E(\Psi)$ is trivially equal to $\int V_{\text{ext}}(x) \varrho(x) d\mathbf{x}$, and therefore the above equation is an implicit proof that the existence and validity of density-based treatment equals to the existence of the $F(\Psi) = F(\varrho)$ functional which comprises kinetic energy as well as all terms of interaction between the N electrons. This $F(\varrho)$ functional is called the universal part of energy functional, since it is the same for every system containing N electrons.

The first attempt at such a scheme was the Thomas–Fermi method [15, 35] with its simple kinetic energy functional and total neglection of exchange and correlational energies (a term approximating exchange energy was later added by Dirac [9] and the kinetic energy part was improved somewhat by Weizsäcker [37]), that is a very simplistic universal functional. This approximate density-based method is far from fulfilling the (1.4) equivalence precisely, and serves barely more than as a historical example today.

The very success of density-based quantum-chemical methods had begun with the theoretically strict and exact formulation of density-functional theory based on the Hohenberg–Kohn theorems that establish the validity of handling electronic density instead of wavefunction as the basic variable of calculation. Validity is ensured by the existence of a $F(\varrho)$ universal functional that makes the (1.4) equivalence exact. However, the actual form of this $F(\varrho)$ functional is unknown, and thus it can only be approximated in practical calculations. Based on the Hohenberg–Kohn theorems, Kohn and Sham founded the most efficient calculation method up to date that calculates density as that of non-interacting electron-like quasiparticles.

1.1.2 The Hohenberg–Kohn theorems

The first Hohenberg–Kohn theorem establishes that different problems necessarily have different ground state electron densities, or equivalently, no two different external potentials can lead to the same ground-state electronic density with the same number of electrons. The proof is simple: if both the $V_1(\mathbf{x})$ and $V_2(\mathbf{x})$ external potentials give $\varrho(\mathbf{x})$ as ground-state density and Ψ_1, Ψ_2 are the two ground-state wavefunctions for the two potentials, respectively, then

$$F(\Psi_1) + \int \varrho(\mathbf{x}) V_1(\mathbf{x}) d\mathbf{x} \leq F(\Psi_2) + \int \varrho(\mathbf{x}) V_1(\mathbf{x}) d\mathbf{x} \tag{1.5}$$

since Ψ_1 is the ground state of the system with V_1. In the same way

$$F(\Psi_2) + \int \varrho(\mathbf{x}) V_2(\mathbf{x}) d\mathbf{x} \leq F(\Psi_1) + \int \varrho(\mathbf{x}) V_2(\mathbf{x}) d\mathbf{x} \tag{1.6}$$

since Ψ_2 is the ground state of system 2 (here and in (1.4) we denoted the universal part of wavefunction-dependent energy functional with F, but although it is not the same as the F density functional, this leads to no ambiguity). The two inequalities together say that $F(\Psi_1) = F(\Psi_2)$ and therefore the value of F may be assigned to ϱ. With this, in a non-degenerate case

$$E_1 = F(\varrho) + \int \varrho(\mathbf{x}) V_1(\mathbf{x}) > E_2 + \int \varrho(\mathbf{x}) \left(V_1(\mathbf{x}) - V_2(\mathbf{x})\right) \tag{1.7}$$

if we denote the ground-state energies of problem 1 and 2 with E_1 and E_2, respectively. The inequality holds because ϱ is the ground-state density of problem 2, and therefore $F(\varrho) + \int \varrho V_2 = E_2$. Similarly

$$E_2 = F(\varrho) + \int \varrho(\mathbf{x}) V_2(\mathbf{x}) > E_1 - \int \varrho(\mathbf{x}) \left(V_1(\mathbf{x}) - V_2(\mathbf{x})\right) \tag{1.8}$$

because ϱ is the ground-state energy of problem 1. If we add (1.7) and (1.8) together, we get

$$E_1 + E_2 > E_1 + E_2 \tag{1.9}$$

which is clearly a contradiction. We silently omitted treating degenerate cases, when the sides of above inequalities become equal. The theorem also holds in this more complicated case, but the proof is not that easy. As a plausibilization instead of the proof, it must be noted that for the degenerate equations to hold, it would need a very quirky situation: two ground states which are degenerate ground states of two distinct Hamiltonians in parallel, but with the same density.

It is true therefore that a ground-state density can not belong to more than one external potential, and thus ground-state electronic density determines the external potential of the problem.

A corollary of the first Hohenberg–Kohn theorem is that since the ground state determines the potential, it determines the Hamiltonian as well, because the universal part is a constant operator. Through the Hamiltonian, the ground-state density of a quantum-chemical problem determines the whole spectrum, the ground-state wavefunctions and all of other eigenstates of it.

Another corollary of the above theorem can be the first stage of the proof: the universal part of energy functional exists and it is well-defined. Its actual form is not known, and is of unknown complexity, though.

The second Hohenberg–Kohn theorem states that the ground state density and energy of a quantum-chemical system can be calculated minimizing the

$$E(\varrho) = F(\varrho) + \int \varrho(\mathbf{x}) V_{\text{ext}}(\mathbf{x}) d\mathbf{x} \tag{1.10}$$

energy functional. The proof can be regarded as a third corollary of the first theorem, it is based on having a ground-state wavefunction determined by V_{ext} and N. Since this ground-state wavefunction is at the minimum of the wavefunction-based energy functional, and $E(\Psi) = E(\varrho_\Psi)$, $E(\varrho)$ must take its minimum at ϱ_Ψ, the charge density determined by Ψ.

A further corollary of the Hohenberg–Kohn theorems (the Levy constrained-search formulation) is that if the actual form of $F(\varrho)$ were known, the ground-state of a system would be found minimizing the density-dependent energy functional first, then getting the ϱ_0 ground-state density, and finally minimizing

$F(\Psi)$ over the Ψ wavefunctions which have ϱ_0 as their density. This corollary is again based on the energy-minimum property of ground state, and it introduces a theoretical implementation of $F(\varrho)$:

$$F(\varrho) = \min_{\varrho_\Psi = \varrho} F(\Psi). \tag{1.11}$$

1.1.3 The Kohn–Sham equations

The invention of Kohn and Sham about calculating the $F(\varrho)$ universal functional was calculating it with a method that is highly accurate compared to earlier attempts, but circumvents the direct construction of an $F(\varrho)$ functional. Instead, the density is calculated as a

$$\varrho(\mathbf{x}) = \sum_i^{\text{occ.}} \bar{i}(\mathbf{x}) i(\mathbf{x}) \tag{1.12}$$

density sum of independent, non-interacting electronic orbitals, the so-called Kohn–Sham orbitals, and being the Kohn–Sham electrons non-correlated, the kinetic energy part of universal functional is simply:

$$T_{\text{KS}}(\varrho) = -\sum_i^{\text{occ.}} \int_{\mathbf{x}} \bar{i}(\mathbf{x}) \frac{\Delta}{2} i(\mathbf{x}) d\mathbf{x}. \tag{1.13}$$

In the Kohn–Sham machinery, the number of used orbitals equals to the number of electrons, i.e. there are no unoccupied Kohn–Sham orbitals in the original scheme. Formulae can be upgraded, however, to the non-zero-temperature case by changing $\sum_i^{\text{occ.}}$ to $\sum_i n_i$ where n_i are the appropriate occupation numbers. To provide the collection of i Kohn–Sham orbitals with a Schrödinger-like system of equations to calculate them, one places them into the *noninteracting reference system* of the original problem. This reference system has an external potential composed of the original external potential and the effective potential of electrons, called the Kohn–Sham potential:

$$V_{\text{KS}}(\mathbf{x}) = V_{\text{ext}}(\mathbf{x}) + V_{\text{C}}(\mathbf{x}) + V_{\text{xc}}(\mathbf{x}) \tag{1.14}$$

where V_{C} is the Coulomb potential of electrons

$$V_{\text{C}}(\mathbf{x}) = \int_{\mathbf{y}} \frac{\varrho(\mathbf{y})}{|\mathbf{x} - \mathbf{y}|} d\mathbf{y}, \tag{1.15}$$

and V_{xc} is an effective potential arising from everything else, namely

- the error of (1.13) Kohn–Sham kinetic energy with respect to the true one,
- Coulomb exchange terms not present in the (1.15) classical Coulomb field,
- correlational terms not present in the calculations with the multi-electron Kohn–Sham wavefunction, that is a determinant made of Kohn–Sham orbitals.

The Kohn–Sham orbitals of noninteracting reference system obey a Schrödinger equation of the form

$$\hat{H}_{\mathrm{KS}}|i\rangle = (\hat{T}_{\mathrm{KS}} + \hat{V}_{\mathrm{KS}})|i\rangle = \varepsilon_i|i\rangle \tag{1.16}$$

defining the $\hat{H}_{\mathrm{KS}}$ Kohn–Sham Hamiltonian. This is equivalent to the

$$0 = \delta\left[\sum_i^{\mathrm{occ}}\langle i|\hat{H}_{\mathrm{KS}}|i\rangle + \sum_i^{\mathrm{occ}}\varepsilon_i\langle i|i\rangle\right] \tag{1.17}$$

variational problem if we use a zero-temperature occupation of states as the simplest case. Here, the (1.12) condition of mimicking the electronic density of the real system is included by Lagrangian multipliers.

To derive the Kohn–Sham effective potential, we take total energy into parts first.

$$\begin{aligned} E(\varrho) &= T + J(\varrho) + K + \int V_{\mathrm{ext}}\varrho \\ &= T_{\mathrm{KS}}(\varrho) + (T - T_{\mathrm{KS}}(\varrho)) + J(\varrho) + K + \int V_{\mathrm{ext}}\varrho \end{aligned} \tag{1.18}$$

where quantities written as depending on ϱ are known to be a functional of it, either in a known or a not known functional form, and K is the amount of quantum mechanical Coulomb energy deviation from the classical one (Coulombic exchange and correlational terms). Making the implicit definition of E_{xc} as 'everything else' more explicit,

$$E_{\mathrm{xc}} = E(\varrho) - J(\varrho) - T_{\mathrm{KS}}(\varrho), \tag{1.19}$$

whence it will be also evindent that E_{xc} is also a well-defined functional of ϱ.

Knowing that all relevant parts of the energy are valid functionals of ϱ, we can define the effective potential as

$$V_{\mathrm{KS}}(\mathbf{x}) = \frac{\delta}{\delta\varrho(\mathbf{x})}\left(E(\varrho) - T_{\mathrm{KS}}(\varrho)\right) = \frac{\delta J(\varrho)}{\delta\varrho(\mathbf{x})} + \frac{\delta E_{\mathrm{xc}}(\varrho)}{\delta\varrho(\mathbf{x})}. \tag{1.20}$$

The exchange-correlational part of Kohn–Sham potential is the most challenging part of the whole construction. While all the other parts are quantum-mechanically motivated and well underpinned, any computationally reasonable $V_{\mathrm{xc}}(\varrho)$ exchange-correlational potential is far from exact and physically correct. Nonetheless, approximations to it proved to be quite precise in quantum chemical calculations, although they are determined with surprisingly simple constructions. The simplest one is the local-density approximation (LDA), which formulates the exchange-correlational energy as

$$E_{\mathrm{xc}} = \int_{\mathbf{x}} \varepsilon(\varrho(\mathbf{x}))\varrho(\mathbf{x})d\mathbf{x}, \tag{1.21}$$

where $\varepsilon : \mathbb{R} \to \mathbb{R}$ is an ordinary scalar to scalar function, thus making V_{xc} a local quantity. The next sophisticated method of approximating E_{xc} is the generalized-gradient method (GGA), which uses almost the same structure,

but ε depends on not only ϱ itself, but also on some of its spatial derivatives. Since GGA's construction is able to take some nonlocality of ε and therefore V_{xc} in a differential neighbourhood of $\mathbf{x}$ into account, it is sometimes called a 'semilocal' approximation of E_{xc}. Further on this way, there are fully nonlocal approximations of exchange-correlational DFT energy available (i.e. $E_{\mathrm{xc}} = \int\int \varrho(\mathbf{x})\varepsilon(\varrho(\mathbf{x}), \varrho(\mathbf{y}))\varrho(\mathbf{y})d\mathbf{x}d\mathbf{y}$, see e.g. [38]), but they are computationally very expensive, and thus they are not that widely applied as the former two ones. Nonetheless, nonlocal xc energy kernels are promising tools to describe e.g. the van der Waals interaction, that local and semilocal xc cannot do, and this remains a strong motivation for further research on them.

In addition to the above scheme of non-locality, E_{xc} can be also calculated as a non-local quantity from the Kohn–Sham orbitals (next to kinetic energy, which is always calculated so in the leading order) as a sum of Hartree–Fock-type exchange terms. In this case, all pairwise combinations of integrals

$$\int_{\mathbf{y}} \int_{\mathbf{x}} \bar{i}(\mathbf{x}) j(\mathbf{y}) \frac{1}{|\mathbf{x}-\mathbf{y}|} i(\mathbf{y}) \bar{j}(\mathbf{x}) d\mathbf{x} d\mathbf{y} \tag{1.22}$$

are summed up with the appropriate weights to give an exchange energy. As DFT-based Kohn–Sham exchange–correlational energies and Hartree–Fock-based ones tend to generate opposite errors in energetics, they are often combined with some weighting to give a viable compromise. These blends of Kohn–Sham and Hartree–Fock exchange-correlational functionals are called hybrid xc functionals.

It can be clearly seen, that the Kohn–Sham method is not a direct density-based method as it would be imagined according to the Hohenberg–Kohn theorems. This method employs the Kohn–Sham orbitals as primary quantities to express $\varrho(\mathbf{x})$, and in addition to this, $T_{\mathrm{KS}}(\varrho)$ is also calculated from the orbitals, in an algorithmically independent calculation (hybrid xc functionals calculate even the xc energy partly with KS orbitals directly). With ϱ one can compute the effective Kohn–Sham potential more precisely, and the cycle begins with calculating new Kohn–Sham orbitals again. This algorithm renders the method an iterative self-consistent-field approximation. Nevertheless, Kohn–Sham DFT proved to be by far the most efficient way of density-based quantum-chemical calculations, when the trade-off between computational expense and precision comes into question.

As a theoretical aspect of Kohn–Sham method, one can notice that an intermediary energy term of it, the so-called Kohn–Sham energy is

$$E_{\mathrm{KS}} = \mathrm{Tr}(\hat{H}_{\mathrm{KS}}\hat{P}) = \mathrm{Tr}\left(\hat{T}_{\mathrm{KS}}\hat{P}\right) + \int_{\mathbf{x}} V_{\mathrm{KS}}(\mathbf{x})\varrho(\mathbf{x})d\mathbf{x} = \mathrm{Tr}\left(\frac{\delta E}{\delta \hat{P}}\hat{P}\right) \tag{1.23}$$

where $\hat{P}$ is the one-electron density operator of the Kohn–Sham system, and $\hat{T}_{\mathrm{KS}}$ is the Kohn–Sham kinetic energy operator. Note that the kinetic energy operator is a constant with respect to $\hat{P}$, this is why $\mathrm{Tr}\left(\hat{P}\frac{\delta}{\delta\hat{P}}\mathrm{Tr}(\hat{T}_{\mathrm{KS}}\hat{P})\right) = \mathrm{Tr}(\hat{T}_{\mathrm{KS}}\hat{P})$. This Legendre-transformation-like construction, as a thermodynamical analogy, makes going over from the external potential to the ground-state density as the basic determinative variable of the problem analogous to changing the N particle number to the

$$\mu = \frac{\partial E}{\partial N} \tag{1.24}$$

chemical potential as an independent variable in classical thermodynamics, that implies distracting an $N\frac{\partial E}{\partial N}$ term from the Helmholtz free energy to get the grand canonical potential. About this thermodynamical analogue and other aspects of this analogy (e.g. even a classical DFT method!), see [3].

The above Kohn–Sham energy is clearly different from the total energy of the interacting system because the effective Kohn–Sham potential contains energy terms arising from the electrons themselves, and therefore the $\int \varrho V_{\mathrm{KS}}$ term contains double-counting. After a Kohn–Sham calculation of orbitals, one determines the total energy by distracting these double-counting terms, resulting in

$$E = E_{\mathrm{KS}} - \frac{1}{2}\int\limits_{\mathbf{x}} \varrho(\mathbf{x})V(\mathbf{x})d\mathbf{x} - \int\limits_{\mathbf{x}} \varrho(\mathbf{x})V_{\mathrm{xc}}(\mathbf{x})d\mathbf{x} + E_{\mathrm{xc}}(\varrho). \tag{1.25}$$

1.2 DFTB, the tight-binding approximation of Kohn–Sham DFT

1.2.1 The non-self-consistent DFTB

The original, non-self-consistent-charges (non-SCC) DFTB [33] is a tight-binding DFT method to calculate electronic structures of chemical systems. It solves the (1.16) Kohn–Sham equations in an LCAO Hilbert space of wavefunctions that is spanned by the electronic orbitals of the participating atoms.

$$\hat{H}_{\mathrm{KS}} \left|i\right\rangle = [\hat{T} + \hat{V}_{\mathrm{KS}}] \left|i\right\rangle = \varepsilon_i \left|i\right\rangle \tag{1.26}$$

where the $V_{\mathrm{KS}}(\mathbf{x})$ Kohn–Sham effective potential behind the $\hat{V}_{\mathrm{KS}}$ operator is the (1.14) sum of the $V_{\mathrm{C}}(\mathbf{x})$ Coulomb potential generated by the $\varrho(\mathbf{x})$ charge density, the $V_{\mathrm{xc}}(\mathbf{x})$ functional derivative of exchange-correlation energy with respect to $\varrho(\mathbf{x})$, and the $V_{\mathrm{ext}}(\mathbf{x})$ external (non-electronic) potential of the atomic nuclei:

$$V_{\mathrm{KS}}(\mathbf{x}) = \int\limits_{\mathbf{y}} \frac{\varrho(\mathbf{y})}{|\mathbf{x}-\mathbf{y}|}d\mathbf{y} + \frac{\delta E_{\mathrm{xc}}[\varrho(\mathbf{x})]}{\delta\varrho(\mathbf{x})} + V_{\mathrm{ext}}(\mathbf{x}). \tag{1.27}$$

Expressing all the $|i\rangle$ Kohn–Sham electronic orbitals in the atomic orbital basis,

$$\left|i\right\rangle = \sum_{\phi} c_{i,\phi} \left|\phi\right\rangle \tag{1.28}$$

where $|\phi\rangle$ runs over all atomic orbitals around all atomic centres in the entire basis. The stationary Schrödinger equation in (1.26) thus numerically becomes a generalized eigenvalue problem:

$$\sum_{\chi} H_{\phi\chi}c_{i,\chi} = \varepsilon_i \sum_{\omega} S_{\phi\omega}c_{i,\omega} \tag{1.29}$$

where $H_{\phi\chi} = \langle\phi|\hat{H}_{\mathrm{KS}}|\chi\rangle$ is the Hamiltonian matrix and $S_{\phi\omega} = \langle\phi|\omega\rangle$ is the overlap matrix (the matrix of the unit operator in this basis of atomic orbitals).

Strictly speaking, the basis does not consist of *atomic*, but *pseudoatomic* [14] orbitals coming from 'pseudoatoms' with a harmonic contractive potential in addition to the Coulombic nuclear potential. This means

$$v^{(\mathrm{psat})}(r) = v^{(\mathrm{at})}(r) + \left(\frac{r}{r_0}\right)^n = -\frac{Z}{r} + \left(\frac{r}{r_0}\right)^n \tag{1.30}$$

instead of the $v^{(\mathrm{at})}(r)$ atomic Coulomb potential (note that the pseudoatomic potentials are used only at determining (pseudo)atomic quantities, like potentials and orbitals, $V_{\mathrm{ext}}(x)$ is built of atomic ones). This construction makes our atomic orbitals more compressed and thus much more apt for realistic LCAO calculations.

In order to have more degrees of freedom with tuning electronic properties, the above pseudoatomic potential can contain different compressive potentials on top of the atomic Coulomb potential within one course of atomic ab initio calculations that determine atomic densities, total atomic potentials and atomic orbitals. In most cases, the first stages (determining overall electronic density and potentials) of atomic ab initio calculations are carried out with the so-called *density compression radius* in the place of r_0, while calculation of actual electronic orbitals used later in LCAO calculations is made with the so-called *wavefunction compression radius* (denoted with r_1) in the same place. Note that the potentials calculated with the density compression radius are kept and used in the second part, thus this is a bit of inconsistency brought in to get more electronic parameters to be able to tune. Originally, the ability of having multiple compression radii was invented to cancel the possible errors of the so-called 'density superposition' construction of molecular potential (see the end of this section, after (1.36)) semiempirically, but has been being used very often deliberately as another free parameter to improve electronic properties since then. Further tunable parameters can be introduced by applying different compression radii to orbitals of different angular momenta, but this is very rare, though. The usual value of r_0 is about five times the covalent radius of the atom, while a typical r_1 is twice the covalent radius. The whole construction does not depend strongly on the value of n. This arbitrary n used to be 2 in most cases.

With the above compressed pseudoatomic orbitals, it is even possible to get good results without a self-consistent solution of equation (1.26). A Harris-functional-like [18] use of the Kohn–Sham Hamiltonian leads to fairly good energy values in one step, and thus, the non-SCC DFTB is a non-iterative DFT-based method to calculate molecular electronics and chemical energies. The total energy of the calculated chemical system is also calculated like in Kohn–Sham DFT:

$$E = \mathrm{Tr}\left[\hat{P}\left(\hat{H}_{\mathrm{KS}} - \frac{1}{2}\hat{V}_{\mathrm{C}} - \hat{V}_{\mathrm{xc}}\right)\right] + E_{\mathrm{xc}} + E_{\mathrm{nuc}} \tag{1.31}$$

where $\hat{P} = \sum_i n_i \left|i\right\rangle \left\langle i\right|$ is the density operator of the electrons, n_i being the occupation number of state $\left|i\right\rangle$, E_{xc} is the total exchange-correlational energy and

$$E_{\mathrm{nuc}} = \frac{1}{2}\sum_{A,B}^{\mathrm{nuclei}} \frac{Z_A Z_B}{r_{AB}} \tag{1.32}$$

is the energy of nuclear Coulomb repulsion.

The above total energy expression is further simplified in DFTB. First, the atomic core electrons are frozen and they are not accounted for in the quantum-mechanically calculated total electronic energy, they only affect it via the contribution of their $\hat{P}_{\mathrm{cores}}$ and $\varrho_{\mathrm{cores}}(\mathbf{x})$ density to the V_{C} and V_{xc} potentials (naturally, $\hat{P} = \hat{P}_{\mathrm{cores}} + \hat{P}_{\mathrm{valence}}$ and $\varrho = \varrho_{\mathrm{cores}} + \varrho_{\mathrm{valence}}$). Second, the energetics

of atomic cores as well as the part of (1.31) after $E_{\mathrm{KS}} = \mathrm{Tr}[\hat{P}\hat{H}_{\mathrm{KS}}]$ is not calculated with DFT methods, it is substituted with a set of pairwise effective quasiclassical potentials (the repulsive potentials) acting between atoms:

$$E_{\mathrm{rep}} = \mathrm{Tr}\left[\hat{P}_{\mathrm{valence}}\left(-\frac{1}{2}\hat{V}_{\mathrm{C}} - \hat{V}_{\mathrm{xc}}\right)\right] + \mathrm{Tr}\left[\hat{P}_{\mathrm{cores}}\left(\hat{H}_{\mathrm{KS}} - \frac{1}{2}\hat{V}_{\mathrm{C}} - \hat{V}_{\mathrm{xc}}\right)\right] + E_{\mathrm{xc}} + E_{\mathrm{nuc}} \approx \sum_{A\neq B}^{\mathrm{nuclei}} \frac{1}{2} U_{Z_A Z_B}(r_{AB}) \quad (1.33)$$

(we drop the 'valence' index in the sequel and unindexed electronic densities will denote those of the valence electrons from here on). The $U_{Z_A Z_B}(r_{AB})$ potentials which depend on the type of atom pair AB and the r_{AB} distance between them are fitted preliminarily on fit systems against ab initio or experimental energetics, in the process of parametrization.

Third, the Kohn–Sham electronic energy part of total DFTB energy is also simplified. When it is expressed with the basis wavefunctions

$$E_{\mathrm{KS}} = \mathrm{Tr}[\hat{P}\hat{H}_{\mathrm{KS}}] = \sum_i n_i \langle i|\hat{H}_{\mathrm{KS}}|i\rangle = \sum_{i,\phi,\chi} n_i \bar{c}_{i,\phi} \langle\phi|\, \hat{T} + \hat{V}_{\mathrm{KS}}\, |\chi\rangle\, c_{i,\chi}, \quad (1.34)$$

the matrix elements of Kohn–Sham potential in the sum break up to sums of three-center terms

$$\langle\phi|\hat{V}_{\mathrm{KS}}|\chi\rangle = \sum_B^{\mathrm{atoms}} \langle\phi|\, \hat{V}_B\, |\chi\rangle \quad (1.35)$$

since $\hat{V}_{\mathrm{KS}}$ can also be regarded as a sum of $\hat{V}_B$ atomic contributions[2]. From the above sum, proper three-center terms ($\langle A|B|C\rangle$-like terms, where $\phi \in \{A\}$, $\chi \in \{C\}$ i.e. ϕ and χ are centered at atoms A and C, respectively, and $A \neq B$, $B \neq C$, $C \neq A$) are dropped because they are only very small corrections to the energy, yet they are computationally expensive.

Two-center terms of the form $\langle A|B|A\rangle$ (the so-called crystal-field terms) are also neglected due to their magnitude and two further reasons. First, $\langle A|A|A\rangle$-type terms are treated in a special way: $H_{\phi\chi} = \langle\phi|\hat{T}+\hat{V}_A|\chi\rangle$ terms where $\phi, \chi \in \{A\}$ are substituted with their respective free-atom values (matrix elements of atomic potentials with atomic orbitals, $\delta_{\phi\chi}\varepsilon_\phi$ where δ is the Kronecker delta and ε is the atomic, not the pseudoatomic orbital energy) in order to recover free-atom energies in the dissociation limit. Second, crystal-field terms (just like three-center terms, if there were any) would mix valence orbitals with the frozen core electronic states [33] and make a $\varrho = \varrho_{\mathrm{cores}} + \varrho_{\mathrm{valence}}$ or $\hat{P} = \hat{P}_{\mathrm{cores}} + \hat{P}_{\mathrm{valence}}$ breakdown of density to core and valence contributions far from trivial (core states not orthogonal to valence ones would imply a pseudopotential treatment). These reasons leave no room for $\langle A|B|A\rangle$-type contributions in $\langle A|\ldots|A\rangle$.

[2]This is exactly true when the so-called potential superposition is used ($V_{\mathrm{molecular}} = \sum_A^{\mathrm{atoms}} V(\rho_A)$), but it is only 'almost true' when density superposition is used ($V_{\mathrm{molecular}} = V(\sum_A^{\mathrm{atoms}} \rho_A)$) since exchange-correlational energy expressions are not linear. In the latter case, however, the construction of pairwise potentials in (1.36) will handle the problem.

The remaining $\langle A|A|B\rangle$ and $\langle A|B|B\rangle$-type terms are calculated as $\langle A|A+B|B\rangle$ and they are calculated together with kinetic energy integrals

$$H_{\phi\chi}(r_{AB}) = \langle\phi|\,\hat{T} + \hat{V}_A + \hat{V}_B\,|\chi\rangle\,, \tag{1.36}$$

and they are tabulated as functions of atomic distances. These integral tables are used by DFTB to calculate the Kohn–Sham energy without actually calculating any integrals run-time. Building $A+B$-type Hamiltonian terms also handles the problem of density superposition (see footnote 2). In this case, $V(\rho_A+\rho_B)$ is used instead of V_A+V_B, and for the Hamiltonian matrix element in question the difference between $\langle\phi|\hat{V}(\rho_A+\rho_B)|\chi\rangle$ and $\langle\phi|\hat{V}(\sum_A^{\text{atoms}}\rho_A)|\chi\rangle$ can be approximated with the sum

$$\sum_{C\neq A, C\neq B}\int_x \frac{d}{d\rho(\mathbf{x})}\langle\phi|\,\hat{V}_{\text{xc}}(\varrho)\Big|_{\varrho=\rho_A(\mathbf{x})+\rho_B(\mathbf{x})}|\chi\rangle\rho_C(\mathbf{x})d\mathbf{x} \tag{1.37}$$

which is a sum of three-center integrals (characterized by the A, B, C atomic centres) and thus belongs to negligible order.

Shortly summarized, the following cases and types are distinguished calculating the elements of the Kohn–Sham Hamilton matrix (using the $[\phi]$ notation for the atomic centre of orbital ϕ):

$$H_{\phi\chi} = \begin{cases} \delta_{\phi\chi}\varepsilon_\phi & \text{if } [\phi]=[\chi], \\ \langle\phi|\,\hat{T}+\hat{V}_A+\hat{V}_B\,|\chi\rangle & \text{if } \phi\in\{A\} \text{ and } \chi\in\{B\}, \\ 0 & \text{otherwise.} \end{cases} \tag{1.38}$$

Thus the total non-SCC DFTB energy is a Kohn–Sham energy calculated from tabulated pairwise data perturbatively in one non-self-consistent step, with the quasi-classical repulsive energy added. Being a one-step perturbative method, it does not take the energetical effects of charge fluctuations between atoms precisely into account. This behaviour makes non-SCC DFTB reliable with chemical systems containing atoms of nearly the same electronegativity.

1.2.2 SCC-DFTB

To handle the energetics of charge fluctuations, the DFTB method was extended to an iteratively solved self-consistent DFT-like method, called SCC-DFTB [12]. The iteration is done by constructing a new Kohn–Sham Hamiltonian with the new $\varrho(\mathbf{x})$ charge density from the last step instead of the initial $\varrho^{(0)}(\mathbf{x})$ and calculating Kohn–Sham energies, LCAO Kohn–Sham electronic states as well as a more precise charge density in the next step, and so on. This iteration is made until the Kohn–Sham states converge. The actual realisation is detailed below.

We write electronic charge density as a sum $\varrho(\mathbf{x}) = \varrho^{(0)}(\mathbf{x}) + \Delta\varrho(\mathbf{x})$ of the starting charge density (the mere superposition of pseudoatomic electron densities without interatomic interactions) and the fluctuations, and likewise the density operator as $\hat{P} = \hat{P}^{(0)} + \Delta\hat{P}$.

As the charge density is in a very close linear relation with the density operator, we will take the dependence of the $\hat{H}_{\text{KS}}[\varrho(\mathbf{x})]$ Kohn–Sham Hamiltonian

on the charge density into account by expanding $\hat{H}_{\mathrm{KS}}$ as a Taylor series of the $\hat{P}$ density operator up to the first order in $\Delta\hat{P}$. Note that since

$$\hat{H}_{\mathrm{KS}} = \frac{\delta E}{\delta \hat{P}}, \tag{1.39}$$

this is equivalent to examining the second-order term in the Taylor series of E with respect to $\hat{P}$

$$\frac{\delta \hat{H}_{\mathrm{KS}}}{\delta \hat{P}} = \frac{\delta^2 E}{\delta \hat{P} \delta \hat{P}} \tag{1.40}$$

(where we silently did not define all the straightforward details about these Fréchet derivatives with respect to the valence density operator).

Since

$$E = \mathrm{Tr}\left[\hat{P}\left(\hat{T} + \frac{1}{2}\hat{V}_{\mathrm{C}}(\hat{P}) + \hat{V}_{\mathrm{ext}}\right)\right] + E_{\mathrm{xc}}(\hat{P}) + E_{\mathrm{cores}} + E_{\mathrm{nuc}} \tag{1.41}$$

(where E_{cores} is the $\mathrm{Tr}[\hat{P}_{\mathrm{cores}}\ldots]$ term in the (1.33) definition of repulsive energy), the second derivative of E with respect to $\hat{P}$ comes only from the Coulomb and the exchange-correlation energy, the other parts either do not depend on $\hat{P}$ or are only linear in it.

$$\frac{\delta^2 E}{\delta \hat{P} \delta \hat{P}} = \frac{\delta^2 E_{\mathrm{C}}}{\delta \hat{P} \delta \hat{P}} + \frac{\delta^2 E_{\mathrm{xc}}}{\delta \hat{P} \delta \hat{P}} \tag{1.42}$$

where $E_{\mathrm{C}} = \frac{1}{2}\mathrm{Tr}[\hat{P}\hat{V}_{\mathrm{C}}]$.

We investigate the Coulomb part of the above derivative first. For this, $\varrho(\mathbf{x})$, the electronic charge density can be calculated as

$$\varrho(\mathbf{x}) = -\langle \mathbf{x}| \hat{P} |\mathbf{x}\rangle \tag{1.43}$$

where $|\mathbf{x}\rangle$ is the $\mathbf{x}$ position eigenstate. Furthermore

$$\langle \mathbf{x}| \hat{P} |\mathbf{x}\rangle = \langle \mathbf{x}| \left(\sum_i n_i |i\rangle\langle i|\right) |\mathbf{x}\rangle = \sum_i n_i |i(\mathbf{x})|^2, \tag{1.44}$$

or expanding the i states according to (1.28) in the atomic orbital basis

$$\begin{aligned}\langle \mathbf{x}| \left(\sum_i n_i |i\rangle\langle i|\right) |\mathbf{x}\rangle & \\ &= \sum_{i,\phi,\psi} n_i \bar{c}_{i,\phi} c_{i,\psi} \langle \mathbf{x}|\psi\rangle\langle\phi|\mathbf{x}\rangle \\ &= \sum_{i,\phi,\psi} n_i \bar{c}_{i,\phi} c_{i,\psi} \bar{\phi}(\mathbf{x})\psi(\mathbf{x})\end{aligned} \tag{1.45}$$

where $i(\mathbf{x})$, $\phi(\mathbf{x})$ and $\psi(\mathbf{x})$ are position-space wavefunction values of the i Kohn–Sham orbital and the ϕ, ψ basis atomic orbitals, respectively.

The Coulomb potential operator $\hat{V}_C$ belonging to the $\varrho(\mathbf{x})$ charge distribution is

$$\begin{aligned}\hat{V}_C &= \int_{\mathbf{x}} V_C(\mathbf{x}) \left|\mathbf{x}\right\rangle \left\langle\mathbf{x}\right| d\mathbf{x} \\ &= \int_{\mathbf{x},\mathbf{y}} \frac{\varrho(\mathbf{y})}{|\mathbf{x}-\mathbf{y}|} \left|\mathbf{x}\right\rangle \left\langle\mathbf{x}\right| d\mathbf{y}d\mathbf{x} \\ &= -\int_{\mathbf{x},\mathbf{y}} \frac{\left\langle\mathbf{y}\right| \hat{P} \left|\mathbf{y}\right\rangle}{|\mathbf{x}-\mathbf{y}|} \left|\mathbf{x}\right\rangle \left\langle\mathbf{x}\right| d\mathbf{y}d\mathbf{x}. \quad (1.46)\end{aligned}$$

The Coulomb part of the total energy is

$$E_{\mathrm{C}} = \frac{1}{2}\mathrm{Tr}(\hat{P}\hat{V}_{\mathrm{C}}) = \frac{1}{2}\int_{\mathbf{x},\mathbf{y}} \frac{\left\langle\mathbf{y}\right| \hat{P} \left|\mathbf{y}\right\rangle \left\langle\mathbf{x}\right| \hat{P} \left|\mathbf{x}\right\rangle}{|\mathbf{x}-\mathbf{y}|} d\mathbf{x}d\mathbf{y}. \quad (1.47)$$

Using (1.45) for $\left\langle\mathbf{x}\right| \hat{P} \left|\mathbf{x}\right\rangle$ and $\left\langle\mathbf{y}\right| \hat{P} \left|\mathbf{y}\right\rangle$

$$\begin{aligned}E_{\mathrm{C}} = \frac{1}{2} \sum_{i,j,\psi,\omega,\phi,\chi} & n_i n_j \bar{c}_{j,\phi} \bar{c}_{i,\omega} c_{i,\psi} c_{j,\chi} \\ & \times \int_{\mathbf{x},\mathbf{y}} \frac{1}{|\mathbf{x}-\mathbf{y}|} \bar{\phi}(\mathbf{x}) \bar{\omega}(\mathbf{y}) \psi(\mathbf{y}) \chi(\mathbf{x}) d\mathbf{x}d\mathbf{y}. \quad (1.48)\end{aligned}$$

To step further, we rearrange the summation in (1.48):

$$\begin{aligned}E_{\mathrm{C}} = \frac{1}{2} \sum_{A,B} \sum_{\substack{i,j,\chi,\omega \\ \phi\in\{A\},\psi\in\{B\}}} & n_i n_j \bar{c}_{j,\phi} \bar{c}_{i,\omega} c_{i,\psi} c_{j,\chi} \\ & \times \int_{\mathbf{x},\mathbf{y}} \frac{1}{|\mathbf{x}-\mathbf{y}|} \bar{\phi}(\mathbf{x}) \bar{\omega}(\mathbf{y}) \psi(\mathbf{y}) \chi(\mathbf{x}) d\mathbf{x}d\mathbf{y} = \frac{1}{2}\sum_{A,B} I_{AB} \quad (1.49)\end{aligned}$$

defining the pairwise I_{AB} subsums. With different but similar rearrangements, we can also define other pairwise subsums: a constraint $\phi \in \{A\}, \omega \in \{B\}$ in the summation yields J_{AB}, $\chi \in \{A\}, \psi \in \{B\}$ yields K_{AB} and $\chi \in \{A\}, \omega \in \{B\}$ yields L_{AB}. With them

$$E_{\mathrm{C}} = \frac{1}{2}\sum_{A,B} I_{AB} = \frac{1}{2}\sum_{A,B} J_{AB} = \frac{1}{2}\sum_{A,B} K_{AB} = \frac{1}{2}\sum_{A,B} L_{AB}. \quad (1.50)$$

So

$$E_{\mathrm{C}} = \frac{1}{8}\sum_{A,B} \left\{I_{AB} + J_{AB} + K_{AB} + L_{AB}\right\}. \quad (1.51)$$

The above summation can be taken apart to an on-site and an off-site part:

$$\begin{aligned}E_{\mathrm{C}} = E_{\mathrm{C}}^{(\mathrm{on})} + E_{\mathrm{C}}^{(\mathrm{off})} = \frac{1}{8}\sum_{A} & \left\{I_{AA} + J_{AA} + K_{AA} + L_{AA}\right\} \\ & + \frac{1}{8}\sum_{A\neq B} \left\{I_{AB} + J_{AB} + K_{AB} + L_{AB}\right\}. \quad (1.52)\end{aligned}$$

Off-site SCC energy

If, as an approximation, we suppose that all wavefunctions can be regarded point-like relative to the distances of atoms, the off-site part of (1.52) goes into

$$E_{\mathrm{C}}^{(\mathrm{off})} = \frac{1}{8}\sum_{A\neq B}\left\{\sum_{\substack{i,j,\omega,\chi\\ \phi\in\{A\},\psi\in\{B\}}} n_i n_j \bar{c}_{j,\phi} c_{j,\chi} c_{i,\psi} \bar{c}_{i,\omega} \times \frac{1}{|\mathbf{x}_A - \mathbf{x}_B|} S_{\phi\chi} S_{\omega\psi} + \dots\right\} \tag{1.53}$$

where $\mathbf{x}_A$ is the position of the A^{th} atomic centre and $S_{\phi\chi}$ is the overlap matrix (the point-like limit of I_{AB} is presented in the equation, the limit of $J_{AB} + K_{AB} + L_{AB}$ is symbolised by the dots). Defining

$$q_A = -\sum_{\phi\in\{A\},\chi,i} n_i \frac{1}{2}\left(\bar{c}_{i,\phi} c_{i,\chi} S_{\phi\chi} + \bar{c}_{i,\chi} c_{i,\phi} S_{\chi\phi}\right) \tag{1.54}$$

as the Mulliken charge of atom A, the (1.53) form of off-site Coulomb energy part in this point-like approximation easily becomes

$$E_{\mathrm{C}}^{(\mathrm{off})} = \frac{1}{2}\sum_{A\neq B}\frac{q_A q_B}{r_{AB}} \tag{1.55}$$

where $r_{AB} = |\mathbf{x}_A - \mathbf{x}_B|$ is the distance between atoms A and B.

The $\frac{1}{r}$ Coulomb interaction profile of point-like charges must be modified to take into account that these charges cannot be treated point-like approaching each other at the typical molecular neighbour distances. The modified interaction profile is calculated as the interaction energy of two spherically symmetric charge clouds with $e^{-\tau_A r}$ and $e^{-\tau_B r}$ radial distributions for atoms A and B. This gives

$$E_{\mathrm{C}}^{(\mathrm{off})} = \frac{1}{2}\sum_{A\neq B}\gamma_{AB} q_A q_B \tag{1.56}$$

where

$$\gamma_{AB} = \gamma(\tau_A, \tau_B, r_{AB}) \tag{1.57}$$

and $\gamma_{AB} - \frac{1}{r_{AB}} \to 0$ with $r_{AB} \to \infty$. The actual shape of γ_{AB} at short distances is determined by the τ_A and τ_B parameters [13] that depend only on the types of atoms A and B, respectively.

On-site SCC energy

The on-site part is a bit different, as in this case the electronic orbitals cannot be treated point-like in any aspect. To understand what the on-site part is, we construct atomic Mulliken density operators first that give the foundation of the (1.54) Mulliken charges (we use them only briefly here to give an insight on the structure of the on-site energy; for more details, see 3.3.1):

$$\hat{P}_A = \frac{1}{2}\sum_{\phi\in\{A\},\chi,i} n_i \left(\bar{c}_{i,\phi} c_{i,\chi} |\chi\rangle\langle\phi| + \bar{c}_{i,\chi} c_{i,\phi} |\phi\rangle\langle\chi|\right). \tag{1.58}$$

With them,

$$q_A = -\int_{\mathbf{x}} \langle \mathbf{x}| \hat{P}_A |\mathbf{x}\rangle \, d\mathbf{x} = \int_{\mathbf{x}} \varrho_A(\mathbf{x}) d\mathbf{x} \tag{1.59}$$

$\varrho_A(\mathbf{x})$ being the atomic Mulliken charge density of the A^{th} atom (of course, $\sum_A \hat{P}_A = \hat{P}$ and $\sum_A \varrho_A = \varrho$). With these partial atomic density operators we write the on-site part

$$E_{\text{C}}^{(\text{on})} = \frac{1}{2} \sum_A \int_{\mathbf{x},\mathbf{y}} \frac{\langle \mathbf{y}| \hat{P}_A |\mathbf{y}\rangle \langle \mathbf{x}| \hat{P}_A |\mathbf{x}\rangle}{|\mathbf{x}-\mathbf{y}|} d\mathbf{x} d\mathbf{y}$$
$$= \frac{1}{2} \sum_A \int_{\mathbf{x},\mathbf{y}} \frac{\varrho_A(\mathbf{y}) \varrho_A(\mathbf{x})}{|\mathbf{x}-\mathbf{y}|} d\mathbf{x} d\mathbf{y}. \tag{1.60}$$

Thus we see that, just like the off-site part, the on-site part of Coulomb energy is quadratic in $\hat{P}_A$ or ρ_A.

The above on-site part of the Coulomb energy cannot be further simplified and an approximative formula, unlike the off-site case, cannot be derived. To circumvent this, one determines its second derivatives with respect to atomic charges semiempirically. If the energy of a lone atom A with q_A electrons is E_A, then according to Janak's theorem [19], its first derivative is

$$-\frac{\partial E_A}{\partial q_A} = \varepsilon_A \tag{1.61}$$

where ε_A is the energy of the highest occupied atomic orbit of the free atom. Furthermore,

$$\frac{\partial^2 E_A}{\partial q_A^2} = -\frac{\partial \varepsilon_A}{\partial q_A} = U_A \tag{1.62}$$

that is nothing else than the Hubbard parameter or chemical hardness of element Z_A. If we set the τ parameters in (1.57) so that

$$\gamma_{AA} = U_A, \tag{1.63}$$

the second-order change of E_{C} with respect to the electronic density can be written

$$\Delta^2 E = \frac{1}{2} \sum_{A \neq B} \gamma_{AB} \Delta q_A \Delta q_B + \frac{1}{2} \sum_A U_A \Delta q_A^2 = \frac{1}{2} \sum_{A,B} \gamma_{AB} \Delta q_A \Delta q_B. \tag{1.64}$$

Note that the above semi-empirical on-site energy derivative is based on the total energy, not only the Coulomb energy of electrons. This means that not only the second-order change of Coulomb energy in (1.60) is covered by it, but both relevant parts of (1.42) are included (Coulomb and xc). In addition to this, the analytical interpolation [13] that is realized by the γ's between the on-site chemical hardness and the long-range off-site Coulomb interaction can be regarded also as a coarse description of the gradually vanishing second-order xc energy between two neighbouring atoms.

The Hamiltonian

In addition to $\Delta^2 E$, it is also important for the DFTB machinery to construct the $\Delta\hat{H}_{\mathrm{KS}}$ SCC correction of the Hamiltonian. We will construct the Kohn–Sham Hamiltonian as the (1.39) derivative of total energy with respect to the density operator. We start with a total energy expression in the SCC fashion

$$E = \frac{1}{2}\sum_{A,B}\gamma_{AB}q_A q_B. \tag{1.65}$$

Then

$$\left(\hat{H}_{\mathrm{KS}}\right)_{\phi\chi} = \left(\frac{\delta E}{\delta \hat{P}}\right)_{\phi\chi} = \sum_{A,B}\gamma_{AB}\left(\frac{\delta q_A}{\delta \hat{P}}\right)_{\phi\chi} q_B = \sum_{A,B}\gamma_{AB}\frac{\partial q_A}{\partial P_{\chi\phi}}q_B \tag{1.66}$$

where the last step makes matrix elements of the operator derivative explicit. Since

$$P_{\chi\phi} = \sum_i n_i \bar{c}_{i,\phi} c_{i,\chi}, \tag{1.67}$$

(1.54) can be rewritten as

$$\begin{aligned} -q_A = \frac{1}{2}\sum_{\omega\in\{A\},\psi}&\left(P_{\psi\omega}S_{\omega\psi} + \bar{P}_{\psi\omega}S_{\psi\omega}\right) \\ &= \frac{1}{2}\sum_{\omega\in\{A\},\psi}\left(P_{\psi\omega}S_{\omega\psi} + P_{\omega\psi}S_{\psi\omega}\right) \end{aligned} \tag{1.68}$$

(the last equality coming from the self-adjointness of $\hat{P}$). With all this

$$-\frac{\partial q_A}{\partial P_{\chi\phi}} = \begin{cases} \frac{1}{2}S_{\phi\chi} & \text{if } \phi \in \{A\}, \\ \frac{1}{2}S_{\phi\chi} & \text{if } \chi \in \{A\}, \\ S_{\phi\chi} & \text{if } \phi,\chi \in \{A\}, \\ 0 & \text{otherwise,} \end{cases} \tag{1.69}$$

and finally

$$\left(\hat{H}_{\mathrm{KS}}\right)_{\phi\chi} = -\frac{1}{2}S_{\phi\chi}\sum_B(\gamma_{[\phi]B} + \gamma_{[\chi]B})q_B \tag{1.70}$$

where $[\phi]$ and $[\chi]$ denote the respective atomic centres of the orbitals. Because the above Hamiltonian is linear in the Mulliken charges, its change with respect to the non-interacting atoms is

$$\Delta H_{\phi\chi} = \left(\Delta\hat{H}_{\mathrm{KS}}\right)_{\phi\chi} = \frac{1}{2}S_{\phi\chi}\sum_B\left(\gamma_{[\phi]B} + \gamma_{[\chi]B}\right)\Delta q_B. \tag{1.71}$$

Refinement of the on-site SCC energy

Having only one general chemical hardness value for every atom type is quite satisfactory for electronic systems with s or s and p electrons on the valence shell because the respective second energy derivatives for those systems are quite close to each other, regardless of the s or p orbit which the electrons are fluctuating

to or from. With d orbits, however, a refinement of the above U's is necessary. If we split up atomic Mulliken charges to subshell Mulliken charges (or more exactly, if we use subshellwise $\hat{P}_l$, ϱ_l and q_l Mulliken quantities in (1.58), (1.59) and (1.60)), we arrive at calculating a Hubbard matrix

$$U_{ll'} = -\frac{\partial \varepsilon_l}{\partial q_{l'}} \tag{1.72}$$

for every atom type (atom type indices were suppressed for brevity, l and l' denote angular momenta of subshells). With the Hubbard matrix, the second-order on-site energy change for every atom can be calculated as

$$E^{(\mathrm{on})}_{\text{one atom}} = \frac{1}{2} \sum_{l,l'} \Delta q_l U_{ll'} \Delta q_{l'} \tag{1.73}$$

taking into account that electron fluctuation is not restricted to only one atomic subshell.

We are aware of only one publicly available DFTB implementation using different Hubbard parameters for different subshell interactions [2]. But even there, the off-diagonal Hubbard matrix elements are approximated with means of diagonal elements instead

$$U_{ll'} \approx \frac{U_{ll} + U_{l'l'}}{2}, \tag{1.74}$$

following the idea of Köhler et al. [24]. The simplistic, 'semidiagonal' U matrix is a good approximation for elements up to the third period, but it is significantly wrong above (subshell hardness errors going well beyond 10%, see Table 1.1) if d orbitals are present in the atomic basis. The bare magnitude of error in $U_{ll'}$ increases as one goes to the halogens within a period of the periodic table, but the importance of d orbitals decreases in parallel. The resulting overall importance of off-diagonal Hubbard matrix element errors as well as their effective importance at molecular energetics is still a question. Nevertheless, it affects the above semidiagonal Hubbard matrix, that is of great importance according to Köhler et al., e.g. with calculating magnetic properties of iron clusters.

In our treatment of SCC, we will continue using atomwise chemical hardnesses in derivations for the sake of brevity and understandability unless we especially treat refined matrices of chemical hardnesses. The results thus written can be easily extended to matrices of chemical hardnesses.

1.2.3 Further second-order semi-empirical terms

Spin-spin interaction

In the collinear spin model of spin-dependent DFTB [25], the density matrix of electrons depends on the z-aligned spin values too. Thus traces in the spatial representation are summations not only along spatial coordinates, but along spin indices too. This makes a second-order correction to energy like this:

$$\Delta^2 E = \frac{1}{2} \sum_{\alpha,\beta} \int_{\mathbf{x},\mathbf{y}} \frac{\delta^2 E}{\delta \varrho(\mathbf{x},\alpha) \delta \varrho(\mathbf{y},\beta)} \Delta\varrho(\mathbf{x},\alpha) \Delta\varrho(\mathbf{y},\beta) d\mathbf{x} d\mathbf{y} \tag{1.75}$$

Table 1.1: Subshell hardnesses calculated as approximative averages of diagonal Hubbard matrix elements in (1.74) or proper numerical derivatives according to (1.73).

atom	U_{pp}	U_{dd}	U_{pd}	$\frac{U_{\mathrm{pp}}+U_{\mathrm{dd}}}{2}$	relative error
Fe	0.237	0.447	0.303	0.280	0.084
Zn	0.266	0.523	0.345	0.317	0.091
Ga	0.277	0.577	0.365	0.326	0.119
Br	0.376	0.825	0.502	0.428	0.171

where $\varrho(\mathbf{x},\alpha) = \langle \mathbf{x},\alpha|\hat{P}|\mathbf{x},\alpha\rangle$, and $\alpha,\beta = \uparrow,\downarrow$ are spin indices (cf. this expression with $\frac{1}{2}\int \frac{\delta^2 E}{\delta\varrho(\mathbf{x})\delta\varrho(\mathbf{y})}\Delta\varrho(\mathbf{x})\Delta\varrho(\mathbf{y})d\mathbf{x}d\mathbf{y}$ of the spin-independent case). After introducing $\mu(\mathbf{x}) = \varrho(\mathbf{x},\uparrow) - \varrho(\mathbf{x},\downarrow)$, we can write the above energy correction as

$$\Delta^2 E = \frac{1}{2}\int_{\mathbf{x},\mathbf{y}} \frac{\delta^2 E}{\delta\varrho(\mathbf{x})\delta\varrho(\mathbf{y})}\Delta\varrho(\mathbf{x})\Delta\varrho(\mathbf{y}) + \frac{\delta^2 E}{\delta\varrho(\mathbf{x})\delta\mu(\mathbf{y})}\Delta\varrho(\mathbf{x})\Delta\mu(\mathbf{y}) + \frac{\delta^2 E}{\delta\mu(\mathbf{x})\delta\varrho(\mathbf{y})}\Delta\mu(\mathbf{x})\Delta\varrho(\mathbf{y}) + \frac{\delta^2 E}{\delta\mu(\mathbf{x})\delta\mu(\mathbf{y})}\Delta\mu(\mathbf{x})\Delta\mu(\mathbf{y})d\mathbf{x}d\mathbf{y} \quad (1.76)$$

through $\frac{\delta}{\delta\varrho(\mathbf{x},\uparrow)} = \frac{1}{2}\left(\frac{\delta}{\delta\varrho(\mathbf{x})} + \frac{\delta}{\delta\mu(\mathbf{x})}\right)$ and $\frac{\delta}{\delta\varrho(\mathbf{x},\downarrow)} = \frac{1}{2}\left(\frac{\delta}{\delta\varrho(\mathbf{x})} - \frac{\delta}{\delta\mu(\mathbf{x})}\right)$.

After realizing that $\frac{\delta^2 E}{\delta\mu(\mathbf{x})\delta\varrho(\mathbf{y})}$ must be zero due to symmetry reasons[3], the second-order energy correction stemming from magnetization (spin polarization) of electrons can be simplified. The second-order energy change thus becomes

$$\Delta^2 E = \frac{1}{2}\int_{\mathbf{x},\mathbf{y}} \frac{\delta^2 E}{\delta\varrho(\mathbf{x})\delta\varrho(\mathbf{y})}\Delta\varrho(\mathbf{x})\Delta\varrho(\mathbf{y}) + \frac{\delta^2 E}{\delta\mu(\mathbf{x})\delta\mu(\mathbf{y})}\Delta\mu(\mathbf{x})\Delta\mu(\mathbf{y})d\mathbf{x}d\mathbf{y} \quad (1.77)$$

in which the first term is the spin-independent second-order correction constructed with the energy derivatives in (1.42). Its reformulation within the DFTB formalism was treated in 1.2.2. The second part's simplification and inclusion into the DFTB total energy expression goes in the same way, but due to the more localized nature of spin-spin interaction, the sum of interacting spin populations is strictly restricted to on-site terms. The DFTB spin-spin term similar to (1.64) is

$$\frac{1}{2}\sum_A W_A p_A^2 \quad (1.78)$$

in a coarse atomwise approximation, and

$$\frac{1}{2}\sum_{A,l,l'} W_{A,ll'} p_{A,l} p_{A,l'} \quad (1.79)$$

in a finer, subshellwise breakdown of spin populations, where $p_A = q_{\alpha,A} - q_{\beta,A}$

[3]Because the theory is symmetric with respect to reverting the z direction, energy must be an even function of magnetization. This symmetry is easily broken spontaneously by a spin-polarized zeroth-order state of the system, however, but we do not go into details now.

and $p_{A,l} = q_{\alpha,A,l} - q_{\beta,A,l}$ are atomic and subshellwise Mulliken spin populations[4]. The W constants are the appropriate semi-empirical energy derivatives with respect to the p's (or, as an alternative approach, W's are the DFTB approximations of the spin-dependent part of two-electron integrals in a second-order expansion of total energy, just like U's follow a similar concept in the spin-independent part). The above energy expressions are parallel to the on-site part of (1.64) in the atomwise and (1.73) in the subshellwise case, respectively.

$W_{A,ll'}$ spin constants are calculated as a spin-dependent part of a perturbative response to certain electron population changes, quite similar to (1.72) with chemical hardness

$$W_{A,ll'} = \frac{1}{2}\left(\frac{\partial \varepsilon_{l,\uparrow}}{\partial n_{l'\uparrow}} - \frac{\partial \varepsilon_{l,\downarrow}}{\partial n_{l'\uparrow}}\right). \tag{1.80}$$

With the above DFTB spin-spin interaction energy, e.g. magnetization properties of iron clusters can be computed quite accurately with DFTB [21]. The need of a DFTB code calculating these magnetic properties accurately lead to a subshellwise calculation of Mulliken populations and the respective 'almost complete' subshellwise implementation of atomic hardness mentioned in 1.2.2.

The simple collinear spin model can be generalized to non-collinear spins, it involves extending wavefunctions to two-component non-relativistic spinors, and substituting (1.79) with

$$\frac{1}{2}\sum_{A,l,l'} W_{A,ll'}\mathbf{p}_{A,l}\mathbf{p}_{A,l'} \tag{1.81}$$

where 'Mulliken charges' first become 2×2 matrices with spinor indices (these come from the orbital-times-orbital part of Mulliken density operator) and a decomposition of them to a $q + p_x\sigma_x + p_y\sigma_y + p_z\sigma_z$ linear combination of Pauli matrices leads to the Mulliken charge itself along with spin populations in three spatial dimensions. For an accurate derivation see [24].

Spin-orbit coupling

In the non-collinear treatment of spin effects in the DFTB+ code [2], the spin-orbit coupling Hamiltonian can be easily written as the $\xi\hat{\mathbf{L}}\sigma$ 2×2 (spinor) matrix where $\hat{\mathbf{L}}$ is the angular momentum operator and σ is the vector of Pauli matrices. For a bit deeper insight, see also [24].

Possibly, the non-collinear spin-orbit coupling scheme can also be simplified to a collinear one by collapsing the interaction part into the z direction. This leaves

$$\sum_{\phi} \xi m_\phi q_\phi p_\phi \tag{1.82}$$

that is a straightforward realization of collinear spin-orbit coupling in the DFTB philosophy (m_ϕ is the z-direction magnetic quantum number of ϕ). Collinear spin-orbit coupling does not seem to be implemented in any DFTB code, but

[4] We use p instead of Δp as the spin population increment with respect to $p^{(0)}$ because DFTB systems used to be built of spin-unpolarized atoms as the zeroth step of calculations (this is in a strong correlation with the fact reflected in the previous footnote, that the treatment of spin-polarized zeroth-order states has a limited importance in DFTB traditionally).

it might be a good idea to try this regime as a simpler alternative to the non-collinear case.

Spin-orbit coupling constants are not calculated by atomic DFT codes related to DFTB+ in the way as Hubbard parameters or spin constants, but are imported from other calculations or estimates.

1.2.4 The current practice of parametrization

Parametrization with pair potentials

According to equation (1.33), the repulsive energy is broken down to pairwise potentials:

$$E_{\mathrm{rep}}(\{\mathbf{r}_{\mathrm{atoms}}\}) = \frac{1}{2}\sum_{A\neq B} U_{Z_A Z_B}(r_{AB}) \tag{1.83}$$

where A and B both run over the atoms in the system and $Z_A Z_B$ indicates the type of atom pair AB. Naturally, $U_{Z_A Z_B}(r) = U_{Z_B Z_A}(r)$.

The parametrization process optimizes these $U_{Z_A Z_B}(r)$ pair potentials to cover the difference between the reference energies of certain fit systems and the corresponding electronic DFTB energy. The reference energies may be taken from experimental data or *ab initio* calculations. We prefer the latter as it allows a versatile reference data generation. The best parametrization can be viewed as the one where the set of pair potentials minimizes the error:

$$R = \sum \left(E_{\mathrm{ref}} - E_{\mathrm{DFTB}}\right)^2 = \sum \left(\frac{1}{2}\sum_{A\neq B} U_{Z_A Z_B}(r_{AB}) - \left(E_{\mathrm{ref}} - E_{\mathrm{KS}}\right)\right)^2 = \min. \tag{1.84}$$

Due to the pair approximation of E_{rep} and the otherwise approximative nature of DFTB, parametrizations lack universal transferability, but as the cases of successful parametrizations show, the validity of a good parameter set can extend to a wide range of problems.

Hand-made repulsive potentials

In its usual course, parametrization for a bond type (e.g. the carbon-carbon bond) begins with stretching one bond of that kind in an appropriate molecule, as the simplest case, and creating a $U_{\mathrm{CC}}(r)$ curve based on the energy difference between the DFT reference and DFTB:

$$U_{\mathrm{CC}}(r) = E_{\mathrm{DFT}}(r) - E_{\mathrm{KS}}(r) + \mathrm{const} \tag{1.85}$$

with r being the length of the stretched bond. The constant term covers the limit of $E_{\mathrm{DFT}}(r) - E_{\mathrm{KS}}(r)$ at $r \to \infty$ (this limit contains e. g. the repulsive contributions from non-varying bonds, that may not be known in detail at all) in order to ensure a zero limit for $U_{\mathrm{CC}}(r)$, $r \to \infty$. Of course, one chooses stretched molecules so that stretching affects only one bond (or maybe several bonds, but in a totally equivalent way), all the other pairs of atoms with changing distances remain outside the ranges of their respective repulsives.

One can construct a reasonable curve for a given atom pair type by merging curve sections created for different molecules which represent different chemical

bonds between the considered elements. For example, a carbon-carbon pair potential can be constructed by taking the sections near 1.2 Å, 1.34 Å and 1.54 Å from ethyne, ethene and ethane, respectively, in order to take single, double and triple carbon bonds into account. The resulting compound curves can then be heuristically improved by comparing DFTB results on some test systems to DFT data, and fine-tuning them by hand. Unfortunately, the fine-tuning involves a tremendous amount of human work, making the fast extension of a given set or creating a new set from scratch rather difficult.

Chapter 2

Improvements to handling repulsive energy

2.1 Automatization of the parametrization process

In order to reduce the work involved in creating repulsive potentials, we propose an automatic algorithm based on least-squares fitting of repulsive potentials to reference energy values. During our early automatic fitting attempts we had begun experimenting with genetic algorithms based on the early steps of Knaup et al. [20], but the simpler least-squares fits, which were being used originally only for checking purposes, turned out to be easier to handle and far less resource-hungry while delivering results of the same or even better quality. Knowing that the human work needed for parametrization consists of not only the fitting itself, the process to be described below is not limited to the bare fitting of repulsive potentials $U_{ZZ'}(r)$. It also helps selecting and producing fit systems and fit data, tuning the priorities of different systems or properties etc., making the whole parametrization process largely automatic.

2.1.1 Least-squares fitting of repulsive potentials

In order to make a least-squares fitting for the pairwise repulsive potentials possible, we express them in terms of some arbitrary basis functions as

$$U_{ZZ'}(r_{AB}) = \sum_{\nu} \alpha_{ZZ',\nu} f_{ZZ',\nu}(r_{AB}), \tag{2.1}$$

where ZZ' is the type of atomic pair AB. Substituting this into the pair potential structure of E_{rep} from equation (1.83), the total repulsive energy for a given system becomes a linear combination

$$E_{\text{rep}} = \sum_{Z,Z',\nu} \alpha_{ZZ',\nu} X_{ZZ',\nu} \tag{2.2}$$

of the structure-dependent quantities

$$X_{ZZ',\nu} = \frac{1}{2} \sum_{\substack{Z_A Z_B = ZZ' \\ A \neq B}} f_{ZZ',\nu}(r_{AB}). \tag{2.3}$$

The sum runs over all possible atom pairs where the pair AB belongs to pair type ZZ'.

Using the above, the best $\alpha_{ZZ',\nu}$ coefficients may be easily approximated by a least-squares fit to energy values of several different distortions of a chemical system as a function of the changing X values. Due to the linearity of the energy as a function of $X_{ZZ',\nu}$'s, this fitting is a multidimensional linear regression.

Running over a sequence of distortions denoted by s of the same system (we will call this sequence a *fit path* and the distortions *fit steps*), the least-squares fit minimizes the overall error

$$\begin{aligned} R &= \sum_{s}^{\text{all steps}} \left(E_{\text{rep}}^{(s)} - (E_{\text{ref}}^{(s)} - E_{\text{KS}}^{(s)}) \right)^2 \\ &= \sum_{s}^{\text{all steps}} \left(\sum_{Z,Z',\nu} \alpha_{ZZ',\nu} X_{ZZ',\nu}^{(s)} - (E_{\text{ref}}^{(s)} - E_{\text{KS}}^{(s)}) \right)^2, \end{aligned} \tag{2.4}$$

where E_{KS} is the Kohn–Sham energy of DFTB, that is the Kohn–Sham energy of valence electrons. With expression (2.2) of the total repulsive energy, the stationary condition

$$\frac{\partial}{\partial \alpha_{ZZ',\nu}} R[\alpha_{ZZ',\nu}] = 0 \tag{2.5}$$

of the above error leads to a matrix expression of the coefficients $\alpha_{ZZ',\nu}$:

$$\mathbf{A} = \left(\mathbf{X}\mathbf{X}^{\mathsf{T}} \right)^{-1} \mathbf{X}\mathbf{E}. \tag{2.6}$$

The matrices $\mathbf{E}$, $\mathbf{X}$ and $\mathbf{A}$ are constructed from the above energies, X structural quantities and α's in the following way:

$$\mathbf{E} = \begin{pmatrix} E_{\text{ref}}^{(1)} - E_{\text{KS}}^{(1)} \\ E_{\text{ref}}^{(2)} - E_{\text{KS}}^{(2)} \\ \vdots \end{pmatrix} \tag{2.7a}$$

$$\mathbf{X} = \begin{pmatrix} X_{\text{HH},1}^{(1)} & X_{\text{HH},1}^{(2)} & \cdots \\ X_{\text{HH},2}^{(1)} & X_{\text{HH},2}^{(2)} & \cdots \\ \vdots & & \\ X_{\text{CH},1}^{(1)} & X_{\text{CH},1}^{(2)} & \cdots \\ X_{\text{CH},2}^{(1)} & \cdots\cdots\cdots & \\ \vdots & & \end{pmatrix} \tag{2.7b}$$

$$\mathbf{A} = \begin{pmatrix} \alpha_{\mathrm{HH},1} \\ \alpha_{\mathrm{HH},2} \\ \vdots \\ \alpha_{\mathrm{CH},1} \\ \alpha_{\mathrm{CH},2} \\ \vdots \end{pmatrix} \tag{2.7c}$$

where, as an example, we assumed that the enumeration of the investigated atomic pairs begins with HH and contains CH.

As an example, a fit path could be built from a propane molecule with its middle carbon atom being shifted by 40 small random displacements around its equilibrium position. Each movement as well as the original configuration is a different fit step. The energy and structure data of these 41 steps would then give enough input to fit $U_{\mathrm{CC}}(r)$ and $U_{\mathrm{CH}}(r)$[1] provided the number of independent fitting parameters $\alpha_{ZZ',\nu}$ is well below 40, i.e. in this specific case the number of basis functions used to describe one pairwise repulsive is well below 20. This criterion is normally fulfilled, but if not, increasing the amount of steps is always a straightforward remedy.

2.1.2 Fitting to multiple fit system types and objectives

An important expectation towards repulsive potentials is their transferability to a broad range of different systems. Usually this requires compromises; transferability can be reached via a trade-off between individual systems. Our automatic parametrization scheme enables the optimization of this trade-off by making the fit possible on multiple test systems (multiple fit paths) at the same time. Staying with the example of the C-C and C-H repulsive fitting, by taking several different carbohydrogen molecules and distorting them, one can generate several molecular fit paths for the fit. Additionally, taking bulk diamond (with various deformations) as an additional fit path, one can tune transferability towards the description of crystalline systems as well.

The goal of fit becomes the minimization of overall error along all fit paths, modifying (2.4) to

$$R = \sum_{p}^{\text{all paths}} \sum_{s \in p} \left(E_{\mathrm{rep}}^{(ps)} - (E_{\mathrm{ref}}^{(ps)} - E_{\mathrm{KS}}^{(ps)}) \right)^2 \tag{2.8}$$

with p enumerating the paths and E_{rep} written as a function of α's and X'es within each path in the same way as the one-path case. It should be noted here that the number of $\alpha_{ZZ',\nu}$ parameters *does not depend* on the number of fit paths (nor on the number of steps in the individual fit paths). Its value is determined only by the choice of the basis functions to describe the repulsive interactions in question.

The **E** column vector of target repulsive energies for the multiple-path fitting

[1] Displacements of a carbon atom in a carbohydrogen molecule alter the C–C and C–H bonds (but not the H–H bonds), and thus enables fitting to these repulsive potentials only.

is created by putting the $\mathbf{E}^{(p)}$ vectors for each path on the top of each other:

$$\mathbf{E} = \begin{pmatrix} \mathbf{E}^{(1)} \\ \mathbf{E}^{(2)} \\ \vdots \end{pmatrix} = \begin{pmatrix} E_{\mathrm{ref}}^{(11)} - E_{\mathrm{KS}}^{(11)} \\ E_{\mathrm{ref}}^{(12)} - E_{\mathrm{KS}}^{(12)} \\ \vdots \\ E_{\mathrm{ref}}^{(21)} - E_{\mathrm{KS}}^{(21)} \\ E_{\mathrm{ref}}^{(22)} - E_{\mathrm{KS}}^{(22)} \\ \vdots \end{pmatrix} \tag{2.9a}$$

while the geometry matrix is created by putting single-path geometry matrices together in a similar way:

$$\mathbf{X} = \left(\begin{array}{c} \mathbf{X}^{(1)} \\ \hline \mathbf{X}^{(2)} \\ \hline \vdots \end{array} \right). \tag{2.9b}$$

This all gives back matrix equation (2.6) on $\mathbf{A}$ for the multiple-path fit.

2.1.3 Fitting to objectives other than energy

The scheme proposed here is not restricted to obtain repulsive potentials by fitting to energy differences between *ab initio* DFT and DFTB calculations. One can naturally extend it to interatomic forces or even Hessians as targets. This way one gains the possibility of not just choosing the transferability range by selecting various systems for the fitting procedure, but also of being able to select the properties which are required to be transferable to the maximum possible amount over those systems. Furthermore, by using energy differences between successive steps as a target instead of the absolute energies, fitting on molecular dynamics (MD) trajectories is also made efficient. Details for these three target extensions (force, Hessian and energy difference), as well as an approximation to the Hessian fit, and fitting to the stress tensor are given in this section. Of the objectives introduced here, three, the force, energy difference and force difference objectives are fully implemented and thoroughly tested in our automaton.

Fitting to forces

The force objective from the repulsive interaction is repulsive force $\mathbf{F}_A$ acting on atom A projected onto a unit vector (a direction) $\mathbf{u}$

$$F_{A,\mathbf{u}} = \mathbf{F}_A \cdot \mathbf{u} = \sum_{B \neq A,\nu} \alpha_{Z_A Z_B,\nu} {f'}_{Z_A Z_B,\nu}(r_{AB}) \frac{\mathbf{r}_{AB}}{r_{AB}} \cdot \mathbf{u}. \tag{2.10}$$

(Note that $B \neq A$ in the summation goes over B values that do not equal to A; A is not a running index.) This can be, similarly to the energy expression (2.2), decomposed into a linear combination

$$F_{A,\mathbf{u}} = \sum_{ZZ',\nu} \alpha_{ZZ',\nu} X^{(i,\mathbf{u})}_{ZZ',\nu} \tag{2.11}$$

with coefficients $\alpha_{ZZ',\nu}$, built of geometry-dependent factors

$$X^{(A,\mathbf{u})}_{ZZ',\nu} = \sum_{\substack{Z_A Z_B = ZZ' \\ B \neq A}} {f'}_{ZZ',\nu}(r_{AB}) \frac{\mathbf{r}_{AB}}{r_{AB}} \cdot \mathbf{u} \tag{2.12}$$

containing the first derivatives of basis functions $f'_{ZZ',\nu}(r)$. Because the α coefficients in these force components are the same as the ones used for the energy fitting, fitting to energies and forces can be unified when both are required. If $(F_{\mathrm{ref}} - F_{\mathrm{KS}})_{A,\mathbf{u}}$ takes the place of $E_{\mathrm{ref}} - E_{\mathrm{KS}}$ and the above new X'es are used as independent variables, fitting to force components can be simply regarded as a set of additional new fit paths (of course, $\mathbf{F}_{\mathrm{ref}}$ and $\mathbf{F}_{\mathrm{KS}}$ are the corresponding derivatives of E_{ref} and E_{KS}). The matrices $\mathbf{E}$ and $\mathbf{X}$ can then be extended in the same way as in equation (2.9a) and (2.9b).

Fitting to MD trajectory energies

A problem that often compromises fitting to MD trajectories (or to large molecules where only a tiny part is distorted) is the fact that equilibrium bond lengths are heavily overweighted by their overwhelming presence in the sample fit paths. This can make efficient fitting to ranges of bond lengths other than the covalent equilibrium impossible with the original energy target described above.

A remedy of this problem can be found by fitting to *energy differences between subsequent fit steps* instead of energies of each fit step. As

$$\Delta E^{(s)}_{\mathrm{rep}} = E^{(s+1)}_{\mathrm{rep}} - E^{(s)}_{\mathrm{rep}} = \sum_{ZZ',\nu} \alpha_{ZZ',\nu} \left(X^{(s+1)}_{ZZ',\nu} - X^{(s)}_{ZZ',\nu} \right) \tag{2.13}$$

is a linear combination of structural quantities of type $X^{(s+1)} - X^{(s)}$, it is a valid target in our least-squares fit scheme. This modified energy target, however, contains virtually nothing arising from those bonds which do not change over the fit path, thus the overweighting of unchanged bonds is avoided. Even if the MD trajectory does not contain many fixed bonds (e.g. with fluids), the distribution of bond lengths is almost always concentrated around equilibrium values and therefore the differences in (2.13) will contain sample data from equilibrium bond lengths with a naturally very low weight. Of course, if fitting to absolute energy values at molecular equilibrium bond lengths is required, it can be brought back by an appropriate weighting between the original energy objective and the current one, or by defining additional molecular fit paths.

As an alternative use, the fit target based on energy differences can also be used in cases where retrieving force data from a DFT reference is for some reasons problematic or meaningless (e.g. with symmetric distortions of symmetric systems atomwise total forces on some symmetrically positioned atoms are constant zero). Using small distortion steps and the energy difference fit target, one automatically obtains a fit mimicking the fit on certain force or stress tensor components.

Fitting to Hessians

Similar to the forces, also the repulsive contribution to the Hessian matrix of a chemical system can be projected onto unit vectors $\mathbf{u}$ and $\mathbf{v}$ (these unit vectors can be regarded as virtual displacements of atoms). When both $\mathbf{u}$ and $\mathbf{v}$ are on the same A^{th} atom (i.e. we examine the A^{th} 'on-site' 3×3 hyperdiagonal block of the $3N \times 3N$ collective molecular Hessian),

$$\begin{aligned} H_{A,\mathbf{uv}} = \mathbf{uHv} &= \sum_{B \neq A,mn} u_m \frac{\partial^2 U_{Z_A Z_B}(r_{AB})}{\partial x_{A,m} \partial x_{A,n}} v_n \\ &= \sum_{B \neq A,mn,\nu} \alpha_{Z_A Z_B,\nu} u_m \frac{\partial^2 f_{Z_A Z_B,\nu}(r_{AB})}{\partial x_{A,m} \partial x_{A,n}} v_n \\ = \sum_{ZZ'} \sum_{\substack{Z_A Z_B = ZZ' \\ B \neq A,\nu}} \alpha_{Z_A Z_B,\nu} &\left(\frac{1}{r^2} \frac{\partial^2 f_\nu}{\partial r^2} - \frac{1}{r^3} \frac{\partial f_\nu}{\partial r} \right) (\mathbf{u} \cdot \mathbf{r})(\mathbf{v} \cdot \mathbf{r}) + \frac{1}{r} \frac{\partial f_\nu}{\partial r} (\mathbf{u} \cdot \mathbf{v}). \end{aligned} \tag{2.14}$$

(with $\mathbf{r}_{AB} = (x_{B,1} - x_{A,1}, x_{B,2} - x_{A,2}, x_{B,3} - x_{A,3})$ at the beginning and $f_\nu = f_{Z_A Z_B,\nu}(r_{AB})$, $r = r_{AB}$, $\mathbf{r} = \mathbf{r}_{AB}$ in the last step). So, with

$$X^{(A,\mathbf{uv})}_{ZZ',\nu} = \sum_{\substack{Z_A Z_B = ZZ' \\ B \neq A}} \left(\frac{1}{r^2} \frac{\partial^2 f_\nu}{\partial r^2} - \frac{1}{r^3} \frac{\partial f_\nu}{\partial r} \right) (\mathbf{u} \cdot \mathbf{r})(\mathbf{v} \cdot \mathbf{r}) + \frac{1}{r} \frac{\partial f_\nu}{\partial r} (\mathbf{u} \cdot \mathbf{v}), \tag{2.15}$$

the usual linear combinations can be written again

$$H_{A,\mathbf{uv}} = \sum_{ZZ',\nu} \alpha_{ZZ',\nu} X^{(A,\mathbf{uv})}_{ZZ',\nu}. \tag{2.16}$$

With the $\mathbf{E}$ vector composed of $(H_{\text{ref}} - H_{\text{KS}})_{A,\mathbf{uv}}$'s and the $\mathbf{X}$ matrix composed of the above X'es, the fitting of the Hessian can be included as an additional path into the fitting scheme.

When $\mathbf{u}$ and $\mathbf{v}$ are on the A^{th} and B^{th} atoms, respectively,

$$H_{AB,\mathbf{uv}} = \mathbf{uHv} = u_m \frac{\partial^2 U_{Z_A Z_B}(r_{AB})}{\partial x_{A,m} \partial x_{B,n}} v_n = -u_m \frac{\partial^2 U_{Z_A Z_B}(r_{AB})}{\partial x_{A,m} \partial x_{A,n}} v_n. \tag{2.17}$$

Therefore a similar construction applies to 'off-site' Hessian parts, but with the opposite sign and without the summation over B.

As a linear combination of the above $\mathbf{u}$ and $\mathbf{v}$ atomic virtual displacements, every collective distortion of a molecule can be constructed. This knowledge can be used to fit to Hessians of DFT reference algorithms that give no detailed Hessian matrix but only vibrational modes and frequencies in their output. If $\mathbf{e}$ is a ($3N$-component) collective eigenmode of the molecular Hessian with ω frequency,

$$\omega^2 \mathbf{Me} = \mathbf{He} = (\mathbf{H}_{\text{KS}} + \mathbf{H}_{\text{rep}})\mathbf{e} \tag{2.18}$$

where $\mathbf{M}$ is the diagonal mass matrix. The vector of equations contained in

$$\omega^2 \mathbf{Me} - \mathbf{H}_{\text{KS}}\mathbf{e} = \mathbf{H}_{\text{rep}}\mathbf{e} \tag{2.19}$$

can then be used as a new fit path with the left hand side as a vector of **E** values and the right hand side as the usual linear combinations coming from the repulsives and using α's as coefficients[2]. Note that the last equation contains explicit Hessian data from DFTB only.

Fitting to force differences as an easy approximation for certain parts of Hessian

Using differences of target quantities as new targets is also possible with repulsive forces. On the analogy of (2.13), differences of $F_{\mathrm{rep},A,\mathbf{u}} = (F_{\mathrm{ref}} - F_{\mathrm{KS}})_{A,\mathbf{u}}$ repulsive forces can be approximated by differences of right hand sides of (2.10). Thus

$$F^{(s+1)}_{\mathrm{rep},A,\mathbf{u}} - F^{(s)}_{\mathrm{rep},A,\mathbf{u}} = \sum_{ZZ',\nu} \alpha_{ZZ',\nu} \left(X^{(s+1;i,\mathbf{u})}_{ZZ',\nu} - X^{(s;i,\mathbf{u})}_{ZZ',\nu} \right) \tag{2.20}$$

defines a set of new targets for steps s and $s+1$.

The above target can be used efficiently in two ways. First, it is an easy-to-implement double (some sort of numerical derivative) of the Hessian target. With dimers, it is able even to fit vibrational frequencies practically at an arbitrary precision. Second, in certain cases it makes a fit to forces more stable when it is used along the vanilla force target.

Fitting to the stress tensor

The repulsive part of the stress tensor in periodical systems is calculated as

$$\begin{aligned} \sigma_{mn} = -\frac{1}{\tilde{V}} \frac{\partial \tilde{E}_{\mathrm{rep}}}{\partial \varepsilon_{mn}} &= \frac{1}{\tilde{V}} \sum_{\substack{A \in \text{a cell} \\ B}} F_{AB,m} r_{AB,n} \\ &= -\frac{1}{\tilde{V}} \sum_{\substack{A \in \text{a cell} \\ B}} \frac{1}{r_{AB}} \frac{\partial U(r_{AB})}{\partial r_{AB}} r_{AB,m} r_{AB,n} \\ &= -\frac{1}{\tilde{V}} \sum_{\substack{A \in \text{a cell} \\ B}} \alpha_{Z_A Z_B,\nu} f'(r_{AB}) \frac{r_{AB,m} r_{AB,n}}{r_{AB}} \end{aligned} \tag{2.21}$$

where ε_{mn} is the strain tensor, $\tilde{V}$ is the unit cell volume, $\tilde{E}_{\mathrm{rep}}$ is the cellwise repulsive energy, $r_{AB,m}$ is a component of the relative position vector $\mathbf{r}_{AB}$ from the A^{th} atom to the B^{th} and r_{AB} is the length of it. A double projection of σ_{mn} onto unit vectors **u** and **v** can be written

$$\sigma_{\mathbf{uv}} = \sum_{mn} \sigma_{mn} u_m v_n = \sum_{ZZ',\nu} \alpha_{ZZ',\nu} X^{(\mathbf{uv})}_{ZZ',\nu} \tag{2.22}$$

[2]An important issue is whether we must compare DFT-equilibrium Hessians to DFTB-equilibrium Hessians or we must compare Hessians of the very same geometry (practically the DFT equilibrium geometry, as DFT calculators tend to compute (real) eigenvalues and eigenmodes instead of outputting raw Hessian matrices). From a theoretical point of view, the latter comparison is more valid while from a semiempirical (practical) point of view, the former comparison is much more justified.

if our structural quantities are

$$X^{(\mathbf{uv})}_{ZZ',\nu} = -\frac{1}{\tilde{V}} \sum_{\substack{Z_A Z_B = ZZ' \\ A \in \text{a cell} \\ B}} f'(r_{AB}) \frac{(\mathbf{r}_{AB}\mathbf{u})(\mathbf{r}_{AB}\mathbf{v})}{r_{AB}}. \tag{2.23}$$

So with the above X'es, $\sigma_{\mathbf{uv}}$ can be another valid target of our repulsive fitting algorithm.

2.1.4 Weighting of fit targets

In the formalism described so far, every fit step contributes to the R overall error with the same weight. As this may not always be the desired behaviour, we allow each step in each path to have an individual weight for its contribution to the total error. If the fit is done for multiple physical properties (e.g. energies and forces) each property can also be weighted differently.

The weighting issues come to play mainly in two areas. First, one typically would overweight near-equilibrium geometries to assure a higher precision at near-equilibrium bond lengths at the cost of less precise description for strongly distorted geometries. Furthermore, weighting becomes a key issue when multiple physical properties are invoked into the fit, since the numerical values of the differences in the various properties (energy, force, etc.) must be converted to the same scale. This requires some experimenting but it offers the possibility of balancing the performance of repulsives for various physical quantities. For example, heavy weights for forces are usually necessary when the fitted repulsives give poor results with geometry optimization otherwise.

2.1.5 Basis function shapes

We have experimented with several different $f_\nu(r)$ basis functions for the repulsive fitting. The splines used in most of the current DFTB implementations turned out to be inappropriate for a fitting procedure as they tend to give very oscillatory behaviour. As a straightforward alternative, we decided for the (2.24) cut-off polynomials first. They were used in the earliest DFTB implementation [31] and still retain popularity with making parametrization by hand, since most of the parametrizations up to now have been able to be done with them. The zeroth and first-degree terms are omitted from such a polynomial to ensure a smooth decay at its cutoff distance r_0:

$$f_\nu(r) = \begin{cases} (r - r_0)^\nu & \text{if } r < r_0 \text{ and } \nu \geq 2, \\ 0 & \text{otherwise.} \end{cases} \tag{2.24}$$

This representation showed to be successful at the relatively easy hydrocarbon parametrization, among other examples.

To emulate spline-like behaviour in our scheme, we also tested bases containing the above cut-off polynomials, but having no universal cutoff value (these bases can be regarded as sums of multiple single-cutoff bases). Bases with two cutoff values are very efficient at improving polynomial repulsives, while more cutoff values bring up the oscillatory nature of splines. Less successful but still noteworthy examples of spline-like bases are wavelet bases, which we also

probed. It must be noted here that experiments have also begun with regularization schemes that refrain the oscillatory nature of above bases. Although these experiments have not been going for a long time so far, regularization has found another interesting usage: the level of overbinding needed may be reduced by suppressing higher than first derivatives at the 'Sprungschanze' region (see 2.3.2 and Figure 2.2), and thus making the resulting unphysical minimum in the dissociation curve (see Figure 2.3) shallower or even away.

Another important basis was the family of exponential functions. $e^{-a_\nu r^\nu}$ ($\nu = 1, 2, 3, \ldots$) and their linear combinations, which seem to be a very natural choice for a repulsive function basis. These exponential functions proved to be a successful basis for our fittings with Ti and Zn. In these cases a fairly tiny set of exponential basis functions (one to three of them) was quite enough to fit remarkably good parameter sets.

2.1.6 Further automation in the parametrization workflow

Besides the automatized fitting process itself, there are three subprocesses of the parametrization workflow in which our program substantially lowers the human contribution.

- The path building methods mentioned so far and some others are implemented to be executed automatically. They include bond stretchings, displacing atoms, uniform volume changes, linear interpolations between two configurations, and using predefined paths (e.g. MD trajectories or reaction paths).

- Instead of using fixed sets of metaparameters (input parameters determining the parametrization itself) for the fitting process, batch fits can use intervals of them, e.g. instead of setting the longest chlorine-oxygen polynomial cutoff to a fixed value of 2.5 ångströms, we can make a probe-through from 2.3 up to 2.8 by steps of 0.1 Å. Scanning over all of these values in all of these intervals in every combination spares a lot of try-and-fail cycles for the user. At the end of the batch run, the set with lowest total error on the targets (as defined in (2.8)) is picked as the fittest solution.

- A module for defining test systems is built into our program too. It tests the energetical and geometrical performance of fitted repulsives on the specified test systems. This way it can give a first-glance feedback about the performance of the fitted repulsive set on systems that were not necessarily fit systems.

2.1.7 Optimizing electronic parameters?

Batch fitting of parameters outlined in the previous section is not only able to run over large sets of metaparameters, but it is also capable of brute-force choosing from a set of different electronic parameters. This means changing electronic parameters (the pseudoatomic compression radii) defined in 1.2.1 step by step, just like metaparameters of the fitting process, and then picking the one that allowed the best fit. The best fit means the same as in the previous section: the smallest accumulated error of repulsive targets defined in (2.8).

Of course, switching electronic parameters between batch steps needs more than switching metaparameters. When electronic parameters change in the batch, a full regeneration of Slater–Koster integral tables is necessary before going on to the fitting step itself. This and the direct, batch-like probe-through algorithm of comparing different electronic parameters instead of something more sophisticated algorithm earns the 'brute-force' title for the way of electronic parameter fitting proposed here.

Up to now, very little has been produced with the above electronic parameter fitting strategy in the traditional DFTB parametrization framework. As results show so far, influence of electronic parameters on the quality of fitted repulsives is less than expected, and this is in parallel with the contemporary practice: electronic parameters are tuned almost always only to get better electronic properties, e.g. band structures of crystals resembling to reference ones, improving energetics is handled by repulsive fitting later. Three changes in the machinery can make electronic parameters more influencing, however. First, if improvements of SCC-DFTB proposed in this thesis makes DFTB so precise that differences between repulsives on top of different electronics become harsher, repulsives fitted with different electronics will become more distinguishable. Second, if the ab-initio-like calculation of (first-guess) repulsive potentials prevails (see section 2.4), electronic parameters remain the only adjustable parameters of DFTB at the first, ab-initio-like level. This will make differences in electronics more important than ever before. In the current state of this project, optimization of electronic parameters seems to play a promising role, see 2.4.3. Third, if a good method can be found to make electronic properties (band structures, etc.) of DFTB-calculated systems an objective of the fitting algorithm, the proposed brute-force electronic fitting will be able to optimize these electronic properties with choosing optimal electronic parameters.

2.2 Applications of the parametrizer

Since the molecular reference *ab initio* calculations in the hand-made sets were mostly done using the Gaussian [17] code, we also used it as a reference for molecular systems. For the periodic systems, however, we have found the Siesta [34] code far more stable (less prone to convergence failures) in our automatic fitting environment, where distorted systems far from the equilibrium must be calculated very often. Apart from stability issues, this choice is also a good cross-calculator and cross-methodology (even between different xc functionals in DFT references) consistency check of our algorithm and in general for the DFTB parametrization philosophy. As it will be seen from the results, this mixing of DFT references did not pose any problem.

The DFT calculations of the last application example, the half halogen-organic set were not made with the above ad hoc machinery, but with the NWChem [36] code, the B3LYP exchange-correlation functional and a cc-pVTZ basis. This setting was in line with the other part of the halogen-organic project, carried by other authors.

The DFTB calculations were carried out using the DFTB+ package [2].

2.2.1 Carbohydrogens

The carbohydrogen case is a relatively easy case of parametrization in the sense that quite useful parameter sets can be fitted to it even with a small effort. Fitting to DFT references with the PBE [30] exchange-correlation functional, the resulting parameter sets produce, according to our experiences, geometrical errors typically within a few 10^{-2}Å and atomization energy errors in the range of a few 10^{-2} a. u. This quality, which is almost comparable with the hand made mio set [12], is pretty easy to reach at an automatic fit with a non-trivial handful of fit systems and a couple of hours working with them.

Adding more configurations, the results can be further improved. In order to demonstrate the automatism in our procedure, we give the instructions used to generate those configurations:

- a methane molecule with its central carbon atom randomly displaced on five shells within a sphere[3] of diameter 0.75 Å;
- an ethane molecule with one carbon atom displaced on ten equidistant shells within a 0.75 Å sphere;
- a butane molecule with its 1-2 carbon-carbon bond stretched in fifteen 0.1 Å steps, from a shortening of 0.6 Å to a lengthening of 0.9 Å;
- a benzene ring with one of its carbon atoms displaced on five equidistant shells within a 0.75 Å diameter sphere;
- an ethene molecule with one carbon atom displaced on five shells in a 0.75 Å diameter sphere;
- a series of random displacements similar to the above with an ethyne molecule;
- a hydrogen molecule with its only bond shortened in eight and lengthened in twelve 0.025 Å steps;
- an isobutane molecule with its central carbon atom displaced in a 1 Å diameter sphere.

As the mio set, the basis of comparison, was fitted to calculations with the B3LYP xc functional and the 6-31G* basis, we also used this as a reference. The force objective had a weight of three while energy had a weight of one, and each path had its near-equilibrium steps (at most three steps away from equilibrium) overweighted by five. For the diamond test system we used the CRYSTAL2003 code [32] (because of the problems with Gaussian mentioned above) with a 6-21G* [11] basis set and a k-space mesh of an $8 \times 8 \times 8$ Monkhorst–Pack scheme.

During the fitting process the automaton was allowed to sweep over the following metaparameters to search for the best fit:

[3] 'Displaced on n shells in a sphere' means that the atom is dislocated with a random vector on n spherical shells around its original position; the n equidistant shells are defined within the largest sphere, from radius 0 up to the largest radius. The random vectors are generated isotropically, one with length zero, and at least four on each non-trivial shell. This way, a path with an atom jumping around n times contains at least $4n$ steps, plus one for the original configuration.

- The cutoff of C–C: 2.0 Å – 2.3 Å,
- The cutoff of C–H: 1.3 Å – 2.1 Å,
- The cutoff of H–H: 1.3 Å – 2.1 Å,
- The highest degree of polynomials: 10 – 12.

The best fit was achieved with values of 2.3 Å, 2.1 Å, 1.3 Å and 11 for the above metaparameters, respectively. For the sake of smoothness, the polynomials contained a minimal power of 4. Table 2.1 shows the performance of the resulting repulsives in comparison to the mio set (columns 'mio' and 'hom') on the respective equilibrium structures. As our method aims at not only describing equilibrium properties as close to *ab initio* results as possible, but also to provide a reasonable accuracy when dealing with structures out of equilibrium, we calculated also the energy errors over all non-equilibrium configurations in the fit paths. They remained generally within the error of several 10^{-2} hartrees compared to DFT reference except some of the extremely distorted geometries.

Table 2.1: Molecular and crystalline data calculated with the three parameter sets (the mio set [12] and the two automatically fitted ones) compared to reference values. ΔE means atomization energy error relative to the reference in kcal/mol and Z–Z' atom pairs denote distances of the appropriate neighbouring atoms in Å. The column 'hom' contains a fit without dissociation energy correction, 'inhom' contains a fit with it. Values in parentheses indicate errors for the set with dissociation energy correction when used in a DFTB implementation without this correction scheme. Italicized names denote systems that were fit systems too, the other molecules are the rest of the carbohydrogen part of the G2 [8] test set.

property	reference	mio	hom	inhom
methane				
ΔE	0	7.3	-2.5	-0.1 (52.9)
C–H	1.093	1.089	1.094	1.080
ethane				
ΔE	0	17.7	-1.0	0.1 (94.8)
C–C	1.531	1.501	1.535	1.516
C–H	1.096	1.098	1.102	1.088
ethene				
ΔE	0	14.6	-2.4	-3.6 (68.6)
C=C	1.331	1.327	1.327	1.326
C–H	1.087	1.094	1.099	1.084
ethyne				
ΔE	0	21.7	10.2	-3.5 (53.1)
C≡C	1.205	1.203	1.200	1.204
C–H	1.067	1.075	1.080	1.066
benzene				
ΔE	0	52.9	-1.7	0.8 (170.8)
C–C	1.397	1.396	1.405	1.397
C–H	1.087	1.098	1.104	1.090

butane				
ΔE	0	38.7	2.8	1.6 (179.8)
(1, 2) C–C	1.547	1.519	1.555	1.537
(2, 3) C–C	1.536	1.518	1.552	1.534
(1) C–H	1.097	1.097	1.102	1.088
isobutane				
ΔE	0	38.0	1.9	1.5 (178.7)
C–C	1.535	1.518	1.552	1.534
C–H	1.097	1.098	1.102	1.088
diamond				
C–C	1.555	1.540	1.575	1.558
cyclobutane				
ΔE	0	40.0	7.3	13.4 (169.2)
C–C	1.557	1.539	1.569	1.534
C–H	1.095	1.102	1.107	1.094
isobutene				
ΔE	0	36.2	0.5	-2.7 (153.0)
C–C	1.509	1.493	1.524	1.505
C=C	1.337	1.341	1.34	1.339
C–H (in CH_3)	1.099	1.100	1.104	1.090
C–H (in CH_2)	1.087	1.093	1.099	1.084
bicyclobutane				
ΔE	0	26.9	-2.1	10.3 (143.4)
C–C (edge)	1.510	1.464	1.549	1.486
C–C (middle)	1.900	2.003	2.112	1.980
C–H (in CH_2)	1.112	1.195	1.161	1.158
C–H (in CH)	1.095	1.066	1.021	1.065
cyclobutene				
ΔE	0	29.5	-1.8	7.4 (140.6)
C–C	1.573	1.569	1.597	1.538
C=C	1.519	1.524	1.548	1.493
C–H (in CH_2)	1.097	1.104	1.109	1.097
C–H (in CH)	1.087	1.097	1.103	1.089
cyclopropane				
ΔE	0	18.9	-9.6	-0.2 (113.8)
C–C	1.509	1.489	1.523	1.502
C–H	1.087	1.096	1.100	1.087
propane				
ΔE	0	27.7	0.2	0.0 (136.6)
C–C	1.532	1.509	1.544	1.525
C–H (end)	1.097	1.098	1.102	1.088
C–H (middle)	1.099	1.107	1.110	1.097
cyclopropene				
ΔE	0	12.2	-13.8	-7.7 (83.7)
C–C	1.508	1.495	1.528	1.508
C=C	1.295	1.319	1.319	1.318
C–H (opposite to C=C)	1.095	1.107	1.109	1.096
C–H (neighbour to C=C)	1.080	1.090	1.095	1.081

spiropentane				
ΔE	0	29.4	-18.9	-2.0 (173)
C–C ('radial')	1.485	1.479	1.508	1.488
C–C (outer)	1.530	1.508	1.547	1.524
C–H	1.088	1.097	1.102	1.088
methylene-cyclopropane				
ΔE	0	25.9	-10.6	-4.5 (128.7)
C=C	1.322	1.328	1.327	1.327
C–C ('radial')	1.470	1.465	1.491	1.472
C–C (outer)	1.540	1.512	1.551	1.529
C–H (in CH_2)	1.088	1.095	1.101	1.086
C–H (on ring)	1.089	1.098	1.102	1.089
propadiene				
ΔE	0	21.2	-2.6	-7.8 (83.6)
C=C	1.307	1.312	1.312	1.312
C–H	1.088	1.096	1.102	1.087
1,3-butadiene				
ΔE	0	49.9	16.2	10.0 (143.2)
C–C	1.439	1.436	1.457	1.441
C=C	1.392	1.372	1.373	1.370
C–H (middle)	1.089	1.098	1.103	1.089
C–H (end)	1.086	1.104	1.085	1.095
2-butyne				
ΔE	0	38.8	6.5	-1.2 (132.0)
C–C	1.462	1.455	1.477	1.461
C≡C	1.209	1.209	1.205	1.209
C–H	1.097	1.100	1.105	1.091
propyne				
ΔE	0	30.3	8.3	1.2 (92.6)
C–C	1.460	1.453	1.475	1.459
C≡C	1.207	1.206	1.203	1.207
C–H (in CH_3)	1.097	1.100	1.104	1.090
C–H (in CH)	1.066	1.074	1.079	1.066
propene				
ΔE	0	24.9	-1.5	-3.7 (110.3)
C–C	1.502	1.485	1.517	1.497
C=C	1.333	1.334	1.334	1.333
C–H (in CH_3)	1.098	1.100	1.105	1.091
C–H (in CH)	1.091	1.102	1.106	1.092
C–H (in CH_2)	1.087	1.093	1.098	1.084

Using one-body repulsive terms

With this carbohydrogen fit, we also experimented with using one-body terms in the repulsive energy

$$E_{\text{rep}}(\{R_{\text{nuclei}}\}) = \frac{1}{2}\sum_{A\neq B} U_{Z_A Z_B}(r_{AB}) + \sum_A U_{Z_A} \tag{2.25}$$

(see (2.45)). One-body terms are a special case of inhomogeneous or dissociation energy terms: they represent a fixed, geometry-independent energy part as a sum of atomwise parts, that does not come from the linear combinations of pairwise basis functions, and that remains the asymptotic value of E_{rep} at the dissociation limit. One-body energies are the only mathematically correct means of putting any correction to dissociation energy because only a sum of one-atomic dissociation energy terms behaves like an extensive quantity, i. e. is a additive function of stoichiometry. This fact strongly encourages investigating their use.

As the results in Table 2.1 illustrate (column 'inhom'), one-body terms can slightly improve geometry results via eliminating the need of trying to set absolute atomization energy levels by the pair potential profiles. The resulting one-body terms were $U_{\mathrm{C}} = 0.030633\mathrm{H}$ and $U_{\mathrm{H}} = 0.017967\mathrm{H}$ for C and H atoms, respectively. The optimal cutoff distances were (determined by a similar batch) equal to those of the homogeneous case.

To maintain compatibility with the current DFTB implementations lacking one-body repulsive parts, we also took another way of improving results by one-body terms into account. Using them only at the fitting process but dropping them after it retains improved geometries and reaction energies calculated with the produced set, yet leaves the pair potential structure of the repulsive energy built in DFTB intact (deteriorated bare atomization energy values are shown in parentheses in the appropriate column of Table 2.1).

2.2.2 Zinc-oxides

As a further demonstration for our fitting procedure, we attempted to create a parametrization for the Zn-O interaction. A high-quality and well-tested parameter set had been recently created manually for the zinc-organic chemistry by Moreira et al. [27] which should serve as an etalon for our Zn-O repulsive. For the DFT references, the same settings had been used as for the hand-made parametrization (PBE functional, double-ζ polarized basis, norm-conserving Troullier–Martins pseudopotentials, $8 \times 8 \times 8$ Monkhorst–Pack scheme for k sampling). The fit paths were made with distortions applied to the test systems (see table 2.2) in addition to Zn-Zn and Zn-O dimers with very low weights. The distortions applied to crystalline paths were uniform volume scaling and moving a Zn atom around. We show a comparison between the performance of the two Zn-O sets in 2.2. As fit targets, we used the two energy targets (energy and energy differences between steps weighted by 1:10), step weighting was by 10 and 2 in the immediate and in a wider neighbourhood of equilibria. Here, the basis of repulsives consisted of exponential functions of type $e^{-a_2 r^2}$ and $e^{-a_3 r^3}$, as these shapes offered good results quickly in situations where absolute energy targets were not heavily weighted. As it can be seen in Table 2.2, the resulting set is superior in reproducing crystalline geometries to the hand-made one.

2.2.3 Titanium-organics

Our next test of the fitting automaton was producing a titanium-oxygen set and extending it to a titanium-organic set. For this parametrization a good-quality hand-made set (tiorg) has been recently created by Dolgonos et al. [10]. We

Table 2.2: Reference data and its comparison with previous hand-made parametrization [27] ('znorg') and the automatically created one ('auto') for Zn and ZnO crystals. The values given here refer to the equilibrium structure of each system. ΔE denotes the atomization energy difference with respect to the reference in kcal/mol. Atom pairs denote distances in Å.

property	reference	znorg	auto
Zn hcp			
ΔE (per Zn_2)	0	115.5	94.1
Zn–Zn (#1)	2.523	2.796	2.433
Zn–Zn (#2)	2.886	2.864	2.931
Zn–Zn (#3)	3.831	4.051	3.788
Zn–Zn (#4)	4.591	4.872	4.524
ZnO zincblende			
ΔE (per ZnO)	0	22.3	-1.1
Zn–O	2.005	2.015	2.011
Zn–Zn	3.274	3.290	3.281
ZnO wurtzite			
ΔE (per Zn_2O_2)	0	46.5	-0.7
Zn–O	2.017	2.015	2.018
Zn–O′	2.037	2.014	2.004

used the same reference structures and ab initio reference data (various molecular systems calculated with the B3LYP functional and with mixed SDD+ basis set) augmented with crystalline reference systems. For the reference calculations of the periodic systems, the PBE functional, double-ζ plus polarized basis functions and norm-conserving Troullier–Martins pseudopotentials had been used. K-point sampling was set to an $8 \times 8 \times 8$ Monkhorst–Pack scheme with both Siesta and DFTB in this fit session.

In order to fit repulsive potentials for the Ti-Ti and Ti-O interactions, we used a fit set including a titanium dimer (with a very low weight), a TiO_2 molecule, a planar Ti_2O_2 molecule, a tribridged Ti_2O_4, the bulk hcp titanium, and the bulk anatase and rutile forms of TiO_2. The molecular fit paths were created by stretching bonds and displacing titanium atoms while the crystalline paths were created by uniformly changing the volume of the crystal lattices and by using crystals with displaced titanium atoms. We used both energy and force targets (generally weighted 1:2) in the fit.

In a fit session of a few days, we were able to produce a set of Ti-Ti and Ti-O repulsive potentials which reproduce energy and geometrical data in the same quality as the reference hand-made set. A detailed comparison is given in Table 2.3. These results were obtained using $e^{-a_1 r}$ and $e^{-a_2 r^2}$-type exponential functions as basis functions for the fit because this analytical basis gave very good results quickly with the Ti and Ti-O chemistry.

After creating the repulsives for the Ti–Ti and Ti–O interactions, we extended the set to a complete Ti-organic set, still using exponential basis functions for expressing the repulsive potentials. The extension turned out to be more difficult than expected, mainly due to the sudden cutoff in the hand-made Ti-Ti repulsive giving a very stable 3 Å Ti–Ti distance in hcp titanium, titanium nitride and titanium carbide. This feature (shown in Figure 2.1) can be

Table 2.3: Titanium-oxygen compound reference data and its comparison with previous hand-made parametrization [10] ('tiorg') and the automatically created one ('auto'). The values given here refer to the equilibrium structure of the various systems. ΔE means atomization energy difference with respect to the reference in kcal/mol. Atom pairs denote neighbour distances in Å, triples denote angles in degrees (double distance values show artificially broken symmetries of DFTB-optimized lattices). Italicized system names denote fit systems.

property	reference	tiorg	auto
TiO			
ΔE	0	55.0	40.2
Ti–O	1.586	1.592	1.586
Ti_2O_2 planar			
ΔE	0	87.7	69.4
Ti–Ti	2.198	2.355	2.092
Ti–O	1.857	1.891	1.866
Ti_2O_2 non-planar			
ΔE	0	68.0	57.6
Ti–Ti	2.127	2.249	2.133
Ti–O	1.838	1.888	1.826
Ti_2O_4 #1 (dibridged with end O atoms in cis position)			
ΔE	0	49.4	81.3
Ti–Ti	2.716	2.800	2.635
bridging Ti–O	1.848	1.887	1.812
end Ti–O	1.622	1.606	1.589
O–Ti–Ti (ending O)	126.1	124.7	123.7
Ti_2O_4 #2 (dibridged with end O atoms in trans position)			
ΔE	0	145.7	82.8
Ti–Ti	2.709	2.726	2.709
bridging Ti–O	1.840	1.831	1.806
end Ti–O	1.625	1.608	1.590
O–Ti–Ti (ending O)	123.7	122.3	122.2
Ti_2O_4 #3 (tribridged with an O atom at one end)			
ΔE	0	123.3	66.4
Ti–Ti	2.394	2.540	2.399
bridging Ti–O (opposite to end O)	1.763	1.801	1.742
end Ti–O	1.628	1.606	1.586
Ti hcp			
ΔE (per Ti)	0	-40.6	5.4
Ti–Ti	2.900	2.993	2.915
TiO_2 anatase			
ΔE (per TiO_2)	0	22.5	-4.5
shortest Ti–Ti	3.028	2.996	3.082
shortest Ti–O	1.933	1.921 1.995	1.957 1.958
TiO_2 rutile			
ΔE (per TiO_2)	0	19.4	1.1
shortest Ti–Ti	3.559	3.613	3.605
shortest Ti–O	1.974	1.914 1.992	1.976 1.995

Figure 2.1: Comparison of the tiorg (dashed) and the automatically generated (solid line) Ti-Ti repulsives in the area of the sharp cutoff of the former.

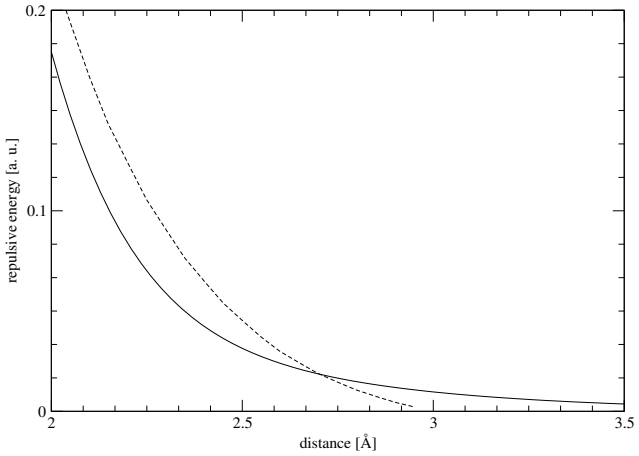

hardly reconstructed with analytical sets. Although this peculiar shape is the numerically most convenient way to confine the range of the Ti-Ti repulsive well below the second-neighbour distance as well as it gives good results for various systems, it may be an interesting question for future investigations whether it is a precise representation of the underlying physics.

Similar to the case of the titanium-oxygen fit, we used the same molecules (TiH_4, $Ti(CH_3)_4$, $Ti(NH_2)_4$) as during the hand-made parametrization [10] extended by crystalline fit systems (TiN and TiC). The fit paths were similar constructions to the titanium-oxygen case: every molecule had two fit paths with the relevant bonds stretched and the titanium atom displaced, while the crystalline systems had a volume change path and a path with a titanium atom displaced. We handled the relative difficulty of Ti-C and Ti-N fitting compared to Ti-Ti and Ti-O by lowering the relative weights of the energy targets in the Ti-C and Ti-N case. As it can be seen from the results (Table 2.4), this resulted in fairly good geometries at the expense of less accuracy in energies (one-body terms as a tool for resolving the conflict between energy and geometry accuracy were not used here).

2.2.4 Halogen-organics

The halogen-organic project part summarized here[4] includes producing *Z*–H, *Z*–N and *Z*–O repulsive potentials where *Z* means Cl, Br and I. As it was given in the introduction, the DFT reference side of these fittings use the NWChem [36]

[4] These fits, or their possible improved versions will constitute a part of a halogen-organic series of fittings that extend the mio organic set and the fluor-organic parameters included in the pbc set [22] to a complete halogen-organic set up to iodine. Production of electronic tables and the carbon-halogen and heteroatomic halogen-halogen fits are being made by Tomáš Kubar and Michael Gaus. The whole product will be published [23] and released for general use.

Table 2.4: Reference data and its comparison with previous hand-made parametrization [10] ('tiorg') and the automatically created one ('auto') for various titanium compounds. The values given here refer to the equilibrium structure of each system. ΔE denotes the atomization energy difference with respect to the reference in kcal/mol. ΔE_b indicates the binding energy between the central Ti atom and the ligands compared to the reference value in kcal/mol. Atom pairs denote neighbour distances in Å, triples denote angles in degree. Italicized system names refer to fit systems.

property	reference	tiorg	auto
Ti(CH$_3$)$_4$			
ΔE_b	0	64.6	180.2
Ti–C	2.072	2.096	2.025
Ti(CH$_3$)$_2$			
ΔE_b	0	-38.8	93.4
Ti–C	2.038	2.096	2.025
C–Ti–C	113.7	110.2	109.9
crystalline TiC			
ΔE	0	111	91.7
Ti–C	2.141	2.159	2.170
Ti–Ti	3.024	3.047	3.067
Ti(NH$_2$)$_4$			
ΔE_b	0	30.6	287.4
Ti–N	1.899	1.902	1.853
H$_3$Ti(NH$_2$)			
ΔE_b	0	12.0	76.2
Ti–N	1.846	1.898	1.837
HN=Ti=NH			
ΔE_b	0	15.5	156.1
Ti–N	1.707	1.703	1.671
N–Ti–N	114.8	114.7	113.7
crystalline TiN			
ΔE	0	196.6	192.2
Ti–N	2.094	2.159	2.115
Ti–Ti	2.958	3.043	2.982
Ti$_2$H$_2$ (dibridged planar)			
ΔE	0	123.5	131
Ti–Ti	1.985	1.967	2.011
Ti–H	1.868	1.827	1.899
Ti–H–Ti	64.2	65.2	63.9

code with the B3LYP xc functional[5] and a cc-pVTZ basis.

In order to give a novel systematic and reconstructible treatment of the problem of dissociation levels and overbindings written in 2.3.2, we use the following scheme here. A preliminarily fixed ('natural') one-body repulsive energy is calculated for every Z atom type by halving the 'binding energy' of the heavily stretched Z_2 dimer. 'Heavy stretching' means here a quasidissociated state with a distance of ten atomic covalent radii between the two atoms (and therefore its energy with respect to the two free atoms may be considered a numerical corrective term rather than a physical binding energy). As the above one-body energies would give a huge overbinding, they are reduced then to 20% of their original amount. (For the sake of preciseness, we note that the latter reduction was achieved by generating the final parameter set as a 20%–80% weighted sum of dissociation-corrected and dissociation-uncorrected sets, but a new fit with the reduced one-body terms would have resulted in roughly the same parameters.) These reduced one-body energies (see Table 2.5) provided enough overbinding to eliminate the unphysical second minima of dissociation curves (see Figure 2.3).

Table 2.5: One-body repulsives used for halogen–organics. Note that pairwise sums of them give equivalent traditional pairwise overbinding values.

atom	one-body rep [eV]	
	natural	reduced
H	0.0525	0.0105
N	1.8266	0.3653
O	2.1182	0.4236
Cl	0.8363	0.1673
Br	0.6911	0.1382
I	0.5817	0.1163

The cutoff values of polynomials building the repulsives were partly allowed to vary during fitting. The optimized values of these metaparameters are shown in Table 2.6. The quality of parameters is illustrated by tables 2.7–2.16.

[5] It would be worth investigating that fitting to a B3LYP reference is much more difficult than fitting to PBE or PBE0 (with which these fits were made more successfully, but they were rejected for a compatibility reason with mio's B3LYP reference). The most straightforward explanation is that DFTB itself uses integral tables produced with PBE, but there may or may not be other reasons in the background too. Cf. this with the similar note at the beginning of 2.2.1.

Table 2.6: Cutoff values in the repulsives (note that close multiple values come from the parts of blended parameter sets, while more distant values come from multiple-cutoff fits).

pair	cutoff(s) [Å]
Cl–H	1.9, 2.0
Cl–O	1.5, 1.95, 2.8
Cl–N	2.8
Cl–Cl	2.8
Br–H	1.9, 2.1
Br–O	1.8, 2.1, 3.0
Br–N	3.0
Br–Br	3.0
I–H	2.4
I–O	1.9, 2.0, 2.3, 3.2
I–N	3.1
I–I	3.4

Table 2.7: Results with chlorine compounds. ΔE: atomization energy in eV ($\Delta E'$: calculated with one-body terms on the DFTB side), doubles are bond lengths (distinguished with bond quality if needed) in Å, triples are angles in degrees.

property	ref.	DFTB	error	rel. error.
Cl_2				
ΔE	-2.3482	-2.6858	-0.3377	0.14379
$\Delta E'$	-2.3482	-2.3513	-0.0031	0.00134
Cl–Cl	2.02249	2.02366	0.00117	0.00058
Cl_2O				
ΔE	-4.1138	-6.9317	-2.8179	0.68500
$\Delta E'$	-4.1138	-6.1736	-2.0598	0.50071
O–Cl	1.71496	1.64923	-0.0657	-0.0383
Cl–O–Cl	112.572	113.370	0.79738	0.00708
HCl				
ΔE	-4.5256	-4.5718	-0.0462	0.01022
$\Delta E'$	-4.5256	-4.3941	0.13154	-0.0291
Cl–H	1.28337	1.28587	0.00250	0.00195
HClO				
ΔE	-7.0008	-8.7040	-1.7033	0.24330
$\Delta E'$	-7.0008	-8.1026	-1.1019	0.15739
O–Cl	1.70813	1.63403	-0.0741	-0.0434
H–O–Cl	102.955	106.920	3.96446	0.03851
$HClO_2$				
ΔE	-8.3690	-10.127	-1.7580	0.21006
$\Delta E'$	-8.3690	-9.1019	-0.7329	0.08758
Cl–O	1.72867	1.66153	-0.0671	-0.0388
Cl=O	1.52336	1.5859	0.06254	0.04105
O–Cl=O	112.334	98.5918	-13.742	-0.1223
$HClO_3$				
ΔE	-10.810	-13.217	-2.4067	0.22263
$\Delta E'$	-10.810	-11.768	-0.9580	0.08862
Cl–O	1.73379	1.75060	0.01682	0.0097
Cl=O	1.46299	1.47015	0.00716	0.00489
O–Cl=O	104.575	100.075	-4.5007	-0.0430
O=Cl=O	112.646	108.001	-4.6452	-0.0412
$HClO_4$				
ΔE	-12.761	-17.304	-4.5427	0.35599
$\Delta E'$	-12.761	-15.431	-2.6704	0.20927
Cl–O	1.68073	1.66307	-0.0177	-0.0105
Cl=O	1.43962	1.41986	-0.0198	-0.0137
O–Cl=O	100.908	104.382	3.47457	0.03443
O=Cl=O	115.073	115.582	0.50981	0.00443

Table 2.8: Results with bromine compounds. ΔE: atomization energy in eV ($\Delta E'$: calculated with one-body terms on the DFTB side), doubles are bond lengths (distinguished with bond quality if needed) in Å, triples are angles in degrees.

property	ref.	DFTB	error	rel. error.
Br_2				
ΔE	-2.1199	-2.7969	-0.6770	0.31937
$\Delta E'$	-2.1199	-2.5204	-0.4006	0.18896
Br–Br	2.31469	2.32797	0.01328	0.00574
Br_2O				
ΔE	-3.8942	-6.2094	-2.3152	0.59453
$\Delta E'$	-3.8942	-5.5093	-1.6151	0.41475
O–Br	1.85118	1.79333	-0.0578	-0.0312
Br–O–Br	114.842	115.369	0.52648	0.00458
HBr				
ΔE	-3.9826	-4.0572	-0.0746	0.01872
$\Delta E'$	-3.9826	-3.9085	0.07418	-0.0186
Br–H	1.42494	1.42620	0.00126	0.00089
HBrO				
ΔE	-6.9001	-8.3665	-1.4664	0.21252
$\Delta E'$	-6.9001	-7.7941	-0.8940	0.12957
O–Br	1.84191	1.77491	-0.067	-0.0364
H–O–Cl	103.350	106.842	3.49245	0.03379
$HBrO_2$				
ΔE	-8.4140	-9.8850	-1.4711	0.17483
$\Delta E'$	-8.4140	-8.889	-0.4750	0.05646
Br–O	1.85360	1.80672	-0.0469	-0.0253
Br=O	1.66639	1.72212	0.05572	0.03344
O–Br=O	109.957	96.5473	-13.410	-0.1220
$HBrO_3$				
ΔE	-10.938	-12.864	-1.9254	0.17603
$\Delta E'$	-10.938	-11.444	-0.5058	0.04624
Br–O	1.83944	1.86485	0.02541	0.01381
Br=O	1.61552	1.63254	0.01702	0.01053
O–Br=O	103.646	98.1828	-5.4635	-0.0527
O=Br=O	110.498	106.704	-3.7942	-0.0343
$HBrO_4$				
ΔE	-12.433	-16.220	-3.7873	0.30462
$\Delta E'$	-12.433	-14.377	-1.9440	0.15636
Br–O	1.79985	1.7691	-0.0308	-0.0171
Br=O	1.60099	1.57973	-0.0213	-0.0133
O–Br=O	100.362	103.664	3.30144	0.03290
O=Br=O	115.452	116.522	1.06988	0.00927

Table 2.9: Results with iodine compounds. ΔE: atomization energy in eV ($\Delta E'$: calculated with one-body terms on the DFTB side), doubles are bond lengths (distinguished with bond quality if needed) in Å, triples are angles in degrees.

property	ref.	DFTB	error	rel. error.
I_2				
ΔE	-1.8621	-2.4641	-0.6020	0.32331
$\Delta E'$	-1.8621	-2.2314	-0.3693	0.19834
I–I	2.70438	2.72377	0.01939	0.00717
I_2O				
ΔE	-3.8071	-5.803	-1.9959	0.52427
$\Delta E'$	-3.8071	-5.1467	-1.3396	0.35187
O–I	2.01955	1.96827	-0.0513	-0.0254
I–O–I	118.785	117.962	-0.8224	-0.0069
HI				
ΔE	-3.3792	-3.2881	0.09111	-0.0270
$\Delta E'$	-3.3792	-3.1612	0.21797	-0.0645
I–H	1.62167	1.61546	-0.0062	-0.0038
HIO				
ΔE	-6.8651	-8.2057	-1.3406	0.19528
$\Delta E'$	-6.8651	-7.6552	-0.7901	0.11509
O–I	2.01066	1.94386	-0.0668	-0.0332
H–O–I	104.630	107.344	2.71457	0.02594
HIO_2				
ΔE	-8.7164	-9.8946	-1.1782	0.13517
$\Delta E'$	-8.7164	-8.9205	-0.2041	0.02341
I–O	2.00402	1.97942	-0.0246	-0.0123
I=O	1.83408	1.89457	0.06049	0.03298
O–I=O	106.608	93.5438	-13.065	-0.1225
HIO_3				
ΔE	-11.650	-13.029	-1.3792	0.11839
$\Delta E'$	-11.650	-11.631	0.01857	-0.0016
I–O	1.97381	1.98529	0.01148	0.00581
I=O	1.78899	1.81169	0.02270	0.01269
O–I=O	102.414	95.4984	-6.9158	-0.0675
O=I=O	108.221	106.861	-1.3595	-0.0126
HIO_4				
ΔE	-13.180	-16.474	-3.2941	0.24993
$\Delta E'$	-13.180	-14.652	-1.4726	0.11173
I–O	1.94152	1.90838	-0.0331	-0.0171
I=O	1.78190	1.75823	-0.0237	-0.0133
O–I=O	99.5880	102.241	2.65285	0.02664
O=I=O	116.022	117.937	1.91501	0.01651

Table 2.10: Results with molecules containing chlorine and nitrogen. ΔE: atomization energy in eV ($\Delta E'$: calculated with one-body terms on the DFTB side), doubles are bond lengths (distinguished with bond quality if needed) in Å, triples are angles in degrees.

property	ref.	DFTB	error	rel. error.
NCl_3				
ΔE	-8.8834	-9.9016	-1.0182	0.11462
$\Delta E'$	-8.8834	-9.0345	-0.1511	0.01701
N–Cl	1.78150	1.7784	-0.0031	-0.0017
Cl–N–Cl	107.82	108.165	0.34498	0.0032
$NHCl_2$				
ΔE	-11.234	-11.890	-0.6555	0.05834
$\Delta E'$	-11.234	-11.179	0.05489	-0.0049
N–Cl	1.77056	1.76391	-0.0066	-0.0038
Cl–N–Cl	110.671	110.655	-0.0161	-0.0001
NH_2Cl				
ΔE	-13.486	-13.988	-0.5021	0.03723
$\Delta E'$	-13.486	-13.434	0.05151	-0.0038
N–Cl	1.76834	1.75424	-0.0141	-0.0080
NOCl				
ΔE	-11.168	-13.122	-1.9543	0.17499
$\Delta E'$	-11.168	-12.166	-0.9981	0.08937
N–Cl	2.00064	2.06546	0.06482	0.0324

Table 2.11: Results with molecules containing bromine and nitrogen. ΔE: atomization energy in eV ($\Delta E'$: calculated with one-body terms on the DFTB side), doubles are bond lengths (distinguished with bond quality if needed) in Å, triples are angles in degrees.

property	ref.	DFTB	error	rel. error.
NBr_3				
ΔE	-8.0083	-8.8055	-0.7972	0.09955
$\Delta E'$	-8.0083	-8.0255	-0.0172	0.00215
N–Br	1.94118	1.93520	-0.0060	-0.0031
Br–N–Br	108.829	109.159	0.33077	0.00304
$NHBr_2$				
ΔE	-10.663	-11.218	-0.5556	0.05210
$\Delta E'$	-10.663	-10.566	0.09672	-0.0091
N–Br	1.92381	1.91180	-0.0120	-0.0062
Br–N–Br	112.141	112.255	0.11468	0.00102
NH_2Br				
ΔE	-13.218	-13.680	-0.4625	0.03499
$\Delta E'$	-13.218	-13.155	0.06208	-0.0047
N–Br	1.91561	1.89528	-0.0203	-0.0106
NOBr				
ΔE	-10.871	-12.873	-2.0020	0.18416
$\Delta E'$	-10.871	-11.946	-1.0748	0.09887
N–Br	2.15763	2.16755	0.00991	0.00459

Table 2.12: Results with molecules containing iodine and nitrogen. ΔE: atomization energy in eV ($\Delta E'$: calculated with one-body terms on the DFTB side), doubles are bond lengths (distinguished with bond quality if needed) in Å, triples are angles in degrees.

property	ref.	DFTB	error	rel. error.
NI_3				
ΔE	-7.1962	-7.9194	-0.7233	0.10050
$\Delta E'$	-7.1962	-7.2051	-0.0089	0.00123
N–I	2.13754	2.12806	-0.0095	-0.0044
I–N–I	110.727	110.914	0.18694	0.00169
NHI_2				
ΔE	-10.124	-10.714	-0.5891	0.05819
$\Delta E'$	-10.124	-10.105	0.01945	-0.0019
N–I	2.11405	2.09227	-0.0218	-0.0103
I–N–I	114.775	115.006	0.23122	0.00201
NH_2I				
ΔE	-12.958	-13.463	-0.5052	0.03899
$\Delta E'$	-12.958	-12.960	-0.0025	0.00019
N–I	2.09975	2.06760	-0.0321	-0.0153
NOI				
ΔE	-10.487	-12.566	-2.0789	0.19823
$\Delta E'$	-10.487	-11.661	-1.1736	0.11191
N–I	2.36624	2.36639	0.00015	6.2E-05

Table 2.13: Results with chlorine compound ions. ΔE: atomization energy in eV ($\Delta E'$: calculated with one-body terms on the DFTB side), doubles are bond lengths (distinguished with bond quality if needed) in Å, triples are angles in degrees.

property	ref.	DFTB	error	rel. error.
ClO_3^-				
ΔE	-10.083	-11.589	-1.5062	0.14938
$\Delta E'$	-10.083	-10.151	-0.0680	0.00674
Cl–O	1.51392	1.57624	0.06232	0.04117
O–Cl–O	108.094	108.355	0.26105	0.00242
ClO_4^-				
ΔE	-12.907	-17.487	-4.5805	0.35489
$\Delta E'$	-12.907	-15.625	-2.7187	0.21064
Cl–O	1.47527	1.45669	-0.0186	-0.0126
ClO^-				
ΔE	-4.5841	-5.4154	-0.8313	0.18133
$\Delta E'$	-4.5841	-4.8245	-0.2404	0.05244
Cl–O	1.72102	1.73016	0.00914	0.00531
ClO_2^-				
ΔE	-6.7945	-7.9260	-1.1316	0.16654
$\Delta E'$	-6.7945	-6.9115	-0.1171	0.01723
Cl–O	1.59790	1.66100	0.06310	0.03949
O–Cl–O	115.070	114.049	-1.0205	-0.0089

Table 2.14: Results with bromine compound ions. ΔE: atomization energy in eV ($\Delta E'$: calculated with one-body terms on the DFTB side), doubles are bond lengths (distinguished with bond quality if needed) in Å, triples are angles in degrees.

property	ref.	DFTB	error	rel. error.
BrO^-				
ΔE	-4.5172	-5.0072	-0.4900	0.10848
$\Delta E'$	-4.5172	-4.4454	0.07185	-0.0159
Br–O	1.83584	1.89874	0.0629	0.03426
BrO_2^-				
ΔE	-6.7873	-7.4236	-0.6363	0.09374
$\Delta E'$	-6.7873	-6.4381	0.34923	-0.0515
Br–O	1.73371	1.80432	0.07061	0.04072
O–Br–O	113.866	114.923	1.05687	0.00928
BrO_3^-				
ΔE	-10.199	-11.000	-0.8003	0.07846
$\Delta E'$	-10.199	-9.5905	0.60886	-0.0597
Br–O	1.65927	1.72552	0.06625	0.03993
O–Br–O	107.415	107.868	0.45317	0.00422
BrO_4^-				
ΔE	-12.740	-16.136	-3.3960	0.26657
$\Delta E'$	-12.740	-14.303	-1.5633	0.12271
Br–O	1.62869	1.61748	-0.0112	-0.0069

Table 2.15: Results with iodine compound ions. ΔE: atomization energy in eV ($\Delta E'$: calculated with one-body terms on the DFTB side), doubles are bond lengths (distinguished with bond quality if needed) in Å, triples are angles in degrees.

property	ref.	DFTB	error	rel. error.
IO^-				
ΔE	-4.4664	-4.6689	-0.2025	0.04533
$\Delta E'$	-4.4664	-4.1289	0.33751	-0.0756
I–O	1.97194	2.07088	0.09893	0.05017
IO_2^-				
ΔE	-6.9908	-7.0284	-0.0376	0.00538
$\Delta E'$	-6.9908	-6.0648	0.92603	-0.1325
I–O	1.89059	1.98852	0.09793	0.05180
O–I–O	111.287	115.971	4.68429	0.04209
IO_3^-				
ΔE	-10.785	-10.701	0.08433	-0.0078
$\Delta E'$	-10.785	-9.3134	1.47159	-0.1364
I–O	1.82580	1.90422	0.07842	0.04295
O–I–O	106.672	107.914	1.24267	0.01165
IO_4^-				
ΔE	-13.450	-15.839	-2.3891	0.17763
$\Delta E'$	-13.450	-14.028	-0.5782	0.04299
I–O	1.80423	1.79588	-0.0084	-0.0046
O–I–O	109.471	109.472	0.00114	0.00001

Table 2.16: Vibrational modes of molecules calculated with the reference method and the new parameters (frequencies in cm^{-1}). Data in parentheses are experimental values from [1].

molecule	ref.	DFTB
Cl_2	539.8	547.6
HCl	2945.5	2929.6
HClO	3774.4	3665.3
	1267.8	1364.6
	740.8	1038.4
$HClO_4$	3710.9	3649.5
	1297.2	1350.0
	1211.6	1334.3
	1184.5	1175.2
	1003.9	1107.4
	692.8	771.2
	550.9	526.0
	544.4	524.6
	520.6	496.9
	395.5	394.7
	387.6	363.2
	169.1	96.2
NCl_3	614.0	757.1
	614.0	744.3
	547.5	633.7
	349.6	383.6
	252.6	289.2
	252.6	280.6

molecule	ref.	DFTB
Br_2	469.4 (325.3)	298.3
HBr	2330.0 (2649.0)	2615.6
HBrO	3812.7	3690.7
	1614.4	1282.1
	743.5	898.8
$HBrO_4$	3724.8	3683.3
	1241.8	1092.9
	1030.4	1045.3
	1022.2	1033.4
	895.0	964.4
	678.1	708.4
	488.8	366.8
	471.8	361.5
	404.2	343.9
	305.0	292.3
	302.9	272.5
	212.4	101.7
NBr_3	516.0	667.8
	516.0	652.8
	418.0	493.3
	139.1	240.7
	–	170.9
	–	166.4

molecule	ref.	DFTB
I_2	218.1	202.4
HI	2314.5	2287.6
HIO	3803.2	3715.5
	1135.7	1203.7
	591.6	774.7
HIO_4	3732.9	3737.5
	1039.8	1041.0
	886.1	930.7
	881.0	917.2
	825.6	873.4
	607.2	633.3
	288.2	285.5
	287.9	275.3
	270.1	253.0
	240.3	217.5
	229.7	198.6
	–	114.9
NI_3	511.3	620.0
	511.3	613.7
	360.2	395.0
	156.2	179.3
	104.7	122.3
	104.7	118.6

2.3 Some theoretical aspects of parametrization

2.3.1 On the theoretical validity of parametrization

The representation of E_{rep} in (1.33) as a sum of quasiclassical multibody potentials is not only a matter of convenience. Its validity is strictly underpinned by the fact that E_{rep} does not depend on molecular charge fluctuations in the leading order. This means that E_{rep} is a functional of the superposed $\varrho^{(0)}$ electronic density of atoms (or the corresponding $\hat{P}^{(0)}$ density operator) up to a satisfactory precision, therefore the repulsive energy of a certain chemical system is influenced by only its geometry (i.e. how $\varrho^{(0)}$ is composed from atomic densities), not its particular electronic state. This enables using transferable quasiclassical repulsive potentials.

$E_{\mathbf{rep}}(\hat{P})$ in general. Generally, the E total energy of a chemical system can be approximated with its Taylor expansion by $\hat{P}$, which we investigate here up to the second order:

$$E = E^{(0)} + \mathrm{Tr}\left[\Delta\mathbf{P}\left.\frac{\delta E}{\delta\mathbf{P}}\right|_0\right] + \frac{1}{2}\mathrm{Tr}\left[\Delta\mathbf{P}\left.\frac{\delta^2 E}{\delta\mathbf{P}^2}\right|_0\Delta\mathbf{P}\right]. \tag{2.26}$$

The Kohn–Sham energy of the same system[6] in DFT is then given by

$$E_{\text{KS}} = \mathrm{Tr}\left[\mathbf{P}\frac{\delta E}{\delta\mathbf{P}}\right]. \tag{2.27}$$

In the first-order machinery of non-SCC DFTB, the above Kohn–Sham energy is approximated by

$$\begin{aligned} E^{(1)}_{\text{KS}} = \mathrm{Tr}[\hat{P^{(1)}}\hat{H}^{(0)}_{\text{KS}}] &= \mathrm{Tr}\left[(\mathbf{P}^{(0)} + \Delta\mathbf{P})\left.\frac{\delta E}{\delta\mathbf{P}}\right|_0\right] \\ &= \mathrm{Tr}\left[\mathbf{P}^{(0)}\left.\frac{\delta E}{\delta\mathbf{P}}\right|_0\right] + \mathrm{Tr}\left[\Delta\mathbf{P}\left.\frac{\delta E}{\delta\mathbf{P}}\right|_0\right], \end{aligned} \tag{2.28}$$

and this is supplemented by the repulsive energy to give $E = E^{(1)}_{\text{KS}} + E_{\text{rep}}$. Finally

$$E^{(1)}_{\text{rep}} = E^{(0)} - \mathrm{Tr}\left[\mathbf{P}^{(0)}\left.\frac{\delta E}{\delta\mathbf{P}}\right|_0\right] + \frac{1}{2}\mathrm{Tr}\left[\Delta\mathbf{P}\left.\frac{\delta^2 E}{\delta\mathbf{P}^2}\right|_0\Delta\mathbf{P}\right]. \tag{2.29}$$

Clearly, regardless of any further detail on the structure of E, we can state that in first-order DFTB the repulsive energy does not depend on $\hat{P}$ in the first order. (This follows from the fact that E_{rep} is the Legendre transform of E with respect to $\hat{P}$, this is a direct consequence of (1.23))

[6] In this section, a thorough treatment of energetics would handle the fact that DFTB Kohn–Sham energy belongs to the valence electrons only, but since core electrons are frozen, their energetics is *always* depending on $\varrho^{(0)}_{\text{cores}}$ only. This makes a precise treatment of core electrons unnecessary here.

In the second-order regime of SCC-DFTB, a theoretical, completely consistent Kohn–Sham treatment would imply a refinement of (2.28) to

$$\begin{aligned} E^{(2)}_{\mathrm{KS}} &= \mathrm{Tr}\left[(\mathbf{P}^{(0)}+\Delta\mathbf{P})\left(\left.\frac{\delta E}{\delta\mathbf{P}}\right|_0+\left.\frac{\delta^2 E}{\delta\mathbf{P}^2}\right|_0\Delta\mathbf{P}\right)\right] \\ &= \mathrm{Tr}\left[\mathbf{P}^{(0)}\left.\frac{\delta E}{\delta\mathbf{P}}\right|_0\right]+\mathrm{Tr}\left[\Delta\mathbf{P}\left.\frac{\delta E}{\delta\mathbf{P}}\right|_0\right] \\ &\quad+\mathrm{Tr}\left[\mathbf{P}^{(0)}\left.\frac{\delta^2 E}{\delta\mathbf{P}^2}\right|_0\Delta\mathbf{P}\right]+\mathrm{Tr}\left[\Delta\mathbf{P}\left.\frac{\delta^2 E}{\delta\mathbf{P}^2}\right|_0\Delta\mathbf{P}\right] \end{aligned} \tag{2.30}$$

by the (1.34) definition of the Kohn–Sham energy. The repulsive energy in this case would be

$$\begin{aligned} E^{(2)}_{\mathrm{rep}} &= E-E^{(2)}_{\mathrm{KS}} \\ &= E^{(0)}-\mathrm{Tr}\left[\mathbf{P}^{(0)}\left.\frac{\delta E}{\delta\mathbf{P}}\right|_0\right]-\mathrm{Tr}\left[\mathbf{P}^{(0)}\left.\frac{\delta^2 E}{\delta\mathbf{P}^2}\right|_0\Delta\mathbf{P}\right]-\frac{1}{2}\mathrm{Tr}\left[\Delta\mathbf{P}\left.\frac{\delta^2 E}{\delta\mathbf{P}^2}\right|_0\Delta\mathbf{P}\right], \end{aligned} \tag{2.31}$$

which is clearly not independent of $\Delta\hat{P}$ in the relevant (second) order. However, in SCC-DFTB this second-order Kohn–Sham energy expression is not used. One uses the

$$\hat{H}_{\mathrm{KS}}=\left.\frac{\delta E}{\delta\mathbf{P}}\right|_0+\left.\frac{\delta^2 E}{\delta\mathbf{P}^2}\right|_0\Delta\mathbf{P} \tag{2.32}$$

Kohn–Sham Hamiltonian to calculate electronic states, but total energy is calculated as its first-order DFTB approximation plus the second-order term in its Taylor series:

$$E^{(2)}=E^{(1)}_{\mathrm{KS}}+E_{\mathrm{rep}}+\frac{1}{2}\mathrm{Tr}\left[\Delta\mathbf{P}\left.\frac{\delta^2 E}{\delta\mathbf{P}^2}\right|_0\Delta\mathbf{P}\right]. \tag{2.33}$$

This construction propagates the usage of charge-fluctuation-independent first-order repulsive potentials into SCC-DFTB. Furthermore, if we take a closer look at what E_{rep} in SCC-DFTB is

$$E^{(2)}_{\mathrm{rep}}=E-E^{(1)}_{\mathrm{KS}}-\frac{1}{2}\mathrm{Tr}\left[\Delta\mathbf{P}\left.\frac{\delta^2 E}{\delta\mathbf{P}^2}\right|_0\Delta\mathbf{P}\right]=\mathrm{Tr}\left[\mathbf{P}^{(0)}\left.\frac{\delta E}{\delta\mathbf{P}}\right|_0\right], \tag{2.34}$$

we notice that the repulsive potential of SCC-DFTB is independent of $\Delta\hat{P}$ up to the second order.

In the following, we calculate the repulsive energy part in detail when the total energy is of the well-known structure: $E=E_{\mathrm{C}}+E_{\mathrm{xc}}$, the sum of Coulomb and xc energy (we omit kinetic energy and energy from external potential as they are trivial cases here, e.g. $\mathrm{Tr}\left(\hat{P}\frac{\delta T}{\delta\hat{P}}\right)=T$). Instead of the density-operator formalism, we use $\varrho(\mathbf{x})=\langle\mathbf{x}|\hat{P}|\mathbf{x}\rangle$ as the basic variable.[7]

[7] The transition from density operator formalism to spatial charge density formalism is simply writing the traces in the spatial representation. Thus $\mathrm{Tr}[\hat{P}\hat{A}]$ for a general $\hat{A}$ operator will be $\int\langle\mathbf{x}|\hat{P}|\mathbf{y}\rangle\langle\mathbf{y}|\hat{A}|\mathbf{x}\rangle d\mathbf{x}$, and in the case of a local $\hat{A}$, it is $\int\langle\mathbf{x}|\hat{P}|\mathbf{x}\rangle\langle\mathbf{x}|\hat{A}|\mathbf{x}\rangle d\mathbf{x}=\int\mathbf{x}\varrho(\mathbf{x})\langle\mathbf{x}|\hat{A}|\mathbf{x}\rangle d\mathbf{x}$.

The Coulomb part of total energy is

$$\begin{aligned} E_{\mathrm{C}} &= \frac{1}{2}\int (\varrho(\mathbf{x})V_{\mathrm{C}}(\mathbf{x}))d\mathbf{x} \\ &= \frac{1}{2}\int \varrho^{(0)}(\mathbf{x})V_{\mathrm{C}}^{(0)}(\mathbf{x})d\mathbf{x} + \frac{1}{2}\int \varrho^{(0)}(\mathbf{x})\Delta V_{\mathrm{C}}(\mathbf{x})d\mathbf{x} \\ &\quad + \frac{1}{2}\int \Delta\varrho(\mathbf{x})V_{\mathrm{C}}^{(0)}(\mathbf{x})d\mathbf{x} + \frac{1}{2}\int \Delta\varrho(\mathbf{x})\Delta V_{\mathrm{C}}(\mathbf{x})d\mathbf{x}, \end{aligned} \quad (2.35)$$

if we expand charge density in the first order as $\varrho = \varrho^{(0)} + \Delta\varrho$. Also using that the Coulomb potential itself is a linear function of charge density (i.e. the total Coulomb energy is quadratic in ϱ), we get that

$$\int \varrho^{(0)}(\mathbf{x})\Delta V_{\mathrm{C}}(\mathbf{x})d\mathbf{x} = \int \Delta\varrho(\mathbf{x})V_{\mathrm{C}}^{(0)}(\mathbf{x})d\mathbf{x} \quad (2.36)$$

and therefore

$$E_{\mathrm{C}} = \frac{1}{2}\int \varrho^{(0)}(\mathbf{x})V_{\mathrm{C}}^{(0)}(\mathbf{x})d\mathbf{x} + \int \Delta\varrho(\mathbf{x})V_{\mathrm{C}}^{(0)}(\mathbf{x})d\mathbf{x} + \frac{1}{2}\int \Delta\varrho(\mathbf{x})\Delta V_{\mathrm{C}}(\mathbf{x})d\mathbf{x}. \quad (2.37)$$

Then the Coulomb part of $E_{\mathrm{KS}}^{(1)}$ is

$$E_{\mathrm{KS,C}}^{(1)} = \int \varrho(\mathbf{x})\left.\frac{\delta E_{\mathrm{C}}}{\delta\varrho(\mathbf{x})}\right|_0 d\mathbf{x} = \int (\varrho^{(0)}(\mathbf{x}) + \Delta\varrho(\mathbf{x}))V_{\mathrm{C}}^{(0)}(\mathbf{x})d\mathbf{x}. \quad (2.38)$$

It implies a repulsive energy of the form

$$\begin{aligned} E_{\mathrm{rep,C}}^{(1)} &= E_{\mathrm{C}} - E_{\mathrm{KS,C}}^{(1)} \\ &= -\frac{1}{2}\int \varrho^{(0)}(\mathbf{x})V_{\mathrm{C}}^{(0)}(\mathbf{x})d\mathbf{x} + \int\int \Delta\varrho(\mathbf{x})\frac{1}{|\mathbf{x}-\mathbf{y}|}\Delta\varrho(\mathbf{y})d\mathbf{x}d\mathbf{y}, \end{aligned} \quad (2.39)$$

which is a functional of $\Delta\varrho$ only in the second order in the non-SCC case. In the SCC case, the second-order part is also dropped from the repulsive energy part.

The exchange-correlation energy part of total energy in the LDA DFT approximation in the same system is

$$\begin{aligned} E_{\mathrm{xc}} &= \int_x \varrho(x)\varepsilon(\varrho(x))dx \\ &= \int_x \varrho^{(0)}\varepsilon^{(0)} + \Delta\varrho\varepsilon^{(0)} + \varrho^{(0)}\left.\frac{d\varepsilon}{d\varrho}\right|_0 \Delta\varrho + \Delta\varrho\left.\frac{d\varepsilon}{d\varrho}\right|_0 \Delta\varrho + \varrho^{(0)}\Delta\varrho\frac{1}{2}\left.\frac{d^2\varepsilon}{d\varrho^2}\right|_0 \Delta\varrho dx, \end{aligned} \quad (2.40)$$

where $\varepsilon^{(0)} = \varepsilon(\varrho^{(0)})$. In the above mentioned LDA case, $\frac{d\varepsilon}{d\varrho} = \frac{\partial\varepsilon}{\partial\varrho}$. In a semilocal GGA case of xc functional, the part denoted by $\frac{d\varepsilon}{d\varrho}$ (a part of the $\frac{\delta E_{\mathrm{xc}}}{\delta\hat{P}}$ operator derivative) is a differential operator in this integral representation.

The xc part of first-order DFTB Kohn–Sham energy is

$$\begin{aligned} E^{(1)}_{\mathrm{KS,xc}} &= \int \varrho(\mathbf{x}) \left.\frac{\delta E_{\mathrm{xc}}}{\delta\varrho(\mathbf{x})}\right|_0 d\mathbf{x} = \int (\varrho^{(0)}(\mathbf{x}) + \Delta\varrho(\mathbf{x}))V^{(0)}_{\mathrm{xc}}(\mathbf{x})d\mathbf{x} \\ &= \int \varrho^{(0)}(\mathbf{x}) \left.\frac{\delta E_{\mathrm{xc}}}{\delta\varrho(\mathbf{x})}\right|_0 d\mathbf{x} + \int \Delta\varrho(\mathbf{x}) \left.\frac{\delta E_{\mathrm{xc}}}{\delta\varrho(\mathbf{x})}\right|_0 d\mathbf{x} \\ &= \int_x \varrho^{(0)} \left(\varepsilon^{(0)} + \varrho^{(0)} \left.\frac{d\varepsilon}{d\varrho}\right|_0\right) + \Delta\varrho \left(\varepsilon^{(0)} + \varrho^{(0)} \left.\frac{d\varepsilon}{d\varrho}\right|_0 (\mathbf{x})\right) d\mathbf{x}. \quad (2.41) \end{aligned}$$

The corresponding part of repulsive energy is

$$E^{(1)}_{\mathrm{rep,xc}} = E_{\mathrm{xc}} - E^{(1)}_{\mathrm{KS,xc}} = \int_x \Delta\varrho \frac{1}{2} W_{\mathrm{xc}} \Delta\varrho - \varrho^{(0)} \left.\frac{d\varepsilon}{d\varrho}\right|_0 \varrho^{(0)} d\mathbf{x}, \quad (2.42)$$

where W_{xc} is the second derivative of E_{xc} with respect to ϱ. It may be written

$$W_{\mathrm{xc}} = 2 \left.\frac{d\varepsilon}{d\varrho}\right|_0 + \varrho^{(0)} \left.\frac{d^2\varepsilon}{d\varrho^2}\right|_0, \quad (2.43)$$

where differentials of ε are partial derivatives in LDA, and differential operators in GGA, just like above. Again here, the investigated non-SCC DFTB repulsive energy part depends on $\Delta\varrho$ in the second order only, and even the second-order term is dropped from repulsive energy in SCC-DFTB.

2.3.2 Handling dissociation energy level

Theoretically, if parametrization were a search for a rich-enough set of multibody potentials, there would be no need for several molecular properties as fit targets because a proper fit to forces would give good energies and vice versa, as well as they both would result in good vibrational modes of DFTB molecules. In this ideal world, a fit to any derivative of energy would effectively lead to a fit to energy profiles themselves and the practically infinite flexibility of multibody repulsives would handle all the possible different chemical situations[8].

As we know, however, the above ideal picture is far from practice. First, reducing the form of repulsive energy to a sum of pairwise potentials makes various chemical environments[9] of a bond non-trivially different and therefore leads to our tedious work of balancing between different fitsystem chemistries. Second, a serious contradiction between energy, force and vibrational targets is produced by restricting repulsive energy as a sum of *short-range* pairwise potentials. The latter restriction prevents fitted repulsives from following any difference between DFTB electronic energy and reference energy properly in the middle and far distance region. This produces a conflict between absolute repulsive energy levels and force profiles: bridging the gap between short-range

[8] As there may be only a finite number of other atoms acting as 'influencing neighbours' on an atom, a theoretical fit with multibody potentials up to some high order of centres would be able to describe chemistry in an extremely accurate way, just like calculated with quantum-mechanical methods, within a reasonable range of chemical situations (e.g. high ionization levels and other extremistic states excluded).

[9] With three-body and higher-order multibody parts neglected, the effects of all these appear as 'different chemical environments' for a certain type of atom pair.

Figure 2.2: The Cl-Cl repulsive potential fitted without any overbinding strategy and the one with one-body energies (the upper and lower strong dashed lines, respectively). Long-range $E_{\mathrm{ref}} - E_{\mathrm{KS}}$ differences (dashed thin line originally, solid line shifted to zero dissociation) and the pairwise overbinding potential (dotted) that is equivalent to the applied one-body terms for this dimer are also shown. (Note, however, that one-body energies and pairwise overbinding potentials cannot be equivalent for several distinct stoichiometries; an equivalence is valid only for one stoichiometry, e.g. Cl_2 in this case. Note also the difference between the lower, dissociation-adjusted fitted repulsive and the reference, resulting from the absence of middle-range repulsives.)

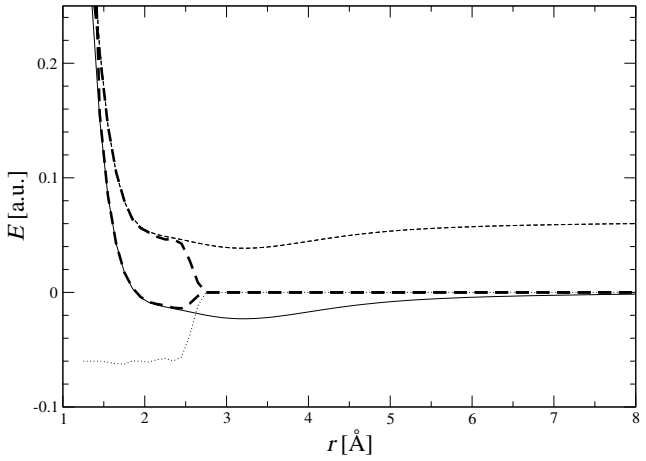

and long-range energies (i.e. a proper energy fit) but having a slope that bridges this gap over a much longer range (a proper force fit) is an unsolvable conflict. As it is also evident from Figure 2.2, covering repulsive energy with short-range potentials is simply not enough. This is the problem that will be studied briefly in this section.

Taking a closer look at Figure 2.2, one can see that discrepancy on this dimer system with respect to the short-range pair potential picture is composed of two main parts. First, the repulsive energy dies out in a much longer range than we implicitly expect with our short-range potentials. Second, there is a remanent discrepancy of repulsive energy in the dissociation limit ($r \to \infty$). While the former difference in pair potential ranges is rather easy to understand (but not to solve!), one may be shocked about the fact that dissociated molecules are not converging energetically to sets composed of lone model atoms in DFTB and the reference method, which means that for a molecule of stoichiometry $Z_l Z'_m \dots Z''_n$,

$$E^{(\mathrm{dissoc})}(Z_l Z'_m \dots Z''_n) \neq lE(Z) + mE(Z') + nE(Z'') \tag{2.44}$$

in the dissociation limit. The most plausible explanation of this phaenomenon is that differences of electronic structures and energies of dissociated chemical

systems with respect to the sum of lone atoms are not the same[10]. Still, if the shifts were consistent with each other in DFTB and in reference methods, the problem would be away (a consistent change in electronics and a consistent shift in atomic energies would cancel even if dissociated systems are not converging to sets of lone atoms in DFTB and the references), but this is ostensibly not the case.

To address the dissociation discrepancies outlined above, traditional parametrization uses the so-called 'overbinding' strategy. This means adding pairwise more or less regularized profiles to each fitted short-range repulsive pair potential in order to kill their sudden slopes at the outer side of the physical first-neighbour region (the so-called Sprungschanze, meaning 'ski jumping hill' in German, see the repulsive without overbinding in Figure 2.2). There are two serious problems with this approach. First, the size of overbinding and its step profile is chosen in a rather ad hoc way. It is set up without any guarantee that it will never affect physical bonding or other interesting situations. The only requirement against it is to eliminate the Sprungschanze on fit systems and thus to produce reasonable dissociation curves. Second, this solution means a pairwise energy correction in the dissociation limit, that is mathematically not feasible (see below). In addition to the two major problems, the shape and sometimes even the magnitude of overbinding used to go rather poorly documented.

To eliminate the shortcomings of traditional overbinding, yet keeping in line with the strict pairwise nature of DFTB and knowing that a fit to higher-order repulsive potentials would be practically impossible, we remain within the framework of using no higher multibody potentials than pairwise ones. In this framework, however, one can use one-body and two-body repulsive terms

$$E_{\mathrm{rep}} = \sum_{A}^{\mathrm{atoms}} U_{Z_A} + \frac{1}{2} \sum_{A \neq B}^{\mathrm{atoms}} U_{Z_A Z_B}(r_{AB}). \tag{2.45}$$

Of the two problems arising from the short-range nature of fitted repulsives, one may try to handle the middle-range problems with middle-range repulsives, and the dissociation problem with one-body and pairwise long-range terms. At least for the first look.

However, infinite-range (dissociation) limit of energy correction cannot be treated with pairwise terms. Energy being an extensive quantity, it must be an additive function of stoichiometry when separated systems are added together

[10] The argumentation of this paragraph is rather sloppy, preparing the unprecise conclusion that one-body repulsive energy terms are the *virtually only* correct solution to the dissociation energy problem. Carefully stated, the remanent dissociation energy discrepancy is present in the *practical, not the actual* dissociation limit, the state where atom pairs have reached distances from each other outside the ranges of respective repulsive potentials (this is a practical $r \to \infty$ state from the point of view of repulsive fitting although all r values are finite, of course.) Therefore in fact, using one-body energies is the only mathematically acceptable way of handling this problem *if* one accepts that any additional information coming from atomic pairs being outside of their respective designated repulsive pair potentials must not influence the physics of DFTB systems. On the contrary, the basic problem of traditional overbinding strategy lies in carrying a 'hidden' knowledge about which atom pairs can be, will be or have ever been in certain types of bonds in their history even beyond the distance of their respective repulsive ranges. *This footnote has been added to the text as a means of clarifying a possible logical flaw* after *submitting the thesis for supervision.*

Figure 2.3: The Cl-Cl dissociation curve calculated with the non-overbinding and the one-body-corrected repulsive of Figure 2.2 (the dotted and the dashed strong lines, respectively). The thin solid line is the DFT reference, and the dashed one is what it seems to be without dissociation adjustment. (Note the middle-range difference between the reference and the dashed strong line also here.)

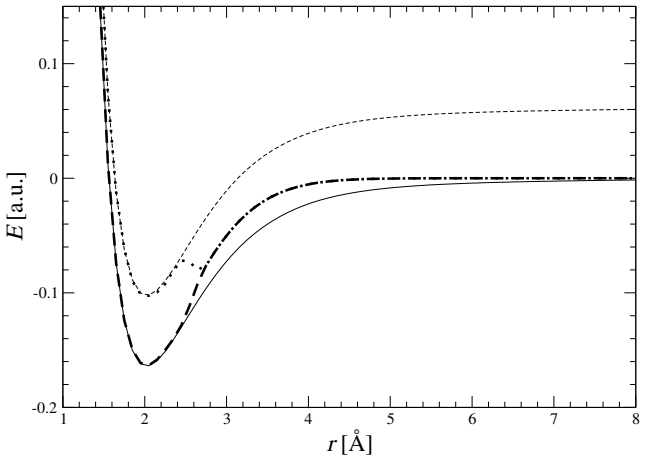

(but kept separated)

$$E^{(\mathrm{dissoc})}(Z_l Z'_m \dots Z''_n + Z_p Z'_r \dots Z''_s) = E^{(\mathrm{dissoc})}(Z_l Z'_m \dots Z''_n) + E^{(\mathrm{dissoc})}(Z_p Z'_r \dots Z''_s) = (l+p)E(Z) + (m+r)E(Z') + \dots (n+s)E(Z''). \quad (2.46)$$

It can be easily derived from the above formula, that only one-body repulsive energy terms fulfill the additivity criterion and can make the two sides of (2.44) if not equal, consistent between reference and DFTB. Therefore, a correct, consistent replacement of traditional overbinding will use one-body repulsive[11] energy parts.

On top of one-body regime, the non-dissociation (short and middle-range) repulsive part in question must be fitted as a sum of pairwise profiles. The fact that pairwise repulsives are not only a short-range phaenomenon can also be seen in Figure 2.2 and Figure 2.3. Unfortunately, the attempts made at fitting middle-range repulsive pair potentials are highly limited by a rather practical circumstance: DFTB and most DFT methods tend not to converge when atoms leave each others region of influence. The chlorine-chlorine dimer used to draw Figure 2.2 and Figure 2.3 was a lucky example to present a long-range behaviour of pair energy, but the usual course of these calculations leads to heavy convergence problems even with simple molecules of chlorine and other

[11] Although it is meaningless to call a one-body energy 'repulsive', we keep this terminology as a name for elements of the parametrized, quasi-classical part of DFTB total energy.

elements. One can try more complex molecules or reaction paths that keep all the partner atoms of a pair bound throughout the whole fit as fit systems, but this leads to an overwhelmingly complicated system of middle-range interactions between participating atoms. This is why repulsive potentials reaching beyond the typical first-neighbour distance are generally rejected as an option when possible ways of improving DFTB parametrizations comes into question.

Anyway, a practical full implementation of the one-body + middle-range strategy outlined and proposed here will need further considerations on the practical side. The one-body part of it can be regarded working and efficient, however.

Fitting one-body repulsives

Having one-body repulsives modifies the (2.2) composition of E_{rep} only slightly;

$$E_{\mathrm{rep}} = \sum_{ZZ',\nu} \alpha_{ZZ',\nu} X_{ZZ',\nu} + \sum_{Z} U_Z N_Z \tag{2.47}$$

where U_Z is the one-body repulsive for atom type Z and N_Z is the number of such atoms in the fit system in question. As it can be seen from the above composition, one-body terms behave just like two-body terms in the fit if U_Z's go along α's and N_Z's along X'es. Thus the (2.7) $\mathbf{X}$ and $\mathbf{A}$ matrices of fitting are modified so:

$$\mathbf{X} = \begin{pmatrix} X^{(1)}_{\mathrm{HH},1} & X^{(2)}_{\mathrm{HH},1} & \cdots \\ X^{(1)}_{\mathrm{HH},2} & X^{(2)}_{\mathrm{HH},2} & \cdots \\ \vdots & & \\ X^{(1)}_{\mathrm{CH},1} & X^{(2)}_{\mathrm{CH},1} & \cdots \\ X^{(1)}_{\mathrm{CH},2} & \cdots\cdots\cdots & \\ \vdots & & \\ N^{(1)}_{\mathrm{H}} & N^{(2)}_{\mathrm{H}} & \cdots \\ N^{(1)}_{\mathrm{C}} & N^{(2)}_{\mathrm{C}} & \cdots \\ \vdots & & \end{pmatrix} \tag{2.48a}$$

$$\mathbf{A} = \begin{pmatrix} \alpha_{\mathrm{HH},1} \\ \alpha_{\mathrm{HH},2} \\ \vdots \\ \alpha_{\mathrm{CH},1} \\ \alpha_{\mathrm{CH},2} \\ \vdots \\ U_{\mathrm{H}} \\ U_{\mathrm{C}} \\ \vdots \end{pmatrix} \tag{2.48b}$$

where we remained at the example composition of systems containing H and C. With the above modifications, the fitting algorithm can fit for one-body terms in the way presented for two-body terms. Of course, fit targets that are homogeneous, in the sense that they do not depend on the absolute value of

E_{rep}, cannot interfere with one-body terms. Thus with energy derivative (e.g. force) and energy difference targets, the corresponding **X** sections contain zeros only. If a fit contains no inhomogeneous energy target, a fit for one-body terms is naturally impossible.

An important detail of one-body repulsive fitting is that for the matrices to have the proper rank, the rows of **X** containing N's must be linearly independent. If this is not the case (e.g. having NCl_3, $NHCl_2$ and NH_2Cl as fit systems, the three rows of N, Cl and H are linearly interdependent), aggregates of one-body energies for each fit system may be fitted as a circumvention. In this case, dissociation energies of single atomic species cannot be calculated. One builds the fit systems' stoichiometries from the aggregates, and the **X** matrix has the rows corresponding to this. In the former example, these aggregates would be NCl_3 and NH_2Cl (then $2NHCl_2 = NCl_3 + NH_2Cl$) or NCl_3 and HCl_{-1} (in the latter case, $NHCl_2 = NCl_3 + HCl_{-1}$ and $NH_2Cl = NCl_3 + 2HCl_{-1}$).

2.4 Ab initio calculation of repulsive energy

In this section, we try to investigate the possibilities of replacing the fitted repulsive potentials of DFTB with directly calculated ones. While this leads to losing flexibility, reasonable first-guess repulsive sets without fitting would mean a tremendous improvement at getting DFTB work with new chemical elements. It must be also noted that being a fit for middle-range repulsive pair potentials problematic (see 2.3.2), calculated repulsives seem to give the only opportunity to produce physical repulsives in this region. In addition to this, the dissociation limit of repulsive energy is also handled correctly with them by nature. [26] can be regarded a very simple first step in this direction, trying to cover pair repulsives with Coulomb interactions of compressed atomic densities with freely optimized compression radii.

2.4.1 Theory

As it was seen in (1.33), the repulsive energy is the sum of the so-called counterterms of double-counting terms in Kohn–Sham energy (for valence electrons), as well as the total energy of core electrons. These together formed

$$E_{\mathrm{rep}} = \mathrm{Tr}\left[\hat{P}_{\mathrm{valence}}\left(-\frac{1}{2}\hat{V}_{\mathrm{C}} - \hat{V}_{\mathrm{xc}}\right)\right] + \mathrm{Tr}\left[\hat{P}_{\mathrm{cores}}\left(\hat{H}_{\mathrm{KS}} - \frac{1}{2}\hat{V}_{\mathrm{C}} - \hat{V}_{\mathrm{xc}}\right)\right] + E_{\mathrm{xc}} + E_{\mathrm{nuc}} \quad (2.49)$$

that may be written using integrals instead of operator traces and dissolving $\hat{H}_{\mathrm{KS}}$ to its parts

$$\begin{aligned}
E_{\mathrm{rep}} =& \mathrm{Tr}[\hat{P}_{\mathrm{cores}}\hat{T}] \\
&+ \int_x \Bigg\{ \int_y -\frac{1}{2}\frac{\varrho(\mathbf{x})(\sigma(\mathbf{y})+\varrho(\mathbf{y}))}{|\mathbf{x}-\mathbf{y}|}d\mathbf{y} \\
&\quad -\varrho(\mathbf{x})V_{\mathrm{xc}}(\sigma(\mathbf{x})+\varrho(\mathbf{x})) \\
&\quad + \int_y \frac{\sigma(\mathbf{x})(\sigma(\mathbf{y})+\varrho(\mathbf{y}))}{|\mathbf{x}-\mathbf{y}|}d\mathbf{y} \\
&\quad +\sigma(\mathbf{x})V_{\mathrm{ext}}(\mathbf{x}) \\
&\quad +\sigma(\mathbf{x})V_{\mathrm{xc}}(\sigma(\mathbf{x})+\varrho(\mathbf{x})) \\
&\quad - \int_y \frac{1}{2}\frac{\sigma(\mathbf{x})(\sigma(\mathbf{y})+\varrho(\mathbf{y}))}{|\mathbf{x}-\mathbf{y}|}d\mathbf{y} \\
&\quad -\sigma(\mathbf{x})V_{\mathrm{xc}}(\sigma(\mathbf{x})+\varrho(\mathbf{x})) \\
&\quad +(\sigma(\mathbf{x})+\varrho(\mathbf{x}))\varepsilon(\sigma(\mathbf{x})+\varrho(\mathbf{x}))\Bigg\}d\mathbf{x} \\
&\quad +E_{\mathrm{nuc}}
\end{aligned} \tag{2.50}$$

where we denote the core and valence electronic charge densities by σ and ϱ. Rearranging the above equation,

$$\begin{aligned}
E_{\mathrm{rep}} = \mathrm{Tr}[\hat{P}_{\mathrm{cores}}\hat{T}] + \int_x \Bigg\{ \int_y -\frac{1}{2}\frac{\varrho(\mathbf{x})\varrho(\mathbf{y})}{|\mathbf{x}-\mathbf{y}|}d\mathbf{y} + \int_y \frac{1}{2}\frac{\sigma(\mathbf{x})\sigma(\mathbf{y})}{|\mathbf{x}-\mathbf{y}|}d\mathbf{y} \\
+ (\sigma(\mathbf{x})+\varrho(\mathbf{x}))\varepsilon(\sigma(\mathbf{x})+\varrho(\mathbf{x})) - \varrho(\mathbf{x})V_{\mathrm{xc}}(\sigma(\mathbf{x})+\varrho(\mathbf{x})) + \sigma(\mathbf{x})V_{\mathrm{ext}}(\mathbf{x})\Bigg\}d\mathbf{x} \\
+ \frac{1}{2}\sum_{A\neq B}^{\mathrm{atoms}} \frac{Z_A Z_B}{r_{AB}}.
\end{aligned} \tag{2.51}$$

The terms of the above sum are nothing else than

- the kinetic energy of frozen core electrons,
- minus the Coulomb energy of valence electrons,
- plus the Coulomb energy of core electrons,
- plus E_{xc},
- minus the Kohn–Sham xc term for valence electrons,
- plus the potential energy of core electrons in the nuclear potentials,
- plus internuclear Coulomb repulsion.

Within the validity range of DFTB approximation, the above integrals can be calculated in pairwise calculations along the Hamiltonian, overlap and position matrix elements. It is an important detail of these calculations that intraatomic Coulomb interactions can be omitted from the sum since they are also constant just like the core kinetic term. Therefore, the terms in (2.51) can be calculated with an A–B atom pair as A–B and B–A interaction energies, A–A and B–B-type terms may be omitted. Thus for an A–B pair of atoms,

$$\begin{aligned} E_{\mathrm{rep}}(AB) = &- \int\int \frac{\varrho_A \varrho_B}{r} + \int\int \frac{\sigma_A \sigma_B}{r} \\ &+ \int (\sigma_A + \sigma_B + \varrho_A + \varrho_B)\varepsilon(\sigma_A + \sigma_B + \varrho_A + \varrho_B) \\ &- \int (\varrho_A + \varrho_B) V_{\mathrm{xc}}(\sigma_A + \sigma_B + \varrho_A + \varrho_B) \\ &+ \int \sigma_A V_{\mathrm{ext},B} + \int \sigma_B V_{\mathrm{ext},A} + \frac{Z_A Z_B}{r_{AB}} \end{aligned} \tag{2.52}$$

(with spatial arguments of the integrands omitted, and $|\mathbf{x} - \mathbf{y}|$ of (2.51) substituted with r). In order to maintain the zero dissociation limit of repulsive pair profiles (see 2.3.2), we must subtract its dissociation limit from the pair repulsive energy. Thus

$$\begin{aligned} U_{AB} = E_{\mathrm{rep}}(AB) &- \int (\sigma_A + \varrho_A)\varepsilon(\sigma_A + \varrho_A) + \int \varrho_A V_{\mathrm{xc}}(\sigma_A + \varrho_A) \\ &- \int (\sigma_B + \varrho_B)\varepsilon(\sigma_B + \varrho_B) + \int \varrho_B V_{\mathrm{xc}}(\sigma_B + \varrho_B). \end{aligned} \tag{2.53}$$

With this definition of U_{AB} it remains true within the precision of negligible three-center terms (see the argumentation about density superposition at the end of 1.2.1) that for any chemical system

$$E_{\mathrm{rep}} = \frac{1}{2} \sum_{A \neq B} U_{AB}(r_{AB}) \tag{2.54}$$

up to a stoichiometry-dependent constant, which is the sum of one-body repulsive energies:

$$E_{\mathrm{rep}}^{(\mathrm{dissoc})} = \sum_A U_A = \sum_A \left(\int (\sigma_A + \varrho_A)\varepsilon(\sigma_A + \varrho_A) - \int \varrho_A V_{\mathrm{xc}}(\sigma_A + \varrho_A) \right). \tag{2.55}$$

If one pursues absolute energy level compatibility (and comparability) with all-electron DFT calculations, the constant terms should contain all the one-atom contributions in the above sum. The terms that constitute the atomic part of the full repulsive energy and must be used instead of the U_A's in (2.55) are

- The kinetic energy of core electrons:

$$T_\sigma^{(A)} = \mathrm{Tr}(\hat{P}_{\mathrm{core},A} \hat{T}) = \sum_{\phi \in \text{core of } A} \langle \phi | T | \phi \rangle \tag{2.56}$$

- The Coulomb energy of core electrons:

$$E^{(A)}_{\text{C, core}} = \frac{1}{2}\int\limits_{\mathbf{x}}\int\limits_{\mathbf{y}} \frac{\sigma_A(\mathbf{x})\sigma_A(\mathbf{y})}{|\mathbf{x}-\mathbf{y}|} d\mathbf{x}d\mathbf{y} \tag{2.57}$$

- The atomic Coulombic counterterms of valence electrons:

$$-E^{(A)}_{\text{C, valence}} = -\frac{1}{2}\int\limits_{\mathbf{x}}\int\limits_{\mathbf{y}} \frac{\varrho_A(\mathbf{x})\varrho_A(\mathbf{y})}{|\mathbf{x}-\mathbf{y}|} d\mathbf{x}d\mathbf{y} \tag{2.58}$$

- The one-atomic xc counterterm in (2.55) for A:

$$E^{(A)}_{\text{xc}} - E^{(A)}_{\text{KS,xc}} = \int(\sigma_A+\varrho_A)\varepsilon(\sigma_A+\varrho_A) - \int \varrho_A V_{\text{xc}}(\sigma_A+\varrho_A) \tag{2.59}$$

- The potential energy of core electrons in their nuclear Coulomb potential:

$$E_{\text{ext,core}} = \int \sigma_A V_{\text{ext},A}$$

2.4.2 Further technical details of repulsive calculation

The specific structure of DFTB machinery gives two more particular aspects which must be considered at repulsive calculations. First, the calculated repulsive energy uses atomic quantities that need to come from distinct pseudoatomic calculations. Exchange-correlational potentials and energy densities come from pseudoatoms compressed with the density compression radius. Densities used as the source of Coulombic potentials also come from these pseudoatoms. Densities, however, which counterbalance $\hat{P}$ terms in counterterms, must be compressed with the wavefunction compression radius. Core densities that are not used to build potentials do not play a role in the Hamiltonian and the Kohn–Sham energy, and they can be attributed a quite arbitrary compression. To avoid further complication of the structure of repulsive calculations, we make them behave always parallel to valence densities. Thus the pair repulsive becomes

$$\begin{aligned} U_{AB} = {} & -\frac{1}{2}\int\int\frac{\varrho'_A\varrho''_B}{r} - \frac{1}{2}\int\int\frac{\varrho''_A\varrho'_B}{r} + \frac{1}{2}\int\int\frac{\sigma'_A\sigma''_B}{r} + \frac{1}{2}\int\int\frac{\sigma''_A\sigma'_B}{r} \\ & + \int(\sigma''_A+\sigma''_B+\varrho''_A+\varrho''_B)\varepsilon(\sigma'_A+\sigma'_B+\varrho'_A+\varrho'_B) \\ & - \int(\varrho''_A+\varrho''_B)V_{\text{xc}}(\sigma'_A+\sigma'_B+\varrho'_A+\varrho'_B) \\ & + \int\sigma''_A V_{\text{ext},B} + \int\sigma''_B V_{\text{ext},A} + \frac{Z_A Z_B}{r_{AB}} \\ & - \int(\sigma''_A+\varrho''_A)\varepsilon(\sigma'_A+\varrho'_A) + \int\varrho''_A V_{\text{xc}}(\sigma'_A+\varrho'_A) \\ & - \int(\sigma''_B+\varrho''_B)\varepsilon(\sigma'_B+\varrho'_B) + \int\varrho''_B V_{\text{xc}}(\sigma'_B+\varrho'_B) \end{aligned} \tag{2.60}$$

and the one-body term for atom A is

$$U_A = \sum_{\phi\in\text{core of } A} \langle\phi''|T|\phi''\rangle + \frac{1}{2}\int\int \frac{\sigma''_A\sigma'_A}{r} - \frac{1}{2}\int\int \frac{\varrho''_A\varrho'_A}{r} + \int(\sigma''_A+\varrho''_A)\varepsilon(\sigma'_A+\varrho'_A) - \int \varrho''_A V_{\text{xc}}(\sigma'_A+\varrho'_A) + \int \sigma''_A V_{\text{ext},A}, \quad (2.61)$$

where quantities marked with $'$ come from an atomic calculation with the so-called density compression radius (which would be better called *potential* compression radius), and those marked with $''$ come from atomic calculations compressed with the so-called wavefunction compression radius. Later, it may be needed to bring in more tunable parameters in calculated repulsives. To fulfill this need, we will let the potential and wavefunction compression radii of repulsive calculation (r_2 and r_3) be other than the same radii of Hamiltonian construction (r_0 and r_1 as it was introduced in 1.2.1).

The second technical detail that needs consideration here, is how potential and density superposition affects calculating repulsive potentials. Clearly, this question affects the

$$\int(\sigma_A+\sigma_B+\varrho_A+\varrho_B)\varepsilon(\sigma_A+\sigma_B+\varrho_A+\varrho_B) - \int(\varrho_A+\varrho_B)V_{\text{xc}}(\sigma_A+\sigma_B+\varrho_A+\varrho_B) \quad (2.62)$$

part of repulsives. In density superposition, the formulae to calculate the xc part of repulsives are literally as above, densities are superposed in the arguments of xc-density-type quantities (ε and V_{xc}). In potential superposition, the dimer xc potential is the $V_{\text{xc}}(\sigma_A+\varrho_A)+V_{\text{xc}}(\sigma_B+\varrho_B)$ superposition of atomic ones, while the dimer ε can be two different ways. Either we leave the above $\varepsilon(\sigma_A+\sigma_B+\varrho_A+\varrho_B)$ xc energy density because we do not want to tinker with the inner structure of ε, or we can use the

$$\tilde{\varepsilon}(\sigma_A+\sigma_B+\varrho_A+\varrho_B) = \frac{(\sigma_A+\varrho_A)\varepsilon(\sigma_A+\varrho_A)+(\sigma_B+\varrho_B)\varepsilon(\sigma_B+\varrho_B)}{\sigma_A+\varrho_A+\sigma_B+\varrho_B} \quad (2.63)$$

weighted sum of atomic xc energy densities (which gives back the potential-superposed V_{xc} as its derivative with respect to ϱ, as well as it gives back the dimer xc energy as the sum of atomic xc energies). In our attempts made so far, we have not tried and experimented with the potential superposition schemes proposed here.

2.4.3 Results

As a first example of C–C repulsive calculation, we took the electronic parameters of the mio set ($r_0 = 7\,\text{a.u.}$, $r_1 = 2.7\,\text{a.u.}$), and optimized the wavefunction compression radius used for the repulsive, independent of the wavefunction compression radius used for the Hamiltonian (the potential compression used for repulsive remained equal with the potential compression used for electronic tables, $r_2 = r_0$). This choice was an ad hoc first trial to calculate repulsives after realizing that letting both compression radii for making repulsives equal to the electronic tabulation counterpart gives unusable results (this problem may be an effect of choosing compression radii rather freely in the world of fitted

repulsives, and may be overcome with an extensive reoptimization of electronic parameters).

The optimization, which was carried out by the brute-force electronic parameter search[12] described in 2.1.7, produced a very unusual result: the optimal wavefunction compression radius for repulsive calculation was as small as possible, $r_3 = 0.01$ a.u. in this optimization (recall that this radius was made independent of the wavefunction compression radius used for integral tables, and therefore this optimization had no effect on the electronic properties of molecules). Despite of the surprisingly small value, the quality of the resulting dissociation curve of C–C dimer (Figure 2.4) encourages further investigation.

To assess the method in real-world circumstances, we optimized a set for carbohydrogens. The hydrogen parameters optimized on the C–H bond behaved similar to the C–C case: an optimal independent wavefunction compression radius of H for repulsives turned out to be the smallest value allowed by the optimization range, 0.001 a.u. in this case. It must be noted that optimizing the C–C repulsive on carbohydrogen systems gave the same optimal parameter (note that only r_3 was optimized here) as the optimization on the C–C dimer. The geometrical and energetical test results of the resulting CH parameter set can be seen in Table 2.17 (the ab initio reference for comparison with calculated repulsives was similarly B3LYP as in 2.2.1). It must be also noted that vibrational frequencies are systematically underestimated with these repulsives by 10–15%, which is an effect of the extremely compressed nature of the wavefunctions used to calculate repulsives. We expect huge improvement from a more thorough reoptimization of *all* electronic parameters.

Another test of the calculated repulsives was a HCO set (an extension of the above set with oxygen). Producing it was a tougher process, as traditional electronic parameters of oxygen turned out to be unusable with our calculations (it was impossible to optimize a reasonable pair of compression radii for repulsives on top of the mio or the matsci [16] electronic tables). After a heuristic search for usable ranges of new tabulation electronic parameters for oxygen, a more systematic optimization of a scheme seen at C and H has been made: a single value for both tabulation and repulsive potential compression radii was optimized with an optimization of the tabulation wavefunction compression in parallel, with the repulsive wavefunction compression fixed to $r_3 = 0.01$ a.u. (this was a guess based on the CH search). The fit systems for this brute-force fit were CO_2, H_2O, O_2 and C_2H_5OH. This resulted in the optimized potential compression radius for electronic tables and repulsives being $r_0 = r_2 = 3.4$ a.u., and the tabulation wavefunction compression being $r_1 = 1.5$ a.u.. The performance of the resulting repulsives is illustrated in Table 2.18. It must be noted here, that this reoptimization of electronic parameters is a foreshadow of a possible *reoptimization of all electronic parameters, based on energetical objectives*, if calculation of repulsives becomes a successful, method and common practice (note the good absolute energy values of C–O and H–O bonds with the more deeply reoptimized oxygen part in Table 2.18).

[12] Of course, the brute-force optimization process was a little bit altered to use calculated repulsives instead of fitted ones: the fitted part was a dummy set while the electronic part contained all the information about calculated repulsives.

Figure 2.4: The C–C dimer dissociation curve. The solid line is the DFT reference, and the dashed line is the one produced with DFTB and a calculated repulsive where electronic parameters of the mio set were used for electronic tables, and the potential compression radius for repulsive was equal to the tabulation one ($r_2 = r_0$). The wavefunction compression radius for repulsive calculation was 0.2 a.u. in the top graph (for a better comparison of curve shapes, both curves were shifted to an arbitrary absolute level determined by the one-body repulsives used here). The same parameter of the bottom graph was optimized further to 0.01 a.u. to give better geometries (this latter parametrization was used for test calculations).

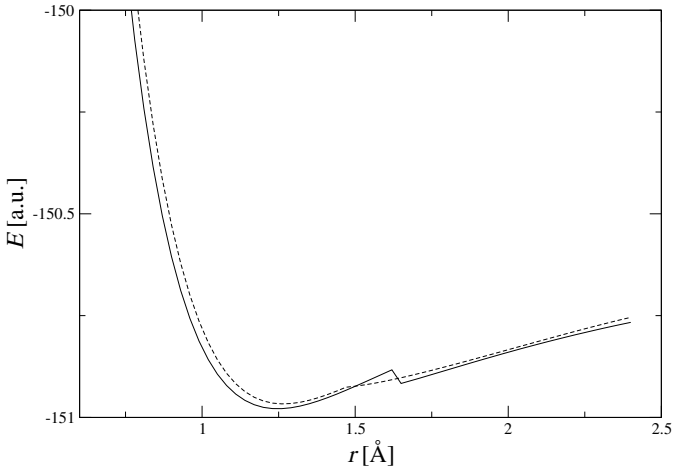

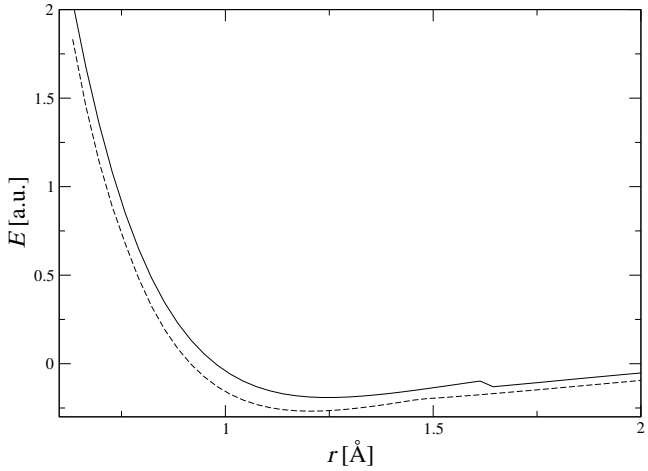

Table 2.17: Test data of first-glance ab initio repulsives for carbohydrogen systems (the G2 [8] test set and diamond). ΔE's are atomization energies in eV, doubles are bond lengths in Å, triples are angles in degrees.

property	ref.	DFTB	error	rel. error
methane				
ΔE	-18.266	-15.344	2.92274	-0.1600
C–H	1.09302	1.10835	0.01533	0.01403
ethane				
ΔE	-30.881	-26.469	4.41151	-0.1429
C–C	1.53061	1.58222	0.05162	0.03372
C–H	1.09615	1.11910	0.02295	0.02093
ethene				
ΔE	-24.437	-21.201	3.23639	-0.1324
C=C	1.33103	1.31039	-0.0206	-0.0155
C–H	1.08743	1.11682	0.02940	0.02703
ethyne				
ΔE	-17.485	-16.442	1.04324	-0.0597
C≡C	1.205	1.15838	-0.0466	-0.0387
C–H	1.06653	1.08725	0.02073	0.01944
benzene				
ΔE	-59.083	-53.143	5.94045	-0.1005
C–C	1.39663	1.41683	0.02021	0.01447
C–H	1.08699	1.12142	0.03444	0.03168
butane				
ΔE	-55.967	-48.644	7.32247	-0.1308
C–C (end)	1.54680	1.60341	0.05661	0.03660
C–C (middle)	1.53643	1.59862	0.06219	0.04048
C–H (end)	1.09667	1.11864	0.02196	0.02003
isobutane				
ΔE	-56.235	-48.835	7.40019	-0.1316
C–C	1.53530	1.59850	0.06320	0.04116
C–H	1.09665	1.11919	0.02254	0.02055
diamond				
C–C	1.555	1.62533	0.08533	0.05541
cyclobutane				
ΔE	-49.524	-43.599	5.92536	-0.1196
C–C	1.55728	1.62048	0.06319	0.04058
C–H	1.09484	1.12521	0.03037	0.02774
isobutene				
ΔE	-50.066	-43.821	6.24536	-0.1247
C–C	1.50876	1.57347	0.06471	0.04289
C=C	1.33658	1.3234	-0.0132	-0.0099
C–H in (CH_3)	1.09898	1.12092	0.02194	0.01996
C–H in (CH_2)	1.08736	1.11584	0.02848	0.02619

bicyclobutane				
ΔE	-39.222	-34.175	5.04709	-0.1287
C–C (edge)	1.51018	1.57435	0.06418	0.04250
C–C (middle)	1.90017	2.08801	0.18785	0.09886
C–H (in CH_2)	1.11157	1.15735	0.04578	0.04119
C–H (in CH)	1.09512	1.12634	0.03122	0.02851
cyclobutene				
ΔE	-43.155	-38.052	5.10254	-0.1182
C–C	1.57318	1.64547	0.07229	0.04595
C=C	1.51869	1.59169	0.07299	0.04806
C–H (in CH_2)	1.09709	1.12671	0.02962	0.02700
C–H (in CH)	1.08716	1.12103	0.03387	0.03115
cyclopropane				
ΔE	-36.872	-31.570	5.302	-0.1438
C–C	1.50922	1.57198	0.06276	0.04158
C–H	1.08659	1.11653	0.02994	0.02755
propane				
ΔE	-43.548	-37.630	5.91752	-0.1359
C–C	1.53199	1.59033	0.05834	0.03808
C–H (end)	1.09717	1.11925	0.02208	0.02013
C–H (middle)	1.09854	1.12985	0.03131	0.02850
cyclopropene				
ΔE	-29.452	-25.360	4.09168	-0.1389
C–C	1.50826	1.57681	0.06855	0.04545
C=C	1.29488	1.30087	0.00599	0.00463
C–H (opposite to C=C)	1.09518	1.12367	0.02849	0.02601
C–H (neighbour to C=C)	1.07983	1.11128	0.03145	0.02913
spiropentane				
ΔE	-55.408	-47.655	7.75290	-0.1399
C–C ('radial')	1.48491	1.55222	0.06731	0.04533
C–C (outer)	1.52990	1.60192	0.07202	0.04707
C–H	1.08815	1.11817	0.03002	0.02758
methylene-cyclopropane				
ΔE	-42.934	-37.323	5.61093	-0.1307
C=C	1.32232	1.30854	-0.0138	-0.0104
C–C ('radial')	1.46992	1.53619	0.06627	0.04508
C–C (outer)	1.53954	1.60484	0.06530	0.04242
C–H (in CH_2)	1.08776	1.11987	0.03210	0.02951
C–H (on ring)	1.08928	1.11842	0.02914	0.02675
propadiene				
ΔE	-30.567	-27.153	3.41345	-0.1117
C=C	1.30686	1.29116	-0.0157	-0.0120
C–H	1.08824	1.12033	0.03209	0.02949

1,3-butadiene				
ΔE	-39.068	-34.610	4.45754	-0.1141
C–C	1.43937	1.49511	0.05574	0.03872
C=C	1.39158	1.36317	-0.0284	-0.0204
C–H (middle)	1.08870	1.12067	0.03197	0.02937
C–H (end)	1.08596	1.12845	0.04249	0.03913
2-butyne				
C–C	1.46169	1.51404	0.05235	0.03582
C≡C	1.20920	1.16399	-0.0452	-0.0374
C–H	1.09707	1.12084	0.02377	0.02167
propyne				
ΔE	-30.483	-27.785	2.69794	-0.0885
C–C	1.46027	1.51272	0.05245	0.03592
C≡C	1.20715	1.16164	-0.0455	-0.0377
C–H (in CH_3)	1.09689	1.12004	0.02314	0.02110
C–H (in CH)	1.06610	1.08671	0.02061	0.01933
propene				
ΔE	-37.260	-32.486	4.77352	-0.1281
C–C	1.50206	1.56603	0.06397	0.04259
C=C	1.33336	1.31711	-0.0163	-0.0122
C–H (in CH_3)	1.09846	1.12126	0.02280	0.02076
C–H (in CH_2)	1.08675	1.11577	0.02902	0.02670
C–H (in CH)	1.09114	1.12569	0.03455	0.03166

2.4.4 Prospects of calculating repulsives

The results shown here illustrate that the proposed machinery of calculating repulsive potentials instead of fitting them is able to produce parametrizations that give less precise results than the best fitted repulsive sets, but they still ensure reasonable, qualitatively good results right at the first glance.

The calculated repulsives still contain parameters that allow semiempirical tuning of them to ensure the least difference with respect to reference methods, but optimization of them means a huge simplification of the parametrization process compared to fitting pair potentials. First, they are two new real numbers per atom, instead of the pair potentials, that have infinite degrees of freedom; and second, they are *atomic*, not pairwise parameters. Once the transferability of these new parameters is proved (this is foreshadowed by the fact that C–C repulsives got from dimer optimization were the same as the C–C parameters from the CH optimization), their atomwise nature ensures that extending a parameter set to a new atomic species means tuning only one set of atomic parameters (two compression radii), not a complete set of new pairwise repulsives between the new species and all the previous members of the parameter set.

The electronic parameters for calculating HCO systems optimized in our first usages of the repulsive calculation scheme seemingly leave more space for further optimization. Besides the performance of the calculated parameters, that is surprisingly good compared with the simplicity of theory, but still lag

Table 2.18: Results with HCO compounds. ΔE: atomization energy in eV, doubles are bond lengths in Å, triples are angles in degrees.

property	ref.	DFTB	error	rel. error
CO_2				
ΔE	-16.851	-16.538	0.31332	-0.0186
O=C	1.16005	1.19163	0.03158	0.02722
H_2C=O				
C–H	1.10671	1.17340	0.06669	0.06026
C=O	1.19896	1.21711	0.01815	0.01513
H–C=O	122.115	122.492	0.37638	0.00308
H_2O				
ΔE	-9.9215	-10.691	-0.7700	0.07760
O–H	0.96107	0.97234	0.01126	0.01172
HCOOH				
ΔE	-21.446	-21.038	0.40824	-0.0190
C=O	1.19023	1.21953	0.02931	0.02462
C–H	1.10330	1.17803	0.07473	0.06773
C–O	1.35071	1.42625	0.07554	0.05593
O–H	0.96462	0.98630	0.02168	0.02247
O=C–H	124.024	126.909	2.88527	0.02326
C–O–H	109.933	109.365	-0.5684	-0.0052
C_2H_5–OH				
ΔE	-34.971	-32.068	2.90355	-0.0830
C–C	1.51430	1.58271	0.06841	0.04517
C–O	1.42674	1.47539	0.04865	0.03410
C–C–O	107.982	107.458	-0.5239	-0.0049
CO				
ΔE	-11.087	-11.486	-0.3994	0.03602
C–O	1.12555	1.12138	-0.0042	-0.0037
CH_3–O–CH_3				
ΔE	-33.057	-29.072	3.98538	-0.1206
C–O	1.37698	1.42937	0.05239	0.03805
C–H	1.09697	1.14405	0.04708	0.04292
CH_3–OH				
ΔE	-22.149	-20.769	1.38017	-0.0623
C–H	1.08850	1.12324	0.03474	0.03192
C–O	1.42018	1.47134	0.05116	0.03603
O–H	0.96029	0.98862	0.02833	0.02950
H_2O_2				
ΔE	-11.228	-14.415	-3.1875	0.28389
H–O	0.96560	0.99593	0.03033	0.03141
O–O	1.46043	1.36649	-0.0939	-0.0643
H–O–O	104.931	104.601	-0.3295	-0.0031
O_2				
O–O	1.21	1.17507	-0.0349	-0.0289

behind that of fitted ones, the actual values of optimized parameters give a hint about their imperfection: the extremely low r_3 values suggest that they try to compensate for a too large r_2. We have tried to re-optimize the CH set with $r_2 = r_3$, in order to keep the number of independent parameters as few as possible, but the resulting parameters were not as good as those presented above. A thorough re-optimization of electronic compression radii may be the solution, however. This new optimization may also be an opportunity to optimize the electronic properties of atoms (through r_0 and r_1) along energetical objectives.

Chapter 3

Enhancement proposals to SCC-DFTB

3.1 Multipole expansion of SCC energy

The off-site energy of interacting atomic charges presented in (1.56) is a very simple approximation; the SCC mechanism based on it considers every atomic excess charge point-like. Remaining within the computational complexity level of present SCC, we can make SCC potentials more precise, however. This is done via a multipole extension of the current SCC scheme.

To derive an extension of SCC with multipole terms, we start with the

$$\int\limits_{\mathbf{x},\mathbf{y}} \frac{1}{|\mathbf{x}-\mathbf{y}|}\bar{\phi}(\mathbf{x})\bar{\omega}(\mathbf{y})\psi(\mathbf{y})\chi(\mathbf{x})d\mathbf{x}d\mathbf{y} \tag{3.1}$$

integrals in (1.48) and expand them as multipole series. A multipole expansion of an expression like

$$\int\limits_{\mathbf{x},\mathbf{y}} \frac{\varrho(\mathbf{x})\sigma(\mathbf{y})}{|\mathbf{x}-\mathbf{y}|}d\mathbf{x}d\mathbf{y} \tag{3.2}$$

around an $\mathbf{x}_0$, $\mathbf{y}_0$ pair of base points is

$$\sum_{m,n}\frac{1}{m!n!}\left(\frac{\partial^m}{\partial\mathbf{x}^m}\frac{\partial^n}{\partial\mathbf{y}^n}\frac{1}{|\mathbf{x}-\mathbf{y}|}\bigg|_{\mathbf{x}_0,\mathbf{y}_0}\right) \times \int\limits_{\mathbf{x}}(\mathbf{x}-\mathbf{x}_0)^m\varrho(\mathbf{x})d\mathbf{x}\int\limits_{\mathbf{y}}(\mathbf{y}-\mathbf{y}_0)^n\sigma(\mathbf{y})d\mathbf{y} \tag{3.3}$$

by simply using its Taylor series instead of the $\frac{1}{|\mathbf{x}-\mathbf{y}|}$ kernel. After rearranging the off-site part of the (1.48) sum (quite similarly to the rearrangement that led to the (1.55) original off-site SCC formula) and using multipole-series expansions instead of the (3.1) integrals, we get a multipole extension of (1.55). It is the same as if we took the atomic Mulliken densities defined in (1.59) as ϱ and σ, and used the multipole expansion of their interaction integrals. Of them, the

$n = 0$, $m = 0$ term is a monopole-monopole interaction, the $n = 1$, $m = 0$ term is a dipole-monopole interaction, etc.

In the course of the above rearrangement, retaining all multipole levels in the series of (1.48) integrals, the rearranged sums of (1.50) become not as simple as in (1.53) but containing a series in the place of

$$\frac{1}{|\mathbf{x}_A - \mathbf{x}_B|} S_{\phi\chi} S_{\omega\psi}, \quad \phi \in \{A\}, \psi \in \{B\}. \tag{3.4}$$

Plausibly we choose atomic centres A and B as base points of the Taylor series in the multipole expansion, and so the first terms of the series taking the place of (3.4) are

$$\begin{array}{c} \frac{1}{|\mathbf{x}_A - \mathbf{x}_B|} S_{\phi\chi} S_{\omega\psi} \\ - \frac{\mathbf{x}_A - \mathbf{x}_B}{|\mathbf{x}_A - \mathbf{x}_B|^3} \mathbf{X}^{(A)}_{\phi\chi} S_{\omega\psi} + \frac{\mathbf{x}_A - \mathbf{x}_B}{|\mathbf{x}_A - \mathbf{x}_B|^3} S_{\phi\chi} \mathbf{X}^{(B)}_{\omega\psi} \\ - \frac{|\mathbf{x}_A - \mathbf{x}_B|^2 - 2(\mathbf{x}_A - \mathbf{x}_B) \circ (\mathbf{x}_A - \mathbf{x}_B)}{|\mathbf{x}_A - \mathbf{x}_B|^5} \mathbf{X}^{(A)}_{\phi\chi} \mathbf{X}^{(B)}_{\omega\psi} + \dots \end{array} \tag{3.5}$$

where the $\mathbf{X}^{(A)}_{\phi\chi}$ position operator matrix is quite similar to the $S_{\phi\chi}$ overlap matrix except that it calculates the first moment of the $\bar{\phi}(\mathbf{x})\chi(\mathbf{x})$ product with respect to the A^{th} atomic centre:

$$\mathbf{X}^{(A)}_{\phi\chi} = \langle \phi | \hat{X} - \hat{X}_A | x \rangle = \int_{\mathbf{x}} \bar{\phi}(\mathbf{x})(\mathbf{x} - \mathbf{x}_A)\chi(\mathbf{x}) d\mathbf{x}. \tag{3.6}$$

We keep the SCC philosophy of including smearing and xc energy via γ profiles instead of the classical Coulomb profile, therefore our new SCC energy will employ the derivatives of γ's[1] instead of those of $\frac{1}{r}$ (which can be regarded the long-distance limit) in (3.5). With this all, the total SCC energy (formerly (1.64) in the monopole-monopole approximation) becomes

$$\begin{aligned} \Delta^2 E = \frac{1}{2} \sum_{A,B} \gamma^{(00)}_{AB} \Delta q_A \Delta q_B + \gamma^{(10)}_{AB} \Delta \mathbf{d}_A \Delta q_B \\ + \gamma^{(01)}_{AB} \Delta q_A \Delta \mathbf{d}_B + \gamma^{(11)}_{AB} \Delta \mathbf{d}_A \Delta \mathbf{d}_B + \cdots \end{aligned} \tag{3.7}$$

where

$$\gamma^{(mn)}_{AB} = \frac{1}{m!n!} \frac{\partial^m}{\partial \mathbf{x}^m_A} \frac{\partial^n}{\partial \mathbf{x}^n_B} \gamma_{AB}, \tag{3.8}$$

and we introduced the $\mathbf{d}_A$ Mulliken dipole moment of the A^{th} atom:

$$\mathbf{d}_A = -\frac{1}{2} \sum_{\phi \in \{A\}, \chi, i} n_i \left(\bar{c}_{i,\phi} c_{i,\chi} \mathbf{X}^{(A)}_{\phi\chi} + \bar{c}_{i,\chi} c_{i,\phi} \mathbf{X}^{(A)}_{\chi\phi} \right). \tag{3.9}$$

$\Delta\mathbf{d}$ is the change of the Mulliken dipole with respect to the non-interacting atoms.

[1] Instead of using derivatives of the old γ's as multipole-multipole interaction profiles, theoretically we could use semiempirical interaction profiles for each level of interaction independent of each other. This is a key feature of improving results with constructions similar to multipole series, for example in neglect of differential overlap methods and their derivatives (see e.g. [7]), but in the case of DFTB, increasing the number of parameters is highly undesired. We also want to make the first steps of enhancing SCC energy relatively simple and theoretically not complicated.

In the following, we will use the very first terms above the original SCC level, the monopole-dipole ones. The construction can be extended to higher terms as well. Up to the desired monopole-dipole level, the SCC Hamiltonian matrix becomes (cf. (1.71) in the monopole-monopole approximation)

$$\begin{aligned}\Delta H_{\phi\chi} = &\frac{1}{2} S_{\phi\chi} \sum_B \left(\gamma^{(00)}_{[\phi]B} + \gamma^{(00)}_{[\chi]B}\right) \Delta q_B \\ &+ \frac{1}{2} S_{\phi\chi} \sum_B \left(\gamma^{(01)}_{[\phi]B} + \gamma^{(01)}_{[\chi]B}\right) \Delta \mathbf{d}_B \\ &+ \frac{1}{2} \sum_B \left(\mathbf{X}^{[\phi]}_{\phi\chi} \gamma^{(10)}_{[\phi]B} + \mathbf{X}^{[\chi]}_{\phi\chi} \gamma^{(10)}_{[\chi]B}\right) \Delta q_B .\end{aligned} \tag{3.10}$$

The transformation rules needed to relate the (3.6) position matrix elements in the molecular coordinate system to the tabulated ones are presented in 3.3.3.

3.2 Semiempirical full chemical hardness matrices and γ profiles

3.2.1 Semiempirical off-site part

As described above in section 1.2.2, the current SCC-DFTB method uses a γ interaction profile in the off-site part of SCC that is an interpolated shape between the Coulombic $\frac{1}{r}$ at $r \to \infty$ and the atomic chemical hardness at $r = 0$. The heuristic derivation of this interpolated shape is based on the classical Coulombic interaction of two exponentially smeared diffuse charges, and then it is renormed to give the chemical hardness at zero distance. The latter correction is considered to take the xc energy into account up to a relevant precision.

Extending the SCC-DFTB philosophy as a pairwise approximation to LCAO DFT with semi-empirical elements and a simplified self-consistency, we can determine the γ profiles (that are semiempirical approximations of two-electron integrals in a proper expansion of DFTB energy, see 3.2.4) with pairwise energy calculations. These calculations use atom pairs, but otherwise they are just like those with lone atoms when chemical hardnesses are determined. As in (1.62), the strength of second-order response is the derivative of the energy of a highest occupied state with respect to a population, but the occupied state and the population belong to two different atoms:

$$\gamma(Z_A, Z_B, r) = -\left.\frac{\partial \varepsilon_A}{\partial q_B}\right|_r \tag{3.11}$$

where atoms A and B, being of types Z_A and Z_B, are in a distance of r, ε_A is the highest occupied electronic energy level of the atom A, and q_B is the total electronic population of atom B. Similarly to the calculation of chemical hardness in traditional SCC scheme, an excess charge on atom B is created by varying the population on its highest occupied orbital.

Because in a self-consistent diatomic calculation the energy levels cannot be attributed to specific atoms, the derivative in (3.11) can be calculated in a perturbative way. If ϕ_A is the atomic state behind ε_A and V_B is the total

potential that electrons feel around atom B,

$$\left.\frac{\partial \varepsilon_A}{\partial q_B}\right|_r = -\frac{\partial \langle \phi_A | \hat{V}_B | \phi_A \rangle}{\partial q_B}. \tag{3.12}$$

3.2.2 γ's in line with subshell hardness

A further improvement of SCC, but independent of the above proposals, could be the usage of the full Hubbard matrix as described in section 1.2.2 as a technical enhancement of the on-site limit of γ with respect to the current DFTB implementations. In line with this, the above semi-empirical γ profiles could also be enriched with a similar matrix structure. Thus (3.11) and (3.12) is modified to

$$\gamma_{ll'}(Z_A, Z_B, r) = -\left.\frac{\partial \varepsilon_{A,l}}{\partial q_{B,l'}}\right|_r = -\frac{1}{2l+1}\sum_m \frac{\partial \langle \phi_{A,l,m} | \hat{V}_B | \phi_{A,l,m} \rangle}{\partial q_{B,l'}} \tag{3.13}$$

where l and l' are the angular momentum indices of the interacting orbitals of atoms A and B, respectively, and m is the magnetic quantum number of the participating A orbitals, over which we make a mean because we want to have a general l-l' interaction profile (angular dependence of SCC interaction which arises due to uneven filling of different-m orbitals is covered by multipole SCC). We do not have to average over magnetic quantum numbers of atom B since $V_B(\mathbf{x})$ is calculated with a spherically symmetric atom.

3.2.3 Fully resolved γ's

At the end of the way described up to now stands a complete refinement of γ's. It goes beyond the Hubbard matrix of (1.72) and the γ of (3.13) and it resolves all the m quantum number cases. Having all the electronic quantum number cases resolved, we can index γ's with orbitals. In this way

$$\gamma_{\phi\chi} = -\frac{\partial \varepsilon_\phi}{\partial q_\chi} = -\frac{\partial \langle \phi | \hat{V}_{[\chi]} | \phi \rangle}{\partial q_\chi} \tag{3.14}$$

where, of course, ε_ϕ is the atomic energy eigenvalue of the ϕ orbital and q_χ is the population sitting on χ, and $[\chi]$ is the atom owning χ (naturally, there are also $U_{\phi\chi}$ Hubbard matrices as the homonuclear, $r = 0$ cases of the above γ's). We do not designate atom types, quantum numbers and the distance of $[\phi]$ and $[\chi]$ explicitly here, as these are all obvious from the ϕ and χ elements of the LCAO basis.

Since the orbitals used for tabulation will not be the same as the ones in the molecular system, the above orbital-indexed γ's have to be built of stored γ's in a similar way to what applies to the other tabulated matrices. The rules are described in 3.3.3.

3.2.4 Further resolution of γ's as operators[2]

Although there is a strong competition between computational costs and calculational precision, that must result in a fair compromise, it is not worthless

[2] This section takes motivation from discussions with Adriel Dominguez and Thomas Niehaus.

investigating where the further resolution of γ's can theoretically lead to. Some aspects of such a further resolution are presented in the following.

'Semioperator' γ's

One step beyond the Mulliken-analysis-based improvement of more and more resolved γ's, one can begin resolving them at least on one 'side' to get fully-fledged orbital-indexed quantities, that is, operators written in the LCAO space, not only the diagonal elements described in 3.2.3. This 'resolution beyond every limit' refines (3.14) on one side to a well-behaved orbital-indexed matrix:

$$\gamma_{\phi\psi;\chi} = -\frac{\partial H_{\phi\psi}}{\partial q_\chi} = -\frac{\partial \langle\phi|\hat{V}_{[\chi]}|\psi\rangle}{\partial q_\chi}. \tag{3.15}$$

These γ's can be used in the calculation of total energy and self-consistent Hamiltonian matrix much easier than former ones. In total energy

$$\Delta^2 E = \frac{1}{2} \sum_{i,\phi,\psi,\chi} \Delta P_{\phi\psi} \gamma_{\phi\psi;\chi} \Delta q_\chi \tag{3.16}$$

would represent the SCC term, where $\Delta P_{\phi\psi}$ is the change of density matrix element $\sum_i n_i \bar{c}_{i,\phi} c_{i,\psi}$ with respect to $P^{(0)}_{\phi\psi}$, and

$$\sum_\chi \gamma_{\phi\psi;\chi} \Delta q_\chi \tag{3.17}$$

is an effective kernel that represents the effective semi-classical interaction of orbital charges with point-like charges accounted for orbitalwise (represented with the same q_χ quantities as in 3.2.3). In the Hamiltonian matrix, the corresponding part is nothing else than the above kernel

$$\left(\Delta \hat{H}_{\mathrm{KS}}\right)_{\phi\psi} = \sum_\chi \gamma_{\phi\psi;\chi} \Delta q_\chi. \tag{3.18}$$

Of course, the advantage of possible refinement of calculation with these new γ's may be less than the disadvantage of tabulating and using $|\{A\}| \times |\{A\}| \times |\{B\}|$ of them[3] for every distance of every atom type pair, where $|\{A\}|$ denotes the number of orbitals centered around A. To remedy the problem of extensive tables, and taking into account that the same refinement may not be needed at either sides of γ, one can begin making the 'source' side more accumulated. This way, even an orbital-center-type set of γ's can be defined:

$$\gamma_{\phi\psi;B} = -\frac{\partial H_{\phi\psi}}{\partial q_B} = -\frac{\partial \langle\phi|\hat{V}_B|\psi\rangle}{\partial q_B}. \tag{3.19}$$

The number of the above γ's is only $|\{A\}| \times |\{A\}|$ per distance step per atom pair type (this means practically $|\{A\}| \times |\{A\}| + |\{B\}| \times |\{B\}|$ entries in an A-B-type table row).

Besides the (3.15) arrangement where the three indices of γ came from centres $AA;B$, we must shortly define all the other possible combinations of centres

[3] This number of $\gamma_{\phi\psi;\chi}$ values is valid when cases with $[\phi] \neq [\psi]$ (i.e. three-center-type ones) are neglected.

in one or two-center-like γ's. As long as we remain at point-like charges at the source (nonoperator) side, calculation of γ's goes as in (3.15) or (3.19). The complexity of dealing with multipole contributions is detailed in the following. Accumulation of the Mulliken side needs further consideration in the non-$AA;B$ case, however. Keeping in line with the importance of Mulliken-side resolution in different cases, an adequate minimization of necessary table sizes may be realized by using a nonuniform resolution of the nonoperator (Mulliken) side; e.g. for off-site γ's an atomwise resolution suffices while on-site γ's (chemical-hardness-type interaction intensities with $AA;A$-type and maybe $AB;A$-type indices) need a subshell or orbitalwise resolution. Note that, depending on the resolution of the quasiclassical side and the number of relevant nonequivalent arrangements of the two atomic centres involved (e.g. $AA;B$ and $AB;A$ in the heteroatomic case of semioperator γ's), the number of integral table entries mentioned above must be multiplied with a small integer, but we will silently omit treating this in detail, as we are only interested in magnitudes of table sizes now.

Another aspect that must be clarified about the semioperator γ's in the future is if some Hartree–Fock-type (HF) exchange energy can be expressed with them, and if yes, how this can go. Certainly, fully operator-like γ's facilitate calculating HF exchange, but it raises two major questions. First, calculating exchange energy implies using a two-electron density operator (or a construction alike), not only the one-electron one used in DFTB and in this thesis. Second, xc parts are also expressed in γ profiles semiempirically, and it is a serious question if we are able to balance between a reduced semiempirical xc energy and a new HF exchange energy correctly.

Handling multipole contributions with semioperator γ's

An above-defined one-sided resolution of operator-level γ's affects the multipole expansion too. Since the operator-like side does not need approximations like multipole expansion any more, only the other side may conserve it. This goes by defining the same Mulliken charges and dipole moments as with the atom-resolved (i.e. non-resolved) or any other finer Mulliken case, but using γ's and energy expressions like in (3.18). In this way, a matrix element of the SCC Hamiltonian looks

$$\left(\Delta\hat{H}_{\mathrm{KS}}\right)_{\phi\psi} = \sum_B \left(\gamma^{(0)}_{\phi\psi;B}\Delta q_B + \gamma^{(1)}_{\phi\psi;B}\Delta\mathbf{d}_B\right). \tag{3.20}$$

Note that higher-multipole γ's are produced also here as derivatives, but this construction affects only one side of γ that is marked by only one derivative index. Being the interacting quantities (atomic potentials and products of electronic orbitals) at γ calculations not spherically symmetrical at both participant centre any more, the derivatives of these γ's cannot be constructed from the bare derivative with respect to the distance between centres. Different derivatives must be calculated in all the three directions of space. This means additionally calculated and stored quantities in a γ table when one wants multipole moments, that negatively affects the usability of semi-operator γ's. In this case, one would store $\gamma^{(0)}$, $\gamma^{(1)}_x$, $\gamma^{(1)}_y$ and $\gamma^{(1)}_z$.

The on-site (one-center) case is a bit more difficult because one has to put dipole moments in atomic DFT calculations by hand to calculate $\gamma^{(1)}_{\phi\psi;B}$ where

$\phi, \psi \in \{B\}$ because there is no distance parameter in chemical hardness with respect to which this profile could be derived, as well as there are no nuclei able to be moved with respect to each other. $\gamma_{\phi\psi;B}$ when $\phi \in \{B\}$ but $\psi \notin \{B\}$ is a similar complicated case: the problem of handling of higher multipole order γ's also applies here because $\phi \in \{B\}$.

There is, however, a possible way to circumvent the calculation of multipole contributions with semi-operator γ's. Because of the symmetry between the two sides of γ (recall that they are nothing else than a complete set of two-electron integrals, or in other words, elements of a kernel of a second derivative of energy), a total sum of all possible multipole contributions above monopole-monopole level in SCC-DFTB can be approximated (exactly at the monopole-dipole level, and with gradually increasing relative errors at higher levels) by

$$\Delta^2 E_{\text{all multipoles}} = 2(\Delta^2 E_{\text{semi-operator}} - \Delta^2 E_{\text{point charges}}), \tag{3.21}$$

where the first term is calculated without any attempt to handle multipole corrections, and the last term is a point-like-charges SCC energy calculated with adequately refined γ's (in (3.11), (3.13) or (3.14)). This makes handling multipoles even with semi-operator γ's unnecessary, because

$$\begin{aligned} \Delta^2 E &= \Delta^2 E_{\text{point charges}} + \Delta^2 E_{\text{all multipoles}} \\ &= 2\Delta^2 E_{\text{semi-operator}} - \Delta^2 E_{\text{point charges}}, \end{aligned} \tag{3.22}$$

containing the old SCC energy in addition the the semi-operator one, which can be calculated far more easily than a multipole extension of semi-operator γ's.

'Two-sided' exact γ operators and their approximations implemented by other schemes

Naturally, one can proceed to refine both sides of γ. This is nothing else than giving back the (1.48) two-electron integrals faithfully in the SCC part. While this means an extremely populous set of $\gamma_{\phi\chi;\psi\omega}$ parameter tables, one can consider neglecting three-center terms also here, arriving at the still very large $|\{A\}| \times |\{A\}| \times |\{B\}| \times |\{B\}|$ number of table entries per atom pair per distance value (this is only an estimation of magnitude, also here). Of course, this regime makes multipole calculations away, and it gives a possibility of calculating HF exchange in a more perfect way.

A useful byproduct of the investigation of operator-like γ's made so far is that we are now able to compare them with Mulliken-level γ's and clarify what and how is simplified in point-like-charges SCC, and what and how is improved in the multipole extension of it. The 'two-sided' operator-like γ's represent the (1.48) four-orbital integrals without any approximation beyond the basic DFTB rules, but with the second derivative of xc energy added to the Coulomb kernel, of course:

$$\gamma_{\phi\chi;\psi\omega} = \int_{\mathbf{x}} \int_{\mathbf{y}} \bar{\phi}(\mathbf{x})\chi(\mathbf{x}) \left(\frac{1}{|\mathbf{x}-\mathbf{y}|} + \frac{\delta^2 E_{\text{xc}}}{\delta\varrho(\mathbf{x})\delta\varrho(\mathbf{y})} \right) \bar{\psi}(\mathbf{y})\omega(\mathbf{y}) d\mathbf{y} d\mathbf{x}. \tag{3.23}$$

The fully-resolved, but not operator-like γ's in 3.2.3 simplify the above plenty of integrals to

$$\gamma_{\phi\chi} = \int_{\mathbf{x}} \int_{\mathbf{y}} \bar{\phi}(\mathbf{x})\phi(\mathbf{x}) \left(\frac{1}{|\mathbf{x}-\mathbf{y}|} + \frac{\delta^2 E_{\text{xc}}}{\delta\varrho(\mathbf{x})\delta\varrho(\mathbf{y})} \right) \bar{\chi}(\mathbf{y})\chi(\mathbf{y}) d\mathbf{y} d\mathbf{x}, \tag{3.24}$$

but considering the structure of the SCC Hamiltonian, this gives also an approximation to the four-indexed γ:

$$\gamma_{\phi\chi;\psi\omega} \approx \frac{1}{4} S_{\phi\chi}(\gamma_{\phi\psi} + \gamma_{\chi\psi} + \gamma_{\phi\omega} + \gamma_{\chi\omega}) S_{\psi\omega}. \tag{3.25}$$

In the subshellwise SCC Hamiltonian, the above structure is maintained while the γ's inside are replaced with an average of e.g. $\gamma_{\phi\psi}$'s resulting in $\gamma_{ll'}$. In the original, atomwise SCC, $\gamma_{ll'}$'s for every atom pair are replaced with the one describing interaction between the respective highest occupied subshells of atoms in the pair.

The multipole expansion makes the above approximation more precise by the multipole regime described in (3.3). This is built of the derivatives of the kernel and the multipole moments of the two 'sides'. Up to the first (monopole-dipole) level, the multipole approximation of the four-indexed γ reads

$$\begin{aligned}
\gamma_{\phi\chi;\psi\omega} \approx{}& \frac{1}{4} S_{\phi\chi}(\gamma^{(00)}_{\phi\psi} + \gamma^{(00)}_{\chi\psi} + \gamma^{(00)}_{\phi\omega} + \gamma^{(00)}_{\chi\omega}) S_{\psi\omega} \\
&+ \frac{1}{4}(X^{[\phi]}_{\phi\chi}\gamma^{(10)}_{\phi\psi} + X^{[\chi]}_{\phi\chi}\gamma^{(10)}_{\chi\psi} + X^{[\phi]}_{\phi\chi}\gamma^{(10)}_{\phi\omega} + X^{[\chi]}_{\phi\chi}\gamma^{(10)}_{\chi\omega}) S_{\psi\omega} \\
&+ \frac{1}{4} S_{\phi\chi}(\gamma^{(01)}_{\phi\psi} X^{[\psi]}_{\psi\omega} + \gamma^{(01)}_{\chi\psi} X^{[\psi]}_{\psi\omega} + \gamma^{(01)}_{\phi\omega} X^{[\omega]}_{\psi\omega} + \gamma^{(01)}_{\chi\omega} X^{[\omega]}_{\psi\omega}),
\end{aligned} \tag{3.26}$$

where $\gamma^{(\cdot\cdot)}_{\cdot\cdot}$'s can be changed to whichever lower-resolution scheme is used. The above formula gives a clear impression about the structural change that multipole extension means to SCC.

It may also be worth taking a look at what approximations the semioperator γ's to operator ones mean. The (3.16) energy expression and the respective (3.18) Hamiltonian implies an approximation

$$\gamma_{\phi\chi;\psi\omega} \approx \frac{1}{2}\left(\gamma_{\phi\chi;\psi} + \gamma_{\phi\chi;\omega}\right) S_{\psi\omega}. \tag{3.27}$$

The (3.22) workaround of computing multipole contributions with semioperator γ's goes beyond the above approximation by doubling it with the operator and quasiclassical sides symmetrized, and then subtracting the fully quasi-classical energy:

$$\begin{aligned}
\gamma_{\phi\chi;\psi\omega} \approx{}& \frac{1}{2}\left(\gamma_{\phi\chi;\psi} S_{\psi\omega} + \gamma_{\phi\chi;\omega} S_{\psi\omega} + S_{\phi\chi}\gamma_{\phi;\psi\omega} + S_{\phi\chi}\gamma_{\chi;\psi\omega}\right) \\
&- \frac{1}{4} S_{\phi\chi}(\gamma_{\phi\psi} + \gamma_{\chi\psi} + \gamma_{\phi\omega} + \gamma_{\chi\omega}) S_{\psi\omega}
\end{aligned} \tag{3.28}$$

where the definition of $\gamma_{\cdot;\cdot\cdot}$'s is self-evident. With a

$$\gamma_{\phi\chi;\psi} = \int_{\mathbf{x}} \int_{\mathbf{y}} \bar{\phi}(\mathbf{x})\chi(\mathbf{x}) \left(\frac{1}{|\mathbf{x}-\mathbf{y}|} + \frac{\delta^2 E_{\mathrm{xc}}}{\delta\varrho(\mathbf{x})\delta\varrho(\mathbf{y})} \right) \bar{\psi}(\mathbf{y})\psi(\mathbf{y}) d\mathbf{y} d\mathbf{x} \tag{3.29}$$

semi-simplified two-electron integral representation of the semioperator γ's, the (3.28) approximation of the exact γ's can be seen quite accurate and able to produce even HF exchange, just like exact ones, yet at a much lower cost (much smaller, but still large integral tables). The quasiclassical side can be even more simplified, an l-indexed resolution seems to be more than satisfactory.

3.3 Supplementary material to SCC improvements

3.3.1 Mulliken charge density operators

At the investigation of on-site Coulombic energy, it was worth introducing the

$$\hat{P}_A = \frac{1}{2} \sum_{\phi \in \{A\}, \chi, i} n_i \left(\bar{c}_{i,\phi} c_{i,\chi} |\phi\rangle\langle\chi| + \bar{c}_{i,\chi} c_{i,\phi} |\chi\rangle\langle\phi| \right) \tag{3.30}$$

atomwise Mulliken density operator. It further implied the ϱ_A atomic Mulliken charge density and the q_A atomic Mulliken charge such that

$$q_A = -\mathrm{Tr}\hat{P}_A = -\int_{\mathbf{x}} \langle \mathbf{x}| \hat{P}_A |\mathbf{x}\rangle \, d\mathbf{x} = \int_{\mathbf{x}} \varrho_A(\mathbf{x}) d\mathbf{x} \tag{3.31}$$

With the atomic Mulliken density operators and using

$$\hat{P} = \frac{1}{2}\left(\hat{P} + \hat{P}^\dagger\right) = \sum_A \hat{P}_A, \tag{3.32}$$

derivation of off-site SCC Coulomb energy with atomwise Mulliken density operators would also have been a bit shorter in 1.2.2, but it would have hidden some intuitive details.

To be seen in a broader view, the Mulliken density operators give a decomposition of the $\hat{P}$ density operator using a complete set of projections in our LCAO space.

$$\hat{P}_A = \frac{1}{2} \sum_{\phi \in \{A\}} (\hat{\Pi}_\phi \hat{P} + \hat{P}^\dagger \hat{\Pi}_\phi^\dagger) \tag{3.33}$$

where

$$\hat{\Pi}_\phi = \sum_{\chi,\psi} |\phi\rangle\langle\chi| \left(S^{-1}\right)_{\chi\psi} \tag{3.34}$$

and

$$\sum_\phi \hat{\Pi}_\phi = 1. \tag{3.35}$$

Similarly to the general refinement of SCC equations to orbital hardnesses and up to orbitally resolved γ's, the Mulliken density operators can also be refined to reflect this structure. An orbitalwise density operator is

$$\hat{P}_\phi = \frac{1}{2}(\hat{\Pi}_\phi \hat{P} + \hat{P}^\dagger \hat{\Pi}_\phi^\dagger) = \frac{1}{2} \sum_{\chi,i} n_i \left(\bar{c}_{i,\phi} c_{i,\chi} |\phi\rangle\langle\chi| + \bar{c}_{i,\chi} c_{i,\phi} |\chi\rangle\langle\phi| \right). \tag{3.36}$$

With this,

$$\hat{P}_A = \sum_{\phi \in \{A\}} \hat{P}_\phi. \tag{3.37}$$

Orbitalwise Mulliken density operators imply orbitalwise Mulliken charge densities and charges, and they may be useful at the investigation of the totally resolved γ's in section 3.2.3.

As an intermediate step between the atomwise and the totally resolved regime, there can be Mulliken densities defined which are resolved only up to the angular momenta of orbitals. They are instruments of studying the 'almost-totally' refined SCC in section 3.2.2.

3.3.2 Properties of the generalized γ functions

Shape

For the original γ shape, see [13]. As the new shapes that we propose in this paper are semi-empirical, there must be analytical shapes (similar to the original ones in [13] or not) fitted to the semi-empirical data in order to be able to carry out derivations on them, if one decides to use them.

Either in the interpolated or in the semiempirical case, the multipole expansion of SCC energy requires derivatives of basic $\gamma^{(00)}$ as higher-order γ's (see (3.8)). Since $\gamma^{(00)}_{AB}(Z_A, Z_B, \mathbf{x}_A, \mathbf{x}_B)$ depends on its $\mathbf{x}_A$ and $\mathbf{x}_B$ arguments as a spherically symmetric function of $r = |\mathbf{r}| = |\mathbf{x}_A - \mathbf{x}_B|$ (for brevity we use $\mathbf{r}$ instead of $\mathbf{x}_A - \mathbf{x}_B$ and we drop the atom-label arguments in the following equations), the higher-order γ's are quite simple, e.g.

$$\gamma^{(10)}(\mathbf{r}) = \frac{\mathbf{r}}{r}\frac{\partial\gamma^{(00)}(r)}{\partial r} \tag{3.38}$$

and the second derivative by components

$$\gamma^{(20)}_{\alpha\beta}(\mathbf{r}) = \frac{1}{2}\frac{\delta_{\alpha\beta}}{r}\frac{\partial\gamma^{(00)}(r)}{\partial r} + \frac{1}{2}\frac{r_\alpha r_\beta}{r^2}\frac{\partial^2\gamma^{(00)}(r)}{\partial r^2}. \tag{3.39}$$

The above formulae can be seen in (3.5) applied to the $\frac{1}{r}$ long-range limit potential in the place of a proper $\gamma^{(00)}$.

As we can see from the above too, higher-order γ's are matrices according to their multipole indices. $\gamma^{(mn)}$ is a matrix of order $m+n$, e.g. $\gamma^{(10)}$ is a vector (not mentioning the atomic centre indices of γ's when they are listed as γ_{AB}).

Identities

As every γ is a $\gamma_{AB} = \gamma(Z_A, Z_B, r_{AB}) = \gamma(Z_A, Z_B, |\mathbf{x}_A - \mathbf{x}_B|)$, it must hold that

$$\frac{\partial\gamma_{AB}}{\partial\mathbf{x}_A} = -\frac{\partial\gamma_{AB}}{\partial\mathbf{x}_B}. \tag{3.40}$$

From physical reasons (from the fact that nothing must depend on the listing order of atoms or from the second-derivative nature of γ's) it is also obvious that

$$\gamma^{(mn)}_{AB} = \gamma^{(nm)}_{BA}. \tag{3.41}$$

In the multipole expansion of SCC energy, the γ's were coefficients of a Taylor series, therefore

$$(m+1)\gamma^{(m+1,n)}_{AB} = \frac{\partial\gamma^{(mn)}_{AB}}{\partial\mathbf{x}_A} = -\frac{\partial\gamma^{(mn)}_{AB}}{\partial\mathbf{x}_B} = -(n+1)\gamma^{(m,n+1)}_{AB}, \tag{3.42}$$

and hence

$$\gamma^{(mn)}_{AB} = (-1)^{m-n}\gamma^{(nm)}_{AB}. \tag{3.43}$$

From the last equation and (3.41)

$$\gamma^{(mn)}_{AB} = (-1)^{m-n}\gamma^{(mn)}_{BA}. \tag{3.44}$$

Based on the above identities, it is enough to calculate a γ for each value of $m+n$, e.g. $\gamma^{(m+n,0)}$, all the other γ's of the same level are of the same shape.

Calculating molecular SCC energy derivatives

Higher-order γ's are not only needed for higher-order multipole terms, but also for calculating the derivatives of SCC energy. As an example, we show how to calculate a molecular SCC force up to the monopole-dipole order.

The molecular SCC force acting on atom B is the negative gradient of (3.7) (now up to the monopole-dipole order) with respect to $\mathbf{x}_B$, and its part that contains γ derivatives is

$$F_{B,\alpha}^{(\partial\gamma)} = -q_B \sum_{A\neq B} \frac{\partial \gamma_{AB}^{(00)}}{\partial x_{B,\alpha}} \Delta q_A - \mathbf{d}_B \sum_{A\neq B} \frac{\partial \gamma_{AB}^{(01)}}{\partial x_{B,\alpha}} \Delta q_A - q_B \sum_{A\neq B} \frac{\partial \gamma_{AB}^{(10)}}{\partial x_{B,\alpha}} \Delta \mathbf{d}_A. \quad (3.45)$$

Writing all the vector quantities by components and using the identities of γ's,

$$F_{B,\alpha}^{(\partial\gamma)} = -q_B \sum_{A\neq B} \gamma_{AB,\alpha}^{(01)} \Delta q_A - \sum_{\beta} \left(d_{B,\beta} \sum_{A\neq B} \gamma_{AB,\alpha\beta}^{(02)} \Delta q_A - q_B \sum_{A\neq B} \gamma_{AB,\alpha\beta}^{(02)} \Delta d_{A,\beta} \right). \quad (3.46)$$

3.3.3 Transformations of tabulated matrices before use

In current SCC-DFTB implementations, there are two matrices of quantum-mechanical integrals tabulated for run-time use with DFTB; the Hamiltonian matrix and the overlap matrix. Using them needs a transformation because the coordinate system in which the tabulated integrals have been carried out is not the same as the molecular coordinate system in which the DFTB calculation takes place (usually, the system of integration is fixed to the line between the participating two atoms, while the molecular one is quite arbitrary).

The overlap and the position matrix

In this section we recall the usage rules of overlap matrix tables in a formalized way, and parallel with it, we construct the similar rules for the position operator matrix.

Let us call the molecular basis ϕ, χ, etc. and the integration basis $\tilde{\phi}$, $\tilde{\chi}$, etc. From the relative orientations of the molecular and the integration coordinate systems, a linear transformation can be set up between the two:

$$\phi = \sum_{\tilde{\phi}} \tilde{\phi} T_{\tilde{\phi}\phi} \quad (3.47)$$

in which orbitals of different angular momenta do not mix, i.e. s, p, etc. orbitals of the molecular basis are linear combinations of integration basis elements of

the same respective types. With this known, the elements of the molecular overlap matrix can be constructed as

$$S_{\phi\chi} = \sum_{\tilde{\phi},\tilde{\chi}} \bar{T}_{\chi\tilde{\chi}} S_{\tilde{\chi}\tilde{\phi}} T_{\tilde{\phi}\phi}, \tag{3.48}$$

similar to the transformation of canned Hamiltonian elements.

In the enhanced SCC scheme, elements of the position operator matrix in (3.6) must be also stored besides the overlap matrix and the Hamiltonian. Taking them out of the box is a bit more difficult since they are not only depending on the orbitals with whom they were integrated, but, as a vector-valued operator, they are also directly depending on the coordinate system chosen. If x_α's are the molecular coordinates, $x_{\tilde{\beta}}$'s are the integration coordinates and

$$x_\alpha = \sum_{\tilde{\beta}} t_{\alpha\tilde{\beta}} x_{\tilde{\beta}} \tag{3.49}$$

is the transformation between the two, a position matrix element with origin **a** in the molecular system is

$$\begin{aligned} X^{(\mathbf{a})}_{\alpha,\phi\chi} &= \int_x \bar{\phi}(x)(x_\alpha - a_\alpha)\chi(x)dx \\ &= \sum_{\tilde{\phi},\tilde{\chi},\tilde{\beta}} \int_x \bar{T}_{\phi\tilde{\phi}} \bar{\tilde{\phi}}(x) \left(t_{\alpha\tilde{\beta}}(x_{\tilde{\beta}} - b_{\tilde{\beta}}) + b_\alpha - a_\alpha \right) \tilde{\chi}(x) T_{\tilde{\chi}\chi} dx \\ &= \sum_{\tilde{\phi},\tilde{\chi},\tilde{\beta}} \bar{T}_{\phi\tilde{\phi}} t_{\alpha\tilde{\beta}} T_{\tilde{\chi}\chi} X^{(\mathbf{b})}_{\tilde{\beta},\tilde{\phi}\tilde{\chi}} + S_{\phi\chi}(b_\alpha - a_\alpha) \end{aligned} \tag{3.50}$$

if the coordinates of origin in the integration reference are $b_\alpha = \sum_{\alpha,\tilde{\beta}} t_{\alpha\tilde{\beta}} b_{\tilde{\beta}}$. This is the transformation of the stored position matrix elements to the molecular system.

In addition to the transformation rules, we note that in the case of the position matrix, there are vanishing elements, just like with the overlap matrix, but the selection rules differ. In the case of the overlap matrix, $S_{\phi\chi}$ was zero if the magnetic quantum numbers of ϕ and χ were different, non-vanishing elements had $m_\chi - m_\phi = 0$ in a coordinate system whose z axis was fixed to the line between the two participating atoms. For $\mathbf{X}^{(\cdot)}_{\alpha,\phi\chi}$ a similar rule applies, but the criterion of a nonzero element includes the coordinate; $m_\alpha + m_\chi - m_\phi = 0$ is the proper selection criterion with m_α being 0 for z, 1 for x and -1 for y (this rule applies to real-valued orbitals, complex ones follow a bit more complicated, yet similar set of rules).

The fully resolved γ's

The definition of orbitalwise γ in (3.14) contains $\langle\phi|\ldots|\phi\rangle$ as the ϕ-dependent part (the $\hat{V}_{[\chi]}$ potential and q_χ are independent from the particular choice of ϕ), therefore it transforms with

$$\gamma_{\phi\chi} = \sum_{\tilde{\phi}} \bar{T}_{\phi\tilde{\phi}} \gamma_{\tilde{\phi}\chi} T_{\tilde{\phi}\phi} \tag{3.51}$$

when we make the transition from $\tilde{\phi}$'s of the integration system to the ϕ's of the molecular calculation. Transformation of the χ index is a bit more complicated to construct, but since $\gamma_{\phi\chi}$ is nothing else than a second derivative of the total energy with respect to q_ϕ and q_χ (or at least an approximation of it), $\gamma_{\phi\chi} = \gamma_{\chi\phi}$ and therefore the transformations in both indices must obey exactly the same rules

$$\gamma_{\phi\chi} = \sum_{\tilde{\phi},\tilde{\chi}} \bar{T}_{\phi\tilde{\phi}} T_{\tilde{\phi}\phi} \bar{T}_{\chi\tilde{\chi}} T_{\tilde{\chi}\chi} \gamma_{\tilde{\phi}\tilde{\chi}}. \tag{3.52}$$

A more precise derivation of the above transformation rules would be built on that the χ-dependent part of the (3.14) definition of $\gamma_{\chi\phi}$ is

$$\frac{\partial \hat{V}_{[\chi]}}{\partial q_\chi} = \int_{\mathbf{x}} \frac{\delta \hat{V}_{[\chi]}}{\delta \varrho_{[\chi]}(\mathbf{x})} \frac{\partial \varrho_{[\chi]}(\mathbf{x})}{\partial q_\chi} d\mathbf{x} \tag{3.53}$$

in which only q_χ is explicitly depending on the particular choice of χ. Being

$$q_\chi = -\frac{1}{2} \sum_{\phi} \left(P_{\chi\phi} S_{\chi\phi} + P_{\phi\chi} S_{\phi\chi} \right), \tag{3.54}$$

it shall follow the transformation rules of a product containing $\langle\chi|$ and $|\chi\rangle$, similar to (3.51).

Note that the (3.52) transformation rules are not of a 'well-behaved' tensor of the LCAO space. A tensor transforming with the product of four transformation matrices should have four independent indices, and all of these four indices should be meaningful. It is supposed, however, that the 'real' four-index $\gamma_{\phi\phi'\chi\chi'}$'s (cf. these four indices with the four orbitals in integrals of (1.48)) are diagonal-dominated in their first and second two indices respectively and the perturbative non-diagonality is approximated with the multipole structure of SCC. The problem of this approximate transformation of γ is naturally away with the operator-like γ's introduced in 3.2.4

3.4 Extensions of TD-DFTB in line with the multipole expansion of SCC

In time-dependent DFTB (TD-DFTB, which is a tight-binding approximation of time-dependent DFT) [28], an improvement of SCC nomenclature comes into play in two aspects. Here, we show these differences very briefly, investigating the details shall take place in further research.

The first aspect shown here is the coupling matrix of TD-DFTB[4]. For singlet transitions in the spin domain, the coupling matrix is nothing else than the second derivative of total energy with respect to the electronic density operator (which gives also the base of a theoretical non-approximated version of the SCC Hamiltonian), except that it contains matrix elements between occupied (i, j) and unoccupied (a, b) Kohn–Sham orbitals:

$$K^{\mathrm{S}}_{ia,jb} = \int_{\mathbf{x}} \int_{\mathbf{y}} \bar{i}(\mathbf{x}) a(\mathbf{x}) \left(\frac{1}{|\mathbf{x}-\mathbf{y}|} + \frac{\delta^2 E_{\mathrm{xc}}}{\delta\varrho(\mathbf{x})\delta\varrho(\mathbf{y})} \right) \bar{j}(\mathbf{y}) b(\mathbf{y}) d\mathbf{y} d\mathbf{x} \tag{3.55}$$

[4] On the usage and construction of the coupling matrix, see section 3 in [28].

As it was shown in 3.2.4, the multipole expansion of two-electron integrals like above is a valid tool of making their approximation better than the point-like Mulliken one. The improvement that the multipole expansion of SCC energy can give to the approximation of the above integrals is also detailed there. As

$$K^{\mathrm{S}}_{ia,jb} = \sum_{\phi,\chi,\psi,\omega} \bar{c}_{i,\phi}\bar{c}_{j,\psi}c_{a,\chi}c_{b,\omega}\gamma_{\phi\chi;\psi\omega}, \tag{3.56}$$

where $|i\rangle = \sum_\phi c_{i,\phi}|\phi\rangle$ etc. with the $\gamma_{\phi\chi;\psi\omega}$ of (3.26), the structure of the improved $K^{\mathrm{S}}_{ia,jb}$ shall be also clear from (3.26).

It must be noted here, however, that the coupling matrix of spin triplet excitations cannot be improved by the multipole expansion introduced in 3.1. As it was written in 1.2.3, spin-spin interaction terms in DFTB are confined to on-site terms, because of the short range of $\frac{\delta^2 E_{\mathrm{xc}}}{\delta\mu(\mathbf{x})\delta\mu(\mathbf{y})}$. In addition to this, on-site multipole-multipole interactions are zero in our approximation above the monopole-monopole level because the (1.62) semiempirical calculation of on-site second-order energy change (the chemical hardness, and its refinements introduced later) includes every level of multipole-multipole interactions. This is also why our new higher-order γ's tend to zero when $r = 0$. Nonetheless, if one wants to make improvements in this part of DFTB, there remains a possibility of using fitted monopole-dipole, etc. interaction strengths, if the underlying physics needs it. The more promising way of improving the description of triplet excitations is including spin-orbit interaction in TD-DFTB. Using some kind of operator-like γ's (see 3.2.4) would be a major improvement in this field, but at rather high cost.

The second aspect of making TD-DFTB better by the multipole SCC which we treat here is the improvement of its oscillator strength expression. The oscillator strength of a transition from state i to a is proportional to the square of a transitional dipole moment

$$f_{ia} \propto \sum_\alpha \left| D^{(ia)}_\alpha \right|^2 = \sum_\alpha \left| \langle i|\hat{X}_\alpha|a\rangle \right|^2 \tag{3.57}$$

where $\alpha = x, y, z$ is the index of spatial coordinates, and $\hat{X}_\alpha$ is the α component of position operator. The above matrix element can be easily calculated with the aid of the previously stored position operator integral table elements discussed in 3.3.3. If $i = \sum_\phi c_{i,\phi}\phi$ and $a = \sum_\chi c_{a,\chi}\chi$, the dipole matrix elements of (3.57) become (the sign is only for conventional reasons)

$$\begin{aligned} -D^{(ia)}_\alpha = &\sum_A^{\text{atoms}} \sum_{\phi\in\{A\}} \sum_B^{\text{atoms}} \sum_{\chi\in\{B\}} \bar{c}_{i,\phi}c_{a,\chi}\langle\phi|\hat{X}_\alpha|\chi\rangle = \\ &\sum_A^{\text{atoms}} \sum_{\phi,\chi\in\{A\}} \bar{c}_{i,\phi}c_{a,\chi}\langle\phi|(\hat{X}_\alpha - R^{(A)}_\alpha) + R^{(A)}_\alpha|\chi\rangle + \\ &\sum_A^{\text{atoms}} \sum_{\phi\in\{A\}} \sum_{B\neq A}^{\text{atoms}} \sum_{\chi\in\{B\}} \bar{c}_{i,\phi}c_{a,\chi}\langle\phi|(\hat{X}_\alpha - R^{(A)}_\alpha) + R^{(A)}_\alpha|\chi\rangle \end{aligned} \tag{3.58}$$

where $R^{(A)}_\alpha$ is the α component of the position of atom A. By the definition of

the tabulated overlap and position matrices (see 3.1), we finally get

$$D_\alpha^{(ia)} = \frac{D_\alpha^{(ia)} + D_\alpha^{(ia)}}{2} =$$
$$-\frac{1}{2}\sum_A^{\text{atoms}} \sum_{\phi\in\{A\},\chi} \bar{c}_{i,\phi} c_{a,\chi} (X^{(A)}_{\alpha,\phi\chi} + S_{\phi\chi} R^{(A)}_\alpha) + \bar{c}_{i,\chi} c_{a,\phi} (X^{(A)}_{\alpha,\chi\phi} + S_{\chi\phi} R^{(A)}_\alpha) =$$
$$\left(\sum_A^{\text{atoms}} \mathbf{d}_A^{(ia)} + q_A^{(ia)} \mathbf{R}^{(A)} \right)_\alpha \tag{3.59}$$

where $\mathbf{R}^{(A)}$ is the vector of the position of atom A, and the first, trivial step is didactically included in order to symbolise that half of the sum over A, B and ϕ, χ is made with a $A \leftrightarrow B$, $\phi \leftrightarrow \chi$ relabelling of the summand. The quantities defined in the last step are called transitional Mulliken charges and dipole moments between states i and a.

Summary

In this dissertation, I treat two areas of improving the DFTB method. The first area of interest is the repulsive part of DFTB energy. There has been a parametrizer automaton developed that performs a least-squares fitting of repulsive potentials as linear combinations of basis profiles through a linear regression of coefficients. It makes fitting of repulsive profiles to multiple fitsystems incomparably easier than before; that is illustrated by several examples as successful usages of the fitter. The automaton is also able to tune electronic parameters. To make the fitting process truly automatic as seen from the user side, the parametrizer does many auxiliary tasks automatically as well, e.g. fitsystem generation. Among the objectives of fits, not only energies can be used, but several other energetical properties (mainly but not exclusively, derivatives of energy). User-input weighting of fit targets ensures the most precise fitting to the most important properties of most important fitsystems selected by the user.

As a further question regarding repulsive energy, its structure is also treated here briefly. It is quite clear now that in addition to the pairwise repulsive profiles, one-body repulsive energy terms can be used too to tune the dissociation behaviour of DFTB. In addition to short-range pair repulsives and one-body terms, there must be middle-range pairwise repulsives also used, but fitting them is not (yet?) feasible.

As a perfect way of building repulsives, calculation of them instead of fitting is also proposed. After deriving the formulas needed for repulsive calculation and implementing them, the first results suggest that this scheme is able to be used to get at least first-glance repulsives for any set of elements that has not been parametrized with DFTB before, if one optimizes atomic electronic parameters successfully. Being able to make transferable parametrizations depending on atomic, not pairwise parameters gives the prospect of producing and extending parametrizations including large sets of elements with reasonable effort.

The second area of DFTB improvement that is investigated here is making its SCC part better. A proposition of a multipole expansion of SCC energy instead of the currently used point-like charges is made as well as a proposition to calculate the effective interaction profiles between atomic excess charges semiempirically, instead of the current heuristical interpolation. Fully derived formulae of the above improvements are ready to implement in SCC. Furthermore, improvements to time-dependent DFTB are also introduced briefly.

The above enhancements, enhancement proposals and descriptions of them are introduced by a thorough derivation of current DFTB method in the very beginning of the thesis, which prepares the methodological improvements, among others, by a formulation of the DFTB equations based on the density matrix. Through treating improvements to DFTB, a deeper understanding of the nature of it, including its approximative self-consistency (SCC) could be achieved too.

Acknowledgements

It is hardly possible to write down how deeply I am grateful to the colleagues who made my doctoral research possible and who helped it. First, I thank to Professor Thomas Frauenheim to give me the opportunity of working at the Bremen Center of Materials Science as a PhD student. As large parts of the research has been carried out in working together with Bálint Aradi, I must acknowledge that my results would have been incomparably less without the help of him.

In addition to the above, cooperations and other discussions canalized a lot of helpful stimuli and other useful impressions from Gotthard Seifert, Martin Persson, Karl Jalkanen, Grygoriy Dolgonos, Thomas Niehaus, Adriel Dominguez, Michael Gaus and Tomáš Kubar into my research.

Many thanks shall go to Christof Köhler and Zoltán Hajnal for facilities I was able to use in Bremen and temporarily in Budapest, respectively.

Last but not least, my thanks go to my family, as well as to my friends in Bremen.

Bibliography

[1] NIST computational chemistry comparison and benchmark database. NIST Standard Reference Database Number 101, `http://cccbdb.nist.gov`. Release 15b, August 2011, Editor: Russell D. Johnson III.

[2] B. Aradi, B. Hourahine, and Th. Frauenheim. DFTB+, a sparse-matrix-based implementation of the DFTB method. *J. Phys. Chem. A*, 111:5678–5684, 2007.

[3] Nathan Argaman and Guy Makov. Density functional theory – an introduction. 1999. `arXiv:physics/9806013v2`.

[4] Zoltán Bodrog and Bálint Aradi. Possible improvements to the self-consistent-charges density-functional tight-binding method within the second order. *Phys. Status Solidi (b)*, 249:259–269, 2012.

[5] Zoltán Bodrog, Bálint Aradi, and Thomas Frauenheim. Automated repulsive parametrization for the DFTB method. *J. Chem. Theory Comput.*, 7:2654–2664, 2011.

[6] Zoltán Bodrog, Bálint Aradi, and Thomas Frauenheim. Atomic-parameter-based repulsive potentials for the density-functional tight-binding method. 2012. To be published soon.

[7] Jiří Čížek. A new method of approximative calculation of polycentric integrals used in the quantum mechanical study of molecular structure. *Mol. Phys.*, 6:19–31, 1963.

[8] Larry A. Curtiss, Krishnan Raghavachari, Paul C. Redfern, and John A. Pople. Assessment of Gaussian-2 and density functional theories for the computation of enthalpies of formation. *J. Chem. Phys.*, 106:1063–1079, 1997.

[9] P. A. M. Dirac. Note on exchange phenomena in the Thomas atom. *Proc. Cambridge Phil. Soc*, 26:376–385, 1930.

[10] Grygoriy Dolgonos, Bálint Aradi, Ney H. Moreira, and Thomas Frauenheim. An improved self-consistent-charges density-functional tight-binding (SCC-DFTB) set of parameters for simulation of bulk and molecular systems involving titanium. *J. Chem. Theory Comput.*, 6:266–278, 2010.

[11] R. Dovesi, M. Causa, R. Orlando, C. Roetti, and V.R. Saunders. Ab-initio approach to molecular-crystals – a periodic hartree-fock study of crystalline urea. *J. Chem. Phys.*, 92:7402–7411, 1990.

[12] M. Elstner. SCC-DFTB: What is the proper degree of self-consistency. *J. Phys. Chem. A*, 111:5614–5621, 2007.

[13] M. Elstner, Dirk Porezag, G. Jungnickel, Joachim Elstner, M. Haugk, Thomas Frauenheim, Sándor Suhai, and Gotthard Seifert. Self-consistent-charge density-functional tight-binding method for simulations of complex materials prooperties. *Phys. Rev. B*, 58:7260–7268, 1998.

[14] H. Eschrig and I. Bergert. An optimized LCAO version for band structure calculations. *Phys. Status Solidi (b)*, 90:621–628, 1978.

[15] Enrico Fermi. Un metodo statistico per la determinazione di alcune proprietà dell'atomo. *Rend. Accad. Naz. Lincei*, 6:602–607, 1927.

[16] J. Frenzel, A. F. Oliveira, N. Jardillier, T. Heine, and G. Seifert. Semi-relativistic, self-consistent-charges Slater-Koster tables for density-functional-based tight-binding (DFTB) for materials science simulations. Technical report, TU Dresden, 2004–2009.

[17] M. J. Frisch, G. W. Trucks, H. B. Schlegel, G. E. Scuseria, M. A. Rob, J. R. Cheeseman, J. A. Montgomery Jr., T. Vreven, K. N. Kudin, J. C. Burant, J. M. Millam, S. S. Iyengar, J. Tomasi, V. Barone, B. Mennucci, M. Cossi, G. Scalmani, N. Rega, G. A. Petersson, H. Nakatsuji, M. Hada, M. Ehara, K. Toyota, R. Fukuda, J. Hasegawa, M. Ishida, T. Nakajima, Y. Honda, O. Kitao, H. Nakai, M. Klene, X. Li, J. E. Knox, H. P. Hratchian, J. B. Cross, V. Bakken, C. Adamo, J. Jaramillo, R. Gomperts, R. E. Stratmann, O. Yazyev, A. J. Austin, R. Cammi, C. Pomelli, J. W. Ochterski, P. Y. Ayala, K. Morokuma, G. A. Voth, P. Salvador, J. J. Dannenberg, V. G. Zakrzewski, S. Dapprich, A. D. Daniels, M. C. Strain, O. Farkas, D. K. Malick, A. D. Rabuck, K. Raghavachari, J. B. Foresman, J. V. Ortiz, Q. Cui, A. G. Baboul, S. Clifford, J. Cioslowski, B. B. Stefanov, G. Liu, A. Liashenko, P. Piskorz, I. Komaromi, R. L. Martin, D. J. Fox, T. Keith, M. A. Al-Laham, C. Y. Peng, A. Nanayakkara, M. Challacombe, P. M. W. Gill, B. Johnson, W. Chen, M. W. Wong, C. Gonzalez, and J. A. Pople. *Gaussian 03*. Gaussian, Inc., Wallingford, CT, 2003.

[18] J. Harris. Simplified method for calculating the energy of weakly interacting fragments. *Phys. Rev. B*, 31:1770, 1985.

[19] J. F. Janak. Proof that $\frac{\partial E}{\partial n_i} = \varepsilon_i$ in density-functional theory. *Phys. Rev. B*, 18:7165–7168, 1978.

[20] J. M. Knaup, B. Hourahine, and Th. Frauenheim. Initial steps toward automating the fitting of DFTB $E_{\mathrm{rep}}(r)$. *J. Phys. Chem. A*, 111:5637–5641, 2007.

[21] Christof Köhler. *Berücksichtigung von Spinpolarisationseffekten in einem dichtefunktionalbasierten Ansatz*. PhD thesis, Universität Paderborn, 2003.

[22] Christof Köhler and Thomas Frauenheim. Molecular dynamics simulations of Cf_x $(x = 2, 3)$ molecules at $\mathrm{Si_3N_4}$ and $\mathrm{SiO_2}$ surfaces. *Surf. Sci.*, 600:453–460, 2006.

[23] Tomáš Kubar, Zoltán Bodrog, and Michael Gaus. Density-functional tight-binding parameters for halogen-organic chemistry. 2012. To be published soon.

[24] Christof Köhler, Thomas Frauenheim, Ben Hourahine, Gotthard Seifert, and Michael Sternberg. Treatment of collinear and noncollinear electron spin within an approximate density functional based method. *J. Phys. Chem. A*, 111:5622–5629, 2007.

[25] Christof Köhler, Gotthard Seifert, and Thomas Frauenheim. Density-functional-based calculations for Fe(n), ($n \leq 32$). *Chem. Phys.*, 309:23–31, 2005.

[26] André Mirtschink. Berechnungen von Bindungsenergien zweiatomiger Moleküle der Elemente der ersten und zweiten Periode im Rahmen der DFTB-Methode. Master's thesis, Technische Universität Dresden, 2010.

[27] Ney H. Moreira, Grygoriy Dolgonos, Bálint Aradi, Andreia L. da Rosa, and Thomas Frauenheim. Toward an accurate density-functional tight-binding description of zinc-containing compounds. *J. Chem. Theory Comput.*, 5:605–614, 2009.

[28] Thomas Niehaus. Approximate time-dependent density functional theory. *J. Mol. Struct. – THEOCHEM*, 914:38–49, 2009.

[29] Robert G. Parr and Weitao Yang. *Density-Functional Theory of Atoms and Molecules*. Oxford University Press, 1994.

[30] J. P. Perdew, K. Burke, and M. Ernzerhof. Generalized gradient approximation made simple. *Phys. Rev. Lett.*, 77:3865–3868, 1996.

[31] Dirk Porezag, Thomas Frauenheim, Thomas Köhler, Gotthard Seifert, and R. Kaschner. Construction of tight-binding-like potentials on the basis of density-functional theory: Application to carbon. *Phys. Rev. B*, 51:12947, 1995.

[32] V.R. Saunders, R. Dovesi, C. Roetti, R. Orlando, C. M. Zicovich-Wilson, N.M. Harrson, K. Doll, B. Civalleri, I. Bush, Ph. D'Arco, and M. Llunell. *CRYSTAL2003 User's Manual*. University of Torino, Torino, 2003.

[33] G. Seifert. Tight-binding density functional theory: An approximate Kohn–Sham DFT scheme. *J. Phys. Chem. A*, 111:5609–5613, 2007.

[34] José M. Soler, Emilio Artacho, Julian D. Gale, Alberto García, Javier Junquera, Pablo Ordejón, and Daniel Sánchez-Portal. The SIESTA method for ab initio order-N materials simulation. *J. Phys.*, 14:2745, 2002.

[35] L. H. Thomas. The calculation of atomic fields. *Proc. Cambridge Phil. Soc.*, 23:542–548, 1927.

[36] M. Valiev, E.J. Bylaska, N. Govind, K. Kowalski, T.P. Straatsma, H.J.J. van Dam, D. Wang, J. Nieplocha, E. Apra, T.L. Windus, and W.A. de Jong. NWChem: a comprehensive and scalable open-source solution for large scale molecular simulations. *Comput. Phys. Commun.*, 181:1477–1489, 2010.

[37] Carl Friedrich von Weizsäcker. Zur Theorie der Kernmassen. *Zeitschrift für Physik*, 96:431–458, 1935.

[38] Oleg A. Vydrov and Troy Van Voorhis. Nonlocal van der Waals density functional: The simpler the better. *J. Chem. Phys.*, 133:244103, 2010.